Materials Today Bio 16 (2022) 100402

Contents lists available at ScienceDirect

Materials Today Bio

journal homepage: www.journals.elsevier.com/materials-today-bio

Strategies to improve bioactive and antibacterial properties of polyetheretherketone (PEEK) for use as orthopedic implants

Zhi Zheng [a,b], Pengjia Liu [c], Xingmin Zhang [a,b], Jingguo xin [a,b], Yongjie wang [a,b], Xiaosong Zou [a,b], Xiaohan Mei [d], Shuling Zhang [d], Shaokun Zhang [a,b,*]

[a] Department of Spinal Surgery, The First Hospital of Jilin University, Changchun, 130021, China
[b] Jilin Engineering Research Center for Spine and Spinal Cord Injury, Changchun, 130021, China
[c] Australian Institute of Bioengineering and Nanotechnology, University of Queensland, St Lucia, QLD, 4072, Australia
[d] National & Local Joint Engineering Laboratory for Synthetic Technology of High Performance Polymer, College of Chemistry, Jilin University, Changchun, 130012, China

ARTICLE INFO

Keywords:
Polyetheretherketone
Orthopedic implants
Modification
Biocompatibility
Antibacterial properties
Coating
Composite

ABSTRACT

Polyetheretherketone (PEEK) has gradually become the mainstream material for preparing orthopedic implants due to its similar elastic modulus to human bone, high strength, excellent wear resistance, radiolucency, and biocompatibility. Since the 1990s, PEEK has increasingly been used in orthopedics. Yet, the widespread application of PEEK is limited by its bio-inertness, hydrophobicity, and susceptibility to microbial infections. Further enhancing the osteogenic properties of PEEK-based implants remains a difficult task. This article reviews some modification methods of PEEK in the last five years, including surface modification of PEEK or incorporating materials into the PEEK matrix. For surface modification, PEEK can be modified by chemical treatment, physical treatment, or surface coating with bioactive substances. For PEEK composite material, adding bioactive filler into PEEK through the melting blending method or 3D printing technology can increase the biological activity of PEEK. In addition, some modification methods such as sulfonation treatment of PEEK or grafting antibacterial substances on PEEK can enhance the antibacterial performance of PEEK. These strategies aim to improve the bioactive and antibacterial properties of the modified PEEK. The researchers believe that these modifications could provide valuable guidance on the future design of PEEK orthopedic implants.

1. Introduction

Orthopedic implants are used in a variety of procedures, such as spinal fusion, joint fusion, fracture fixation, nonunion repair, total hip arthroplasty, and bone defect repair. A variety of materials have been used as orthopedic implants, including metallic materials, autogenous bone, ceramic materials, polymers, and so on. Among them, metal material has a high elastic modulus. It easily leads to stress shielding *in vivo*. In addition, the presence of metal often causes artifacts when taking X-rays images. Autologous bone grafts can cause bone defects at the donor site, which may lead to deformity and disease. Ceramic materials, like metal materials, have high elastic modulus but poor ductility, which cannot meet the requirements of orthopedic implants [1]. There are many kinds of polymers and their properties can be easily changed and tuned. Therefore, polymers may prove to be a practical material for use in orthopedic implants once mechanical properties and biocompatibility are fine-tuned.

PEEK is a specially engineered plastic with a high melting point, high modulus, high strength, corrosion resistance, and excellent processing performance. It also provides excellent wear resistance under a variety of different pressures, temperatures, speeds, and relative roughness contact conditions. Based on the aforementioned advantages, researchers around the world began to consider PEEK as an orthopedic implant in the 1980s. A series of studies have proved that PEEK has stable chemical properties [2]. However, increasing clinical use of PEEK has revealed rather poor osseointegration, likely attributable to the inherent biological inertia of PEEK [3]. Although some shortcomings of PEEK limit its clinical application, the modified PEEK can overcome these shortcomings and is widely used in clinical surgery (Fig. 1).

At present, PEEK implants are increasingly used as spinal cages [4], skull or maxillofacial defect repair implants [5,6], dental implants [7], joint replacements [8], fixation devices [9], and so on. PEEK cages are widely used in spinal fusion due to their radiolucency and low elastic modulus [10–12]. However, the subsidence and migration of PEEK cages

* Corresponding author. Department of Spinal Surgery, the First Hospital of Jilin University, Changchun, 130021, China.
E-mail address: shaokun@jlu.edu.cn (S. Zhang).

https://doi.org/10.1016/j.mtbio.2022.100402
Received 23 June 2022; Received in revised form 11 August 2022; Accepted 12 August 2022
Available online 19 August 2022

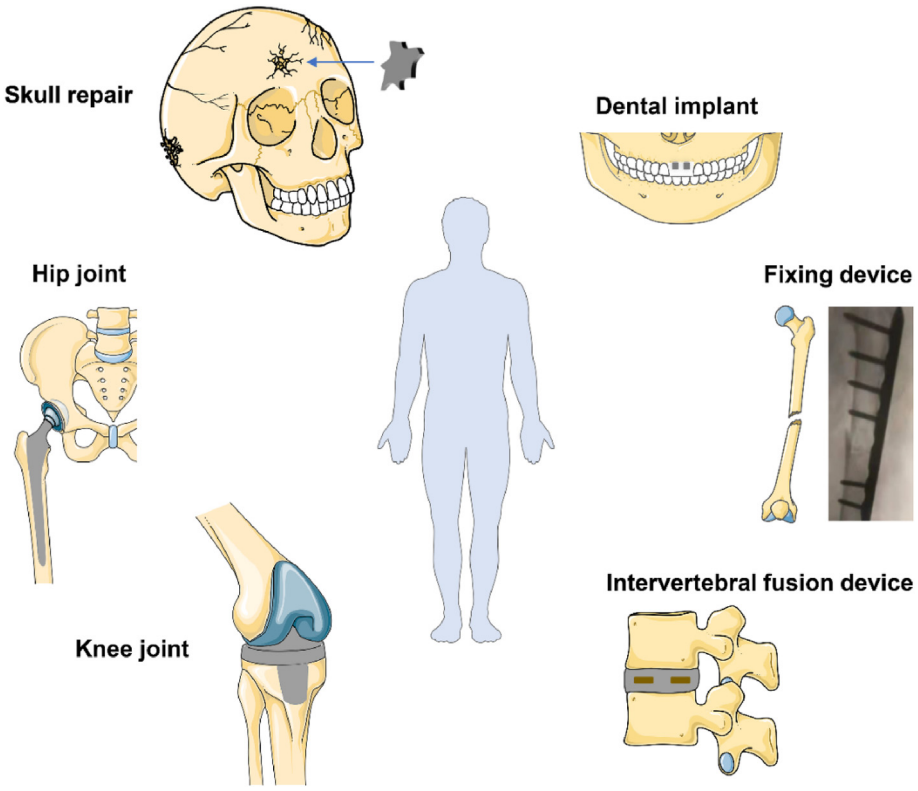

Fig. 1. Example clinical uses of modified PEEK.

often lead to fusion failure [13,14]. This is because PEEK has a hydrophobic surface that cannot absorb proteins and promote cell adhesion [15]. An animal study reported that the surface of PEEK cages was covered by a layer of fibrous tissue [16]; Therefore, changing the shape of the PEEK cage and increasing the bioactivity of PEEK can prevent the subsidence and migration of the PEEK cage. For example, improving the surface roughness of PEEK promotes cell adhesion by sulfonation, sandblasting, or surface coating with hydroxyapatite.

In dental applications, PEEK has an elastic modulus of 3–4 GPa [17], which is close to that of human cancellous bone [18]. By adjusting the ratio of carbon fiber(CF) and PEEK, the elastic moduli of carbon fiber reinforced PEEK (CFR-PEEK) are comparable to those of human cortical bone and dentin [19]. Moreover, the tensile properties of CFR-PEEK are also similar to those of bone, enamel, and dentin [17,20]. In addition, increasing the biological activity of the dental graft can enhance the osseointegration of the graft and alveolar bone. However, studies have shown that CFR-PEEK has mild cytotoxicity [21,22]. Therefore, it is necessary to modify CFR-PEEK or develop new PEEK implant materials.

As for the repair of cranial or maxillofacial defects, PEEK has been widely used in craniocerebral reconstruction in the past few years [23], because PEEK is suitable for 3D printing with CAD surgical planning [24–26]. However, the disadvantages are also obvious, some researchers have reported that implant failure is mainly caused by implant infection [24,27] and poor osseointegration [28]. Therefore, it is the key to increasing the anti-infection ability and osseointegration ability of PEEK implants and designing the shape of the implants. Plasma modification is particularly suitable for biomedical implants with irregular geometries, and plasma modification only changes the surface properties of the material, not the mechanical properties material [29]. Therefore, plasma modification is very suitable for PEEK modification of cranial or maxillofacial repair.

The materials used for joint replacements mainly depend on the design of the biomechanics and tribology of the materials [8,30]. For example, the addition of carbon fibers to PEEK can alter the mechanical properties of PEEK to approximate the elastic modulus of human bone [31,32]. Wear particles generated on the articular surface can cause macrophages to engulf debris particles, trigger the release of inflammatory cytokines, and stimulate osteoclast bone resorption, which can lead to prosthesis loosening [33,34]. Therefore, changing the mechanical properties of PEEK and reducing wear particles are the main focus.

In fracture repair devices, doctors will usually choose stainless steel plates or titanium alloy plates. These metal devices suffer from radiation opacity, elastic modulus mismatch, corrosion, limited fatigue life, susceptibility to cold welding of plates and screws, and osseointegration [35,36]. Because CFR-PEEK can improve these shortcomings [37], some researchers apply CFR-PEEK to fracture repair [9,38]. However, a comparative study pointed out that the disadvantage of CFR-PEEK relative to metal plates is the low tolerance for plastic deformation and the risk of fracture [37]. The researchers are exploring a way to increase the plastic deformation capacity of PEEK while reducing PEEK osseointegration.

This article reviews the last 5 years of developments in the surface treatment of PEEK and the addition of different materials by various techniques to enhance the bioactivity or antibacterial performance (Fig. 3 and Fig. 8). PEEK modified by various methods will increase the bioactivity, osteogenic activity, and antibacterial properties of PEEK (Fig. 2). The literature summarized in this review will provide clues for researchers and surgeons to develop novel ways to enhance the bioactivity or antimicrobial activity of PEEK in orthopedic implants. Table 1 summarizes the modification strategies to enhance the biological activity of PEEK, and Table 3 summarizes the modification strategies to enhance the antibacterial activity of PEEK.

2. Osteogenic activity

2.1. Surface modification

Superficial PEEK modifications mainly include bioactive material

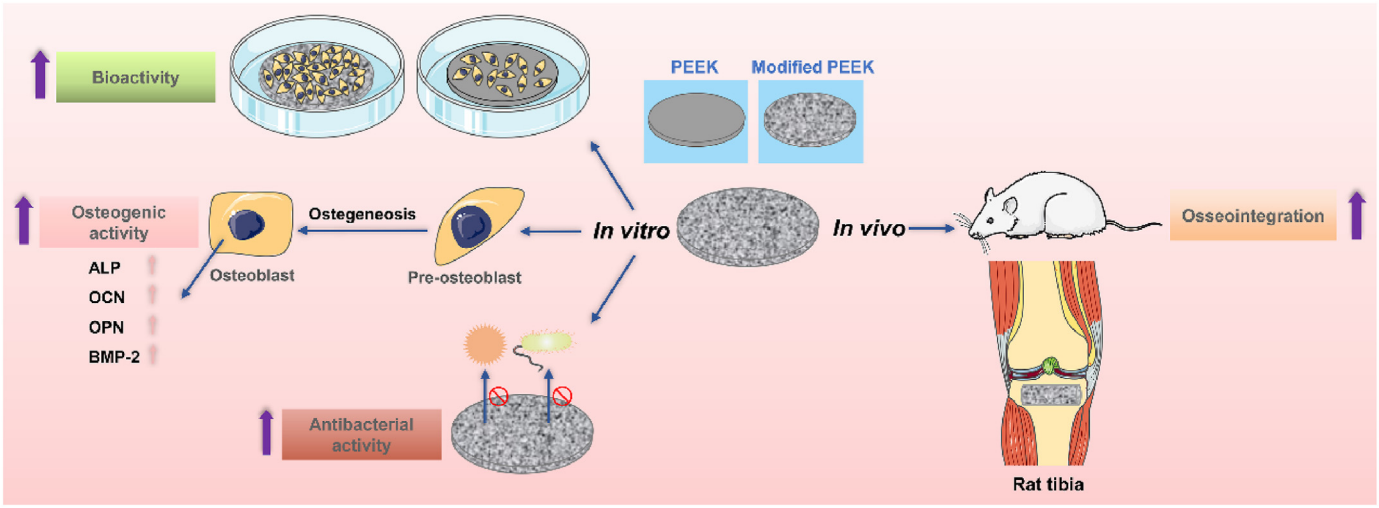

Fig. 2. Characteristics of PEEK implants after modification. **Abbreviation:** ALP, Alkaline Phosphatase; OCN, Osteocalcin; OPN, Osteopontin; BMP-2, Bone morphogenetic protein 2.

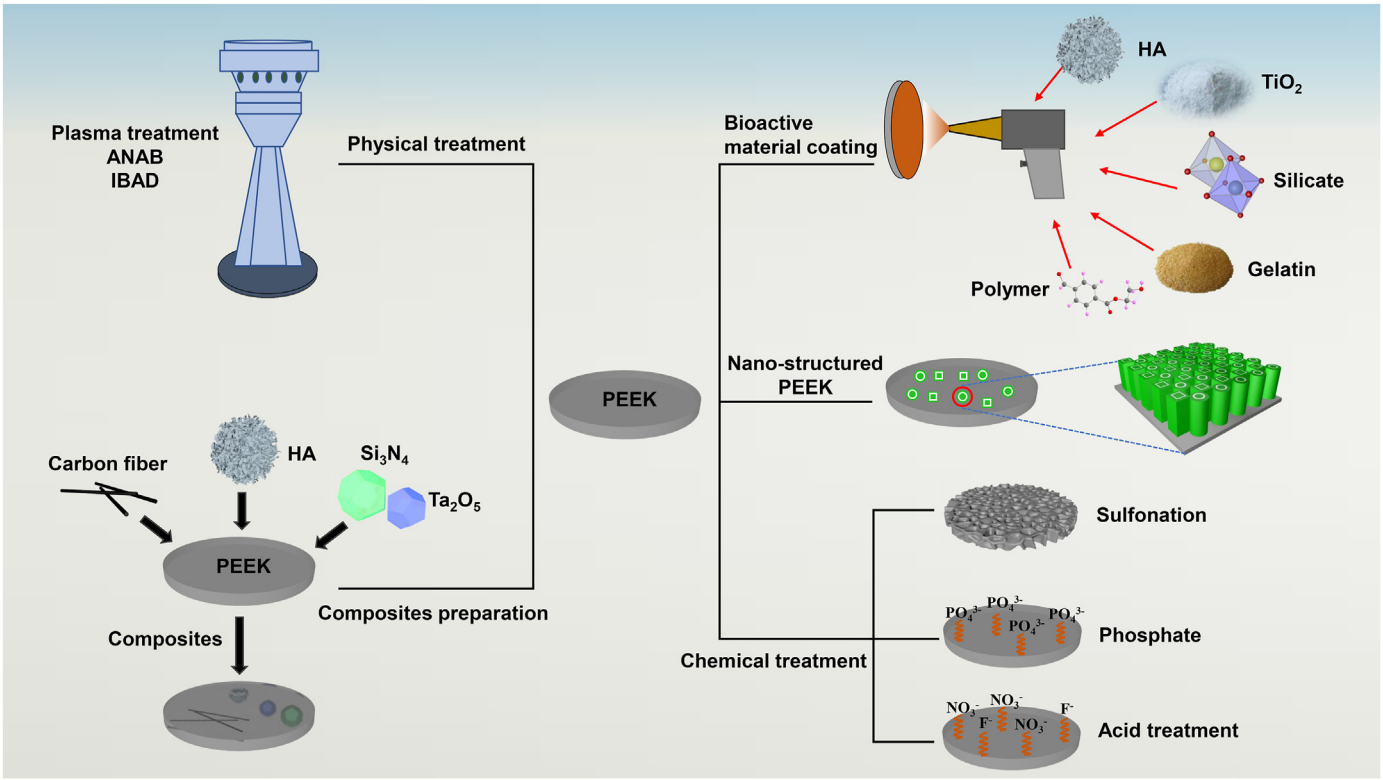

Fig. 3. PEEK modification strategies to improve bioactivity. **Abbreviation:** ANAB, Accelerated Neutral Atom Beam; IBAD, Ion Beam Assisted Deposition; HA, hydroxyapatite.

coating, chemical treatment, and physical treatment (Fig. 3). These surface modifications lead to the enhancement of PEEK bioactivity, allowing for easier integration with native bone tissue while maintaining PEEK's original mechanical properties. However, surface modification also has some disadvantages, such as poor adhesion due to changes in material crystallinity and high-temperature conditions [39]. The advantages and disadvantages of some surface modification techniques are summarized in Table 2.

2.1.1. *Bioactive material coating*

Various bioactive materials are used to coat the surface of PEEK, such as HA, titanium, titanium dioxide, silicate, magnesium phosphate, calcium phosphate, gelatin, proteins, etc. The addition of these bioactive coatings greatly enhanced the surface osteogenic activity of PEEK. However, the stability of the PEEK surface coating deserves our attention.

In a case report, a patient's hip prosthesis was impacted by an external force, which resulted in delamination at the PEEK-cobalt-chromium interface [40]. Therefore, it is crucial to evaluate whether the coating will debond from the polymer substrate under the action of external force.

The improved interfacial adhesion is mainly due to physical interactions such as hydrogen bonds [41]. Some previous studies have

Table 1
Modification strategies to enhance the biological activity of PEEK and its enhanced properties.

Modification strategy	Coatings or Fillers	Research results related to the bioactive property	Reference
Hydroxyapatite coating	B-nHA	*In vitro*: increased cytocompatibility, differentiation, COL1A1 mRNA expression, and collagen secretion.	[39]
	Nanoscale HA	*In vivo*: torque values of the tibia and femur in rabbits were higher.	[48]
	Nanoscale HA	*In vivo*: improved the osteogenic ability of the rabbit femur.	[49]
	HA, YSZ	*In vivo*: increased bone integration of rabbit femur.	[47]
Titanium or titanium dioxide coated PEEK	Ti	*In vitro*: increased cytocompatibility, differentiation; *In vivo*: increased regeneration of rabbit tibial.	[54]
	Ti	Clinical cases: better end plate maintenance of bony fusion.	[55]
	TiO_2	*In vitro*: increased cytocompatibility; *In vivo*: enhanced bone integration of rabbit tibia.	[56]
	Methacrylate hyaluronic acid, TiO_2	*In vitro*: increased cytocompatibility.	[57]
Other surface coatings	Silicate	*In vitro*: increased osteogenic potential at the genetic and protein levels; *In vivo*: improved osteointegration in rat models of osteoporosis.	[58]
	AMP	*In vitro*: enhanced apatite formation in SBF, increased osteocalcin expression of MC3T3-E1 cells.	[59]
	Calcium phosphate	*In vitro*: increased cytocompatibility, and enhanced apatite formation in SBF.	[60]
	BMP-2, gelatin	*In vitro*: reduced water contact Angle, increased cytocompatibility.	[64]
	Concentrated sulfuric acid, silk fibroin protein, BMP	*In vitro*: increased cytocompatibility and differentiation.	[65]
	Concentrated sulfuric acid, zinc ions	*In vitro* and *in vivo*: increased anti-inflammatory properties and improved osseous integration.	[66]
	PSS, PAH	*In vitro*: increased hydrophilicity, increased cytocompatibility, and differentiation; *In vivo*: improved osteointegration in rabbit models of osteoporosis.	[67]
	Oxygen, gelatin	*In vivo*: adhesion and proliferation of mouse embryonic fibroblasts	[63]
	Strontium Eucommia polysaccharide	*In vivo*: promoted the proliferation and differentiation of MC3T3-E1	[73]
	Strontium, chondroitin sulfate	*In vitro and in vivo: improved angiogenic and osteogenic abilities*	[77]
Sulfonation modification	Concentrated sulfuric acid	*In vitro*: SPEEK5 increased hydrophilicity and cytocompatibility.	[78]
	SO_3	*In vitro*: increased cytocompatibility; enhanced apatite formation in SBF and protein absorbability.	[87]
	Concentrated sulfuric acid, calcium phosphate particles	*In vitro*: enhanced apatite formation in SBF.	[318]
	Concentrated sulfuric acid, PDA, RGD	*In vitro*: increased cytocompatibility and differentiation; enhanced apatite formation in SBF and protein absorbability.	[89]
	Concentrated sulfuric acid, $Sr(OH)_2$, APN, PDA	*In vitro*: increased cytocompatibility and differentiation.	[90]
	Concentrated sulfuric acid, NaOH	*In vitro*: increased cytocompatibility and differentiation; enhanced apatite formation in SBF; reduced water contact Angle; increased surface roughness; enhanced serum protein adsorption.	[91]
	BMP-2	*In vitro*: increased cytocompatibility and differentiation; enhanced collagen secretion.	[92]
	Concentrated sulfuric acid, ASP, BFP	*In vitro*: increased cytocompatibility and differentiation; improved anti-inflammatory activity.	[93]
	Concentrated sulfuric acid, hydrogen peroxide	*In vitro*: promoted the adhesion and proliferation of human fibroblasts cells	[99]
Nano-structured PEEK surfaces	PAA, PAH	*In vitro*: increased cytocompatibility and differentiation; improved anti-inflammatory activity; *In vivo*: reduced fibrous sac formation and improved bone regeneration of rat femur.	[130]
	Nanoporous lithium, NLS	*In vitro*: increased cytocompatibility and differentiation; enhanced water absorption and protein absorption, apatite formation in SBF; *In vivo*: Enhanced bone formation of rabbit femur in comparison to PKLs and PK.	[131]
	LSNs, PDA	*In vitro*: increased cytocompatibility; enhanced apatite formation in SBF; *In vivo*: promotes bone tissue response of beagle dog's femur.	[132]
	Nano silicon nitride	*In vitro*: increased cytocompatibility and differentiation; improved surface roughness, hydrophilicity, and protein absorption; *In vivo*: stimulated bone regeneration and integration in a rat model of skull defects.	[133]
	Submicron nanostructures surface (No coatings or Fillers)	*In vitro:* adhesion, proliferation, and osteogenic differentiation of MC3T3-E1 cells were enhanced	[136]
	Patterned nanorod arrays surface (No coatings or Fillers)	*In vitro*: promoted the osteogenic differentiation of rat adipose stem cells *In vivo*: promoted the osseointegration of rat femurs	[129]
Phosphate modification	Vinyl phosphonic acid.	*In vitro*: increased cytocompatibility and differentiation; increased hydrophilicity; *In vivo*: improved bone-implant contact.	[100]
	Phosphoryl chloride	*In vitro*: increased cytocompatibility and differentiation; *in vivo*: enhanced osseointegration of rabbit tibia.	[101]
	Phosphoryl chloride, triethylamine, dichloromethane	*In vitro*: increased cytocompatibility and differentiation; improved anti-inflammatory properties; *In vivo*: improved implant-bone bond strength of rat femur.	[102]
	Phosphonates	*In vitro*: increased cytocompatibility and differentiation; *In vivo*: prevented formation of the fibrous sac and promoted osseointegration in a rat model of skull defects.	[103]
Acid treatment	Hydrofluoric acid and nitric acid	*In vitro*: increased cytocompatibility and differentiation; improved anti-inflammatory properties; enhanced hydrophilicity.	[105]
Plasma treatment	Ammonia	*In vitro*: increased cytocompatibility and differentiation; increased hydrophilicity and roughness; *In vivo*: enhanced osteosynthesis of rat femur.	[29]
	Hydrogen, oxygen	*In vitro*: increased cytocompatibility; improved hydrophilicity, surface microhardness, and crystallinity.	[111]
	H_2SO4, alkaline SBF	*In vitro*: enhanced apatite formation in SBF; *In vivo*: improved bone-bonding properties and bone conductivity of rabbit tibia.	[112]
	Hydrofluoric acid	*In vitro*: increased cytocompatibility and differentiation; increased hydrophilicity of PEEK.	[113]
	Calcium	*In vitro*: increased cytocompatibility and differentiation.	[114]

(*continued on next page*)

Table 1 (*continued*)

Modification strategy	Coatings or Fillers	Research results related to the bioactive property	Reference
	Oxygen, nitrogen	*In vitro*: promoted the adhesion and proliferation of MG-63 cells	[115]
ANAB treatment	N/A	*In vitro*: increased metabolic activity, proliferation, and differentiation; improved hydrophilicity of PEEK.	[118]
IBAD treatment	YSZ, HA	*In vitro*: increased cell growth and differentiation.	[120]
CFR-PEEK composites	CF, amino groups	*In vitro*: increased cytocompatibility and differentiation.	[143]
	CF, GO, concentrated sulfuric acid	*In vitro*: increased cytocompatibility and differentiation; no obvious cytotoxicity; *In vivo*: promoted bone formation in a rat model of skull defects.	[140]
	CF, HNO_3, $CaCl_2$	*In vitro*: increased hydrophilicity; increased apatite formation; no cytotoxicity.	[144]
	CF, graphene	*In vitro*: increased cytocompatibility and differentiation; *In vivo*: increased mineral deposition rate and bone formation of rabbit femur.	[145]
	CF, concentrated sulfuric acid, $CaCl_2$	*In vitro*: enhanced apatite formation in SBF.	[146]
	CF, CNT, HA	*In vitro*: increased cell adhesion.	[147]
	CF, concentrated sulfuric acid, HA, GO	*In vitro*: promotes adhesion and proliferation of MC3T3-E1 cells	[148]
PEEK/HA composites	HA	*In vitro*: increased cytocompatibility and differentiation; improved apatite formation.	[157]
	HA	*In vivo*: improved cervical fusion and bone growth in sheep.	[158]
	HA, PGA	*In vitro*: increased cytocompatibility; enhanced apatite formation in SBF.	[159]
3D printing of PEEK composites	N/A	*In vitro*: higher cytocompatibility in the group without polishing and sandblasting.	[161]
	CF	*In vitro*: the density of cells was higher in the group without polishing and sandblasting; no cytotoxicity.	[164]
	Magnesium ion, PDA	*In vitro*: promoted the proliferation, adhesion, and differentiation of MC3T3-E1 cells *In vivo*: promoted osseointegration of rabbit femur	[172]
PEEK nano-composites	MoS_2,	*In vitro*: increased cytocompatibility; improved surface roughness and hydrophilicity.	[175]
	NBG, HK	*In vitro*: higher cytocompatibility and differentiation in mBPC and dmBPC group; good antibacterial activity in mBPC; *In vivo*: induced greater bone formation of rabbit femur in mBPC and dmBPC group.	[176]
	MWCNTs	*In vitro*: increased cytocompatibility; improved surface roughness and hydrophilicity.	[177]
	n-HA, n-CS	*In vivo*: enhanced osseointegration ability of rabbit skull defect model in n-CS/PEEK group and n-HA/PEEK group.	[178]
	n-CS	*In vitro*: increased cytocompatibility; improve hydrophilicity; enhanced apatite formation in SBF.	[179]
PEEK and inorganic ion composites	ST sub-particles	*In vitro*: increased cytocompatibility and differentiation; enhanced compressive strength, surface roughness, thermal properties, hydrophilicity, surface energy, and protein adsorption.	[180]
	Nb_2O_5 sub-particles	*In vitro*: increased cytocompatibility and differentiation; no cytotoxicity; improved hydrophilicity, surface energy, surface roughness, and protein absorbability.	[181]
	Si_3N_4 particles	*In vitro*: increased cytocompatibility and differentiation; enhanced antibacterial ability.	[182]
	AMP	*In vitro*: increased cytocompatibility. Enhanced apatite formation in SBF; *In vivo*: enhanced osseointegration and bone formation of rat femur.	[183]
	Ta_2O_5	*In vitro*: increased cytocompatibility and differentiation; improved hydrophilicity, surface energy, roughness, and protein absorption.	[184]
	PLLA, β-TCP	*In vitro*: increased cytocompatibility and differentiation; *In vivo*: promoted bone formation and regeneration of rabbit radius.	[185]
	MD	*In vitro*: increased cytocompatibility and differentiation; *In vivo*: enhanced osteogenic properties of rabbit femur; increased expression of type I collagen and VEGF.	[186]
	M-MCS, GS	*In vitro*: Cytocompatibility and differentiation increased gradually in MPC, sandblasted MPC, and GS-loaded MPC; *In vivo*: Osteogenic ability was successively enhanced in the above three complexes.	[187]
	Ti particles	*In vitro*: increased cytocompatibility and differentiation.	[188]

N/A, not applicable.

Table 2
The advantages and disadvantages of some surface modification techniques.

Modification methods	Advantages	Disadvantages	Strategies for improvement
Sulfonation	Fast reaction time, suitable for materials of various shapes, increase surface roughness, low cost [124], antibacterial ability [82–86]	Residual acid needs to be removed [82,88], residual sulfonic acid groups can be harmful to cells [79–81]	Control reaction time for best advantage [78], mix with other bioactive fillers for increased cytocompatibility [203]
Plasma treatment	Can change the surface chemical properties and roughness of PEEK at the same time, with good uniformity and good reproducibility [29,108,109]	Long-term instability, the resulting high temperature may degrade PEEK [319,320]	Improve the cooling capacity of the device
Plasma-immersion ion Implantation	Coatings with strong adhesion, good uniformity, and good reproducibility [319]	The resulting high temperature may cause the PEEK to deform [319]	Improve the cooling capacity of the device
Accelerated neutral atom Beam	Ability to reduce surface roughness and shallow penetration compared to other processes [116,117,321,322]	Poor reproducibility and poor product stability [321]	Repeat multiple times to find suitable reaction conditions
Sandblasting	Cheap, simple, convenient, fast [323]	Contamination from abrasive aerosols [324,325], poor reproducibility [325]	Wear protective equipment to prevent inhalation of abrasives [324], repeat multiple times to find suitable reaction conditions

shown that plasma oxidation [42], acid oxidation [43], and ozone treatment [44] can activate the fiber surface to improve the fiber-matrix interface. However, these methods sacrifice single fiber strength and do not greatly improve mechanical properties [41]. Wolinne et al.

Table 3
Modification strategies to enhance the antibacterial activity of PEEK and its enhanced properties.

Modification strategy	Coatings or Fillers	Research results related to the bioactive or antibacterial property	Reference
Study on Surface Modification of Sulfonated PEEK	Concentrated sulfuric acid	*In vitro*: increased cytocompatibility and differentiation on samples with low sulfur content; showed excellent antibacterial activity on samples with different sulfur content *In vivo*: enhanced bone formation and killed pre-injected bacteria.	[82]
	Concentrated sulfuric acid	*In vitro*: biofilms are most effectively suppressed between 2 and 3 h of sulfonation.	[84]
	Concentrated sulfuric acid, argon	*In vitro*: increased cytocompatibility and differentiation of MG-63 cell; showed excellent antibacterial activity.	[85]
	Concentrated sulfuric acid, copper nanoparticles	*In vitro*: showed excellent antibacterial activity; increased phagocytic ability of macrophages; *In vivo*: showed excellent antibacterial activity.	[83]
Study on sulfonation of composite materials.	N-MS, concentrated sulfuric acid	*In vitro*: increased cytocompatibility and differentiation on PCPS; enhanced surface roughness, hydrophilicity, and apatite mineralization of PCPS; showed antibacterial activity on PCPS.	[203]
	Concentrated sulfuric acid, Ta, GS	*In vitro*: TPSG exhibits excellent antibacterial properties; increased cytocompatibility and differentiation of MG-63 cell; *In vivo*: enhanced bone regeneration and osseointegration	[86]
	NTP, concentrated sulfuric acid, GS	*In vitro*: Cytocompatibility and differentiation increased gradually in PN, SPN, and SPNG; showed excellent antibacterial activity on SPNG; *In vivo*: bone formation was successively enhanced in PN, SPN, and SPNG.	[205]
Coating antibiotics	$CaHPO_4{\cdot}2H_2O$, GS	*In vitro*: increased cytocompatibility and differentiation; had incredible antibacterial properties; *In vivo*: exhibited excellent antibacterial activity and osteointegration in femoral defect infection of rat experiments.	[211]
	GS, SF, AgNPs	*In vitro*: increased cytocompatibility and differentiation; had remarkable antimicrobial activity.	[212]
	Dexamethasone, minocycline, liposomes, PDA	*In vitro*: improved osteoblast differentiation; *In vivo*: enhanced anti-inflammatory properties, osteointegration, and antibacterial activity in beagle femoral implant models.	[215]
	GS, PDA	*In vitro* and *in vivo*: excellent osteogenic activity and antimicrobial properties	[213]
Coating antimicrobial peptides	Antimicrobial peptide KR-12, PDA	*In vitro*: increased cytocompatibility and differentiation; showed remarkable antibacterial activity; *In vivo*: promoted femoral osteointegration in rats.	[220]
	MBD-14, concentrated sulfuric acid	*In vitro*: increased cytocompatibility and differentiation; showed antibacterial activity; *In vivo*: enhanced the osteointegration ability of rat femur and inhibited bacterial growth.	[224]
Coating natural antibacterial materials	Sodium butyrate, concentrated sulfuric acid	*In vitro*: increased cytocompatibility, differentiation, and anti-inflammatory activity; *In vivo*: exhibited excellent anti-infective activity and promoted bone formation in a rat model of osteomyelitis.	[225]
	Chlorogenic acid, concentrated sulfuric acid	*In vitro*: increased cytocompatibility; exhibited excellent antimicrobial activity.	[226]
	CMC, CF, n-HA, BFP, PDA	*In vitro*: increased cytocompatibility and differentiation; showed antibacterial activity; *In vivo*: promoted tibial osseointegration in beagles.	[249]
Coating antimicrobial polymers	Lactam-based antibacterial membrane, concentrated sulfuric acid	*In vitro*: no toxicity for plankton growth; significantly inhibited bacterial growth	[241]
	Modified poly(ethylene glycol), quaternized poly(dimethylaminoethyl acrylate)	*In vitro*: no cytotoxicity; reduced bacterial adhesion.	[244]
Coating graphene oxide	Graphene oxide, concentrated sulfuric acid	*In vitro*: exhibits excellent antibacterial properties; increased cytocompatibility and differentiation of MG-63 cell;	[263]
	Graphene oxide nanosheets, PDA nanofilms, oligopeptides	*In vitro*: increased cytocompatibility and differentiation *In vivo*: promotes osseointegration of rabbit femur; powerful antibacterial phototherapy effect	[264]
Zinc-modified PEEK	ZnO, cicada-like bionic pattern layer	*In vivo*: effectively killed bacteria around the implant.	[275]
	Silver ions, zinc ions, concentrated sulfuric acid	*In vitro*: increased cytocompatibility, differentiation on Ag/ZnO modified sulfonated PEEK; inhibited bacterial growth on Ag and Ag/ZnO modified sulfonated PEEK.	[276]
	Zinc and oxygen, CF	*In vitro*: increased cytocompatibility and differentiation; exhibited strong antibacterial activity.	[277]
	Zinc oxide, graphene oxide, concentrated sulfuric acid	*In vitro*: have good biocompatibility, the obvious antibacterial effect	[278]
	Acrylic acid, zinc ions	*In vitro*: promoted the proliferation and differentiation of MC3T3-E1 cells, inhibited the growth of *S. aureus*	[279]
Silver-modified PEEK	Silver nanoparticles	*In vitro*: increased water contact angle; showed no cytotoxicity; improved the antibacterial activity.	[289]
	Silver nanoparticles	*In vitro*: increased cytocompatibility and differentiation; showed excellent antibacterial activity.	[290]
	Copper oxide microspheres, silver nanoparticles, silk fibroin	*In vitro*: promoted bone formation and angiogenesis; had significant antibacterial activity and prevented the formation of biofilm; *In vivo*: promoted the bone regeneration and osseointegration of rabbit tibia.	[291]
	Silver ions, ZIF-8, concentrated sulfuric acid	*In vitro*: showed excellent antibacterial activity.	[292]
Zirconium-modified PEEK	Zirconium ions, CF	*In vitro*: increased cytocompatibility and differentiation; showed obvious antibacterial activity.	[314]
Nitrogen-modified PEEK	Nitrogen	*In vitro*: increased cytocompatibility and differentiation; showed antimicrobial activity.	[317]

developed a vacuum plasma spray process and a laser shock adhesion testing protocol to produce and test the adhesion of coatings on PEEK. Fatigue test results showed that the coating remained uncracked for more than 10 fatigue tests [45]. This measurement scheme opens the way for

the systematic measurement of the adhesion of coatings on polymer substrates [45].

2.1.1.1. HA coating. The most commonly used bioactive material for PEEK surface coating is HA. In human and animal bones, HA occupies 69% of the weight. It has excellent biocompatibility in many forms [46]. Durham et al. used IBAD to coat PEEK with HA and yttrium-stabilized zirconia (YSZ). In the rabbit femur implantation experiment, microscopic CT, histology, and mechanics analyses showed that the HA/YSZ coating group had increased bone integration in comparison to the uncoated PEEK group [47]. PEEK implants and X-rays after implantation are shown in Fig. 4. Gultan et al. treated PEEK by NaOH etching and coating with boron-doped nano-hydroxyapatite (B-nHA). Cell experiments showed that the differentiation and proliferation of MC3T3-E1 cells were enhanced in the B-nHA-coated group. In addition, NaOH etching and B-nHA treatment increased ALP activity, COL1A1 mRNA expression, and collagen secretion. This suggests that B-nHA treatment, NaOH etching, or a combination of the two can enhance osteogenic activity [39]. Johansson et al. used a novel spin coating technique to coat PEEK with nanoscale HA. In animal experiments, they inserted treated and untreated PEEK implants into the tibia and femur of rabbits. Disassembly torque analysis indicates that the torque value of treated PEEK was markedly higher. They hypothesized it may have to do with changes in the bone mass around the HA-PEEK implant [48]. Johansson et al. investigated the bioactivity to PEEK with or without nano-scaled HA coating. They inserted the implant into the femur of the rabbits and performed a histological evaluation. The results showed that PEEK bone-implant covered with nano-HA had a higher contact rate and larger bone area at the healing point versus their uncoated counterpart. This indicates that HA-coated PEEK can significantly improve osteogenic properties [49].

2.1.1.2. Titanium or titanium dioxide coated PEEK. Pure titanium (Ti) and titanium alloys are the stars of orthopedic implants. Pure titanium and titanium alloy have good tolerance to the human body and strong binding ability to bone, so they are excellent implant materials [50]. However, some researchers have reported that titanium particles migrate to distant tissues and deposit in the lungs and lymph nodes years after implantation. This may lead to granulomatous disease [51–53].

Jung et al. developed a 3D printing device and constructed PEEK materials. Then they sputtered printed PEEK with Ti. The cell experiments showed that the PEEK sample modified by Ti had excellent performance in the proliferation and differentiation of preosteoblasts. Animal experiments demonstrated that bone regeneration of defective rabbit tibial was significantly increased with treated PEEK [54]. Hasegawa et al. investigated intervertebral fusion rates in Ti-coated PEEK(-Ti-PEEK) and pure PEEK cages after posterior lumbar interbody fusion (PLIF) surgery. During the operation, they randomly assigned patients to a pure PEEK group or Ti-PEEK group. They used computed tomography to assess fusion rates and patients were followed up one year later. The results of the Low Back Pain Assessment Questionnaire and Disability Index were as follows: PLIF with a Ti-PEEK fixator resulted in better end plate maintenance of bony fusion than PLIF with a pure PEEK fixator. They concluded that rigorous work and exercise can resume much earlier with Ti-PEEK cages [55]. Shimizu et al. modified the surface of PEEK using a sol-gel-derived TiO_2 coating. Before the sol-gel coating, they pretreated it with O_2 plasma or sandblasting and then treated it with acid. Experimental results of the rabbit tibia model indicated that the bone integration ability of modified PEEK was significantly enhanced. Moreover, the treated PEEK showed good biocompatibility with rabbit bone marrow mesenchymal stem cells [56]. Liu et al. grafted methacrylate hyaluronic acid and TiO_2 nanofibers onto PEEK by ultraviolet radiation induction. Cell experiments also showed good biocompatibility of

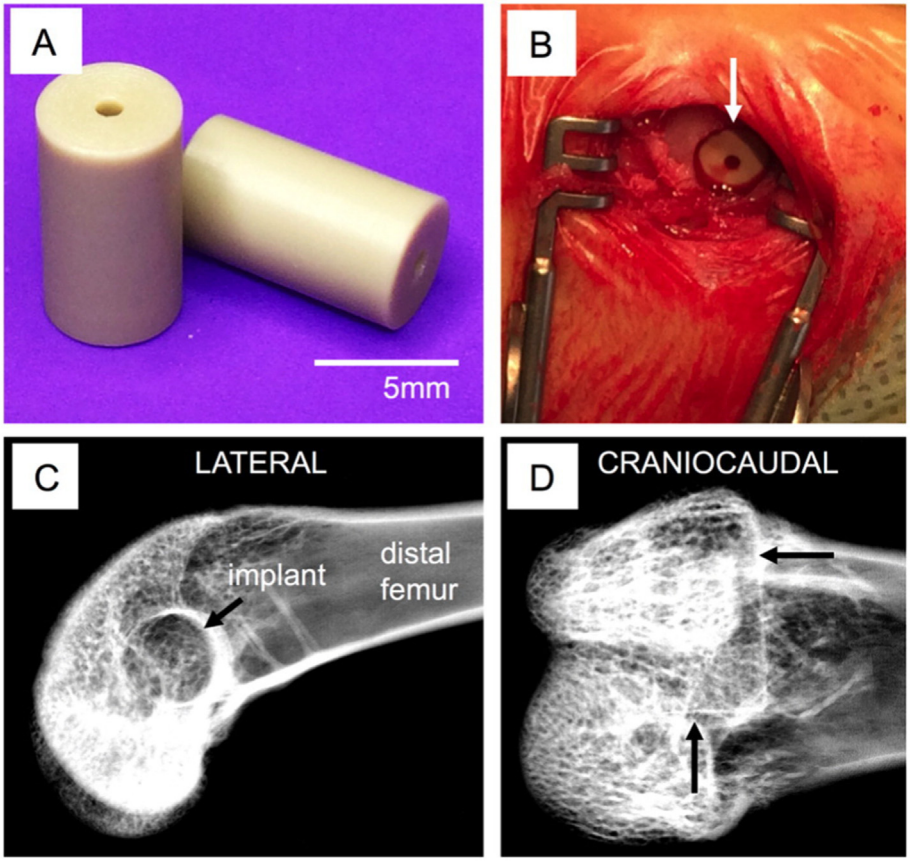

Fig. 4. (A) Size of PEEK implants. (B) Surgical site with an implant inserted. (C, D) X-rays after implantation (arrows indicate the defect boundaries) [47]; Reproduced with permission of Ref.

modified PEEK with rat bone marrow mesenchymal stem cells [57].

2.1.1.3. Other surface coatings. Researchers used a variety of biocompatible materials to coat the surface of PEEK, including silicate, magnesium phosphate, calcium phosphate, gelatin, proteins, zinc ions, and polymers. The biological activity of PEEK can be significantly improved by these surface coatings. For instance, Wen et al. used electron beam evaporation (EBE) to coat biologically active silicate on the surface of bioinert PEEK. The treated PEEK had good biocompatibility as well as the ability to promote the differentiation of bone marrow stem cells. Furthermore, they found that 5 min treatment with EBE had the greatest osteogenic potential by analyzing gene and protein expression. *In vivo* test results also showed that 8 min treatment with EBE improved osteointegration in rat models of osteoporosis. Overall, these results indicate that the application of a bioactive silicate coating to PEEK enhances osseointegration [58]. Ren et al. used microwaves to cover the PEEK surface with amorphous magnesium phosphate (AMP) coating. The apatite formation test showed that the modified PEEK significantly enhanced apatite formation in simulated body fluids (SBF). The cytotoxicity test verified that the modified PEEK had no cytotoxicity. When MC3T3-E1 cells were inoculated with modified PEEK, there was a significant increase in osteocalcin expression, suggesting that modified PEEK may promote osseous integration [59]. Oyane et al. created a laser-assisted biomimetic (LAB) technique to modify PEEK. LAB is performed by laser irradiation of PEEK substrate immersed in supersaturated calcium phosphate solution. After the LAB process, calcium phosphate formed on the surface of PEEK. *In vitro* experiments demonstrated that treated PEEK had good biocompatibility with MC3T3-E1 cells. A dense layer of hydroxyapatite also formed on the treated PEEK in the SBF [60].

Gelatin, a protein derived from collagen, mainly exists in bone and skin and has good biocompatibility, adhesion, and chemical stability [61,62]. However, the protein affinity of the PEEK surface is poor, and direct coating of gelatin on PEEK material cannot make gelatin adhere sufficiently. Omrani et al. modified the PEEK surface with oxygen plasma and then coated the PEEK with gelatin. The results showed that the gelatin-coated surface significantly promoted the adhesion and proliferation of mouse embryonic fibroblasts [63]. Wu et al. loaded BMP-2 onto phosphorylated gelatin. The gelatin was then coated on hydroxylated micro-porous PEEK. The water contact angle of the modified PEEK was significantly reduced. *In vitro* experiments showed that MC3T3-E1 cell adhesion, proliferation, and differentiation were significantly enhanced on modified PEEK [64]. Wang et al. sulfonated the PEEK surface with concentrated sulfuric acid to develop a three-dimensional porous morphology. Silk fibroin and bone formation peptide coating followed. Cellular tests revealed that cells on the modified implant had better cell adhesion, proliferation, and diffusion. Furthermore, peptide-modified fibroin coating resulted in accelerated differentiation and maturation of osteoblasts and osteoblast-like cells [65].

Cytokines released by immune cells are important factors in inducing bone tissue regeneration. Liu et al. used magnetron sputtering to add a layer of zinc ions to sulfonated PEEK (SPEEK) material. *In vitro* and *in vivo* experiments confirmed that Zn-coated SPEEK produces an anti-inflammatory phenotype in macrophages, which then secrete a component of osteoblasts to improve osseous integration [66].

Liu et al. covered PEEK with different layers of polystyrene sulfonate (PSS) and polyallylamine hydrochloride (PAH). They found that 20-layer (20 L) PEEK showed greater hydrophilicity than natural PEEK, and the surface contact angle decreased as the number of layers increased from 5 to 20. *In vitro*, modified PEEK resulted in superior adhesion and proliferation of bone marrow stromal cells, while inducing higher cell growth and alkaline phosphatase levels. *In vivo*, the binding of 20 L PEEK to bone tissue was significantly enhanced in a rabbit osteoporosis model when compared with untreated PEEK [67].

Eucommia is a traditional Chinese medicine that has therapeutic effects on bones [68]. Strontium is an indispensable element in the production of osteoblasts and osteoclasts [69–71]. The previously developed strontium Eucommia polysaccharide was shown to have quite superior biological activity and osteopromoting effect [72]. Zhang et al. introduced strontium Eucommia polysaccharide to the surface of PEEK. Cell experiments showed that the modified PEEK effectively promoted the proliferation and differentiation of MC3T3-E1 [73]. Chondroitin sulfate, a natural glycosaminoglycan, is one of the main components of the extracellular matrix [74,75]. Previous studies have shown that chondroitin sulfate has osteogenic activity [76]. Zheng et al. coated PEEK with strontium and chondroitin sulfate. The modified PEEK significantly improved its angiogenic and osteogenic abilities *in vitro* and *in vivo* [77].

2.1.2. Chemical treatment

2.1.2.1. Sulfonation modification. Sulfonation modification refers to using concentrated sulfuric acid or gaseous sulfur trioxide to react with PEEK for a short time. In doing so introduces-SO_3H groups to bind and form porous structures on the surface of PEEK. PEEK surface sulfonation allows for the retention of excellent mechanical properties. It is a special strategy to improve the osseointegration of PEEK implants by increasing hydrophilicity and roughness [78]. The bioactivity of sulfonated PEEK can be further enhanced by adding bioactive fillers. However, some studies have shown that the sulfur functional groups produced by sulfonation have negative effects on human cells [79–81]. Some studies have also shown that sulfonated PEEK also has antimicrobial activity [82–86], which will be later reviewed in Section 4.1.

PEEK has different surface properties when soaked in concentrated sulfuric acid at different times. Ma et al. explored the optimal sulfonation time and post-treatment method. Concentrated sulfuric acid was soaked for 0.5 min (SPEEK0.5), 1 min (SPEEK1), 3 min (SPEEK3), 5 min (SPEEK5), and 7 min (SPEEK7). Post-treatment methods included acetone flushing (SPEEKT1), hydrothermal treatment (SPEEK-T2), and NaOH immersion (SPEEK-T3). The treated samples were evaluated by scanning electron microscopy (SEM), energy dispersive spectroscopy (EDS), Fourier transform infrared (FTIR) spectra, hydrophilicity, ion release, and cell viability. The results revealed that 5 min sulfonation time was the best choice. Hydrothermal treatment, acetone rinsing, and NaOH immersion showed the same effect in removing residual sulfuric acid. A porous network structure formed on all the sulfonated samples. With the increase in sulfonation time and concentration, the porous structures became more obvious [59]. Wan et al. sulfonated PEEK using gaseous sulfur trioxide (SO_3) to create a porous surface. Mineral deposition of apatite significantly improved after the introduction of –SO_3H groups on the porous surface. Protein absorbability also greatly improved. MC3T3-E1 cells showed remarkably enhanced cell adhesion, proliferation, and extracellular matrix (ECM) secretion [87].

The three-dimensional porous structure formed by sulfonation can get better cell adhesion on the PEEK surface, the three-dimensional porous sulfonated PEEK preparation process is shown in Fig. 5 [88]. Yabutsuka et al. successfully prepared bioactive PEEK by forming pore-like structures on the material's surface. This was done through H_2SO_4 treatment, before O_2 plasma treatment, and the deposition of fine calcium phosphate particles in the pores. They dipped the modified PEEK in SBF liquid for a day and found that HA formed on the surface of the sample. Mechanical anchorage experiments show that the HA layer was closely bound to the PEEK substrate [69]. Zhu immersed PEEK in concentrated sulfuric acid to form a microporous structure, before hydrothermal treatment to reduce residual sulfuric acid. They then treated sulfonated PEEK with oxygen plasma and immersed it in a polydopamine (PDA) solution, giving rise to a PDA layer. Finally, it was immersed in the tripeptide Arg-Gly-Asp (RGD) solution to integrate the RGD onto PEEK's PDA surface coating. The biological properties were evaluated by cell proliferation, real-time reverse transcription polymerase chain reaction (real-time PCR) analysis, alizarin red staining, immunocytochemistry staining, and simulated body fluid immersion. The results showed that,

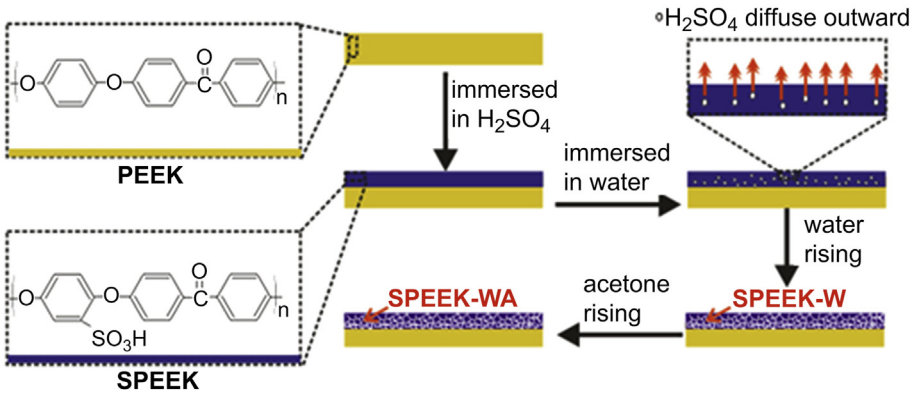

Fig. 5. Schematic diagram of the preparation of three-dimensional porous sulfonated PEEK. SPEEK-W: sulfonated PEEK after drying; SPEEK-WA: sulfonated PEEK rinsed with acetone [88]; Reproduced with permission of Ref.

compared with PEEK control, the modified version yielded significantly improved promotion of cell proliferation, osteogenic differentiation, and osteoid apatite formation *in vitro* [89].

Wang et al. made porous PEEK material by treating it with sulfuric acid. Subsequently, strontium (Sr) was incorporated into the sulfonated PEEK material by hydrothermal reaction in $Sr(OH)_2$ solution. Adiponectin (APN) protein membrane was deposited on the substrate with aid of PDA. *In vitro* experiments showed that proliferation and differentiation of MC3T3-E1 cells significantly increased by modified PEEK [90]. Cheng et al. proposed a strategy that combines sulfonation with alkali treatment. They first sulfonated PEEK-S-3 with 98% concentrated sulfuric acid for 3 min before treatment with NaOH for 24 h to get PEEK-NA-24. *In vitro* bioactivity tests showed that a uniform layer of bony apatite completely covered PEEK-NA-24 by immersion in SBF for only 3 days. Apatite deposition significantly reduced the contact angle of the sample (PEEK-HA) and increased its surface roughness, which resulted in enhanced serum protein adsorption. *In vitro* cell culture showed that the modified samples (PEEK-S-3, PEEK-NA-24, and PEEK-HA) all promoted the adhesion, proliferation, and differentiation of MC3T3-E1, while PEEK-HA had the best effect [91]. Sun et al. used a lyophilized technique to fix bone morphogenetic protein 2 (BMP-2) to sulfonated PEEK. They measured the amount of BMP-2 released from samples immersed in PBS (pH = 7.4) using a BMP-2 ELISA kit. The results show that BMP-2 can be consistently released from PEEK. Cell experiments *in vitro* showed that BMP-2 fixation significantly enhanced the initial adhesion and diffusion of rat bone mesenchymal stem cells (rBMSCs). In addition, PEEK enhanced collagen secretion, extracellular matrix mineralization, and ALP activity of rBMSCs [92]. Yu et al. submerged sulfonated porous PEEK in an aspirin solution and the resulting porous PEEK showed significantly improved anti-inflammatory activity. Subsequently, the grafting of bone-forming peptide (BFP) to porous PEEK greatly enhanced osteogenesis. They investigated the effect of BFP peptides on MC3T3-E1 cell proliferation and ALP activity, as well as the effect of aspirin on inflammation. The results showed that the combination of BFP polypeptide and aspirin can synergistically promote osteoblast proliferation and reduce inflammation [93].

Previous studies have shown that sulfuric acid and hydrogen peroxide solutions can synergistically increase the number of functional groups and increase the hydrophilicity and surface energy of PEEK [94–98]. Santos et al. treated PEEK with sulfuric acid and hydrogen peroxide solution for 60 s, and the experimental results showed that the modified surface promoted the adhesion and proliferation of human fibroblasts cells [99].

2.1.2.2. Phosphate modification. Phosphorylation refers to connecting phosphate groups to PEEK by various approaches, which can increase the biological activity of the material's surface. Zheng et al. introduced phosphate groups to the PEEK surface through single-step UV-induced graft polymerization of vinyl phosphonic acid. Water contact angle measurements show an increase in hydrophilicity after surface phosphorylation. Cell assay and real-time PCR analysis revealed that MC3T3-E1 osteoblasts exhibited enhanced adherence, diffusion, proliferation, and osteogenic differentiation on modified PEEK. *In vivo* biological assessments through animal models of proximal tibial defects in rabbits suggested that modified PEEK improved bone-implant contact. This indicated that the osteogenic activity of phosphorylated PEEK was enhanced [100]. Fukuda et al. prepared rough surface PEEK by sandblasting and modified the phosphate groups with phosphoryl chloride through chemical reactions. Cell experiments showed that the activity of rat mesenchymal stem cells growing on modified PEEK was significantly increased. The expression of osteocalcin and osteoid nodules were also much higher. Furthermore, the modified PEEK enhanced osseointegration in the rabbit tibial implant model [101]. Two years later, their research group modified PEEK by plasma treatment and phosphorylation. *In vitro* experiments demonstrated increased proliferation, alkaline phosphatase activity, and bone-like nodular formation of rat bone marrow stromal cells on phosphate-modified PEEK. In addition, phosphate-modified PEEK reduced the phenotypic polarization of RAW264.7 macrophages induced by LPS to an inflammatory phenotype. Animal experiments revealed that phosphate-modified PEEK exhibited greater pulling force from the femoral cavity than pure PEEK. Thus, they synthesized a new material that enhanced rBMSCs activity, reduced excessive inflammation, and improved PEEK's implant-bone bond strength [102]. Mahjoubi et al. used sandblasting and diazo chemistry to introduce phosphonate groups on PEEK's surface. Cell experiment results showed that modified PEEK improved metabolic activity and mineralization of MC3T3-E1 cells when compared with the unmodified version. Experiments on skull defects in rats demonstrated that fibrous sac formation was prevented by the modified PEEK. Osseointegration between the implant and the surrounding bone was also promoted [103].

2.1.2.3. Acid treatment. Previous studies have shown that fluoride ion surface modification can enhance osteoblast differentiation *in vitro* and osteointegration *in vivo* [104]. Huo et al. treated the PEEK surface with hydrofluoric acid and nitric acid (AFN) to obtain PEEK-AFN. The water contact angle test shows that the modified PEEK had enhanced hydrophilicity. Cell experiments showed that PEEK-AFN promoted adherence, proliferation, and proliferation of rBMSCs. PEEK-AFN also enhances alkaline phosphatase activity. In addition, PEEK-AFN regulates macrophage polarization and down-regulates the expression of pro-inflammatory factors by inhibiting the NF-κB pathway, hence stimulating osteoblast differentiation [105].

2.1.3. Physical treatment

2.1.3.1. Plasma treatment. Plasma modification is the bombardment of

the material surface by ionized gas in a closed container, and the atoms on the original material surface are replaced at the same time [106,107]. Plasma modification can roughen the surface of PEEK and increase the biological activity of PEEK while maintaining good mechanical properties [29,108,109]. Earlier in the article, it was mentioned that sulfonation modification can also increase the roughness of the PEEK surface. Since both modifications are performed on the PEEK surface, neither modification alters the mechanical properties of PEEK [29,87]. Regarding the effect of biological activity, the biological activity of the plasma-modified material depends on the type of plasma [110]. During the sulfonation process, the sulfonic acid groups were bound to the PEEK surface, and the PEEK surface formed a porous structure at the same time [78]. As mentioned earlier, cell adhesion will increase due to increased roughness. However, the sulfonic acid groups generated by sulfonation may adversely affect cells, and the higher the sulfur concentration on PEEK, the more obvious the adverse effect on cells [79–81]. This phenomenon may be improved by coating sulfonated PEEK or adding fillers. Fu et al. treated the PEEK surface with mixed hydrogen and oxygen plasma. They found that the modified PEEK's surface hydrophilicity, microhardness, crystallinity, and adhesion of human osteoblasts significantly improved [111]. Masamoto et al. developed a surface treatment “apatite precursor” (PRA) on PEEK to synthesize PRA-PEEK. The treatment consists of three steps: H_2SO_4 immersion, O_2 plasma discharge, and alkaline SBF treatment. In SBF immersion tests, PRA-PEEK showed excellent apatite formation capability. The mechanical, histological, and radiological analyses showed that PRA provided excellent bone-bonding properties and bone conductivity through the implantation of modified PEEK into rabbit tibia. MC3T3-E1 cell activity was analyzed by the XTT cell proliferation kit, and the modified PEEK did not show cytotoxicity [112]. Chen et al. modified PEEK by plasma immersion ion implantation (PIII) followed by hydrofluoric acid treatment. Compared with the unmodified PEEK, the hydrophilicity of modified PEEK was significantly increased. Cell experiments showed that modified PEEK enhanced the adhesion, proliferation, and ALP activity of rBMSCs [113]. Zhao et al. modified PEEK by water and ammonia PIII. *In vitro* experiments showed that the hydrophilicity and surface roughness of modified PEEK were greatly increased. They also found that MC3T3-E1 cell adhesion, proliferation, ALP activity, and osteogenic differentiation were improved. Furthermore, implantation of modified PEEK in the femur of rats also demonstrated enhanced osteosynthesis ability [29]. Lu et al. incorporated calcium onto the PEEK through calcium PIII (CA-PIII). Cell experiments showed that modified PEEK increased the adherence, proliferation, and differentiation ability of rBMSCs [114].

Injecting a low-temperature plasma induced in gas by an extreme ultraviolet beam into the polymer surface results in the formation of new chemical groups on the polymer surface. Czwartos et al. used extreme ultraviolet-induced oxygen and nitrogen plasma for surface modification of PEEK. The surface roughness of the modified PEEK is increased, and new functional groups are added at the same time. Moreover, the modified PEEK promoted the adhesion and proliferation of MG-63 cells [115].

2.1.3.2. ANAB treatment. ANAB bombardment of any material's surfaces can result in the amorphization of its atomic layer. ANAB can also change the surface morphology of the material. Current studies have shown that ANAB can alter the surface properties of biomaterials and increase their bioactivity, reducing surface roughness without degrading the overall mechanical properties [116,117]. Ajami et al. used ANAB to process PEEK. They found that ANAB treatment increased the surface hydrophilicity of PEEK. Cell experiments showed that modified PEEK increased the metabolic activity and proliferation in human mesenchymal stem cells, human osteoblasts, and skin fibroblasts. Osteogenic differentiation experiments showed that modified PEEK increased the ALP expression of human mesenchymal stem cells [118].

2.1.3.3. IBAD treatment. IBAD can synthesize special thin film materials that are difficult to obtain by conventional means. It can synthesize materials at low temperatures while providing advantageous characteristics like high density and strong adhesion [119]. Durham et al. used IBAD techniques to coat PEEK with YSZ and HA. YSZ is used as a protective layer, and HA is used as the top layer. Cell experiments showed that modified PEEK enhanced cell growth while also improving the maturation and mineralization of osteoblasts [120].

2.1.4. Nano-structured PEEK surfaces

Nanoscale modification is a new technology. This modification technique can avoid debonding coatings and material surfaces caused by conventional modification [121]. In addition, nanoparticles have a higher specific surface area than microparticles, forming a larger interface, which enhances the particle-matrix interaction [122].

Nanotopography, including grooves, pillars, and pores, is widely used in the field of bone tissue engineering [123–126]. Surface nanotopography is a physical topography that can affect osteogenesis in several ways (Fig. 6), including reorganizing the cytoskeleton [127] and affecting cell signaling and metabolism [128]. Zhang et al. established patterned nanorod arrays on PEEK surfaces. The modified nanosurface PEEK promoted the osteogenic differentiation of rat adipose stem cells and the osseointegration of rat femurs [129]. Gao et al. prepared an adhesive film with nanoscale porosity on PEEK. They first treated PEEK with oxygen plasma, followed by depositing poly(acrylic acid) (PAA) and PAH on the treated samples using the layer-by-Layer (LBL) self-assembly technique. *In vitro* experiments demonstrated that modified PEEK not only inhibited the acute inflammatory response of macrophages but also provided a favorable environment for osteogenic differentiation of

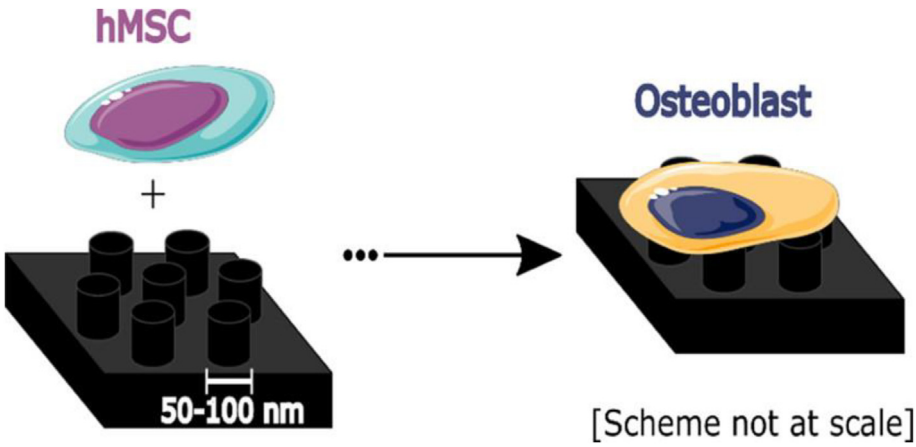

Fig. 6. PEEK surface nanotopography promotes osteoblast differentiation [123]; Reproduced with permission of Ref.

human bone marrow mesenchymal stem cells. *In vivo* results revealed that modified PEEK induced less fibrous sac formation and improved bone regeneration [130]. Wang et al. fabricated the porous surface of polyetheretherketone (PK)-nanoporous lithium-doped magnesium silicate (NLS) blend (PKNLS) on the PEEK surface by layer compression, sintering, and salt leaching. As a control, porous surfaces of PEEK/Lithium-doped magnesium silicate blends (PKLS) and PK were fabricated using the same method. *In vitro* results showed that compared with macroporous PKLS and PK, the surface porosity, water absorption, and protein absorption of PKNLS were significantly enhanced. The apatite mineralization capacity of PKNLS in simulated body fluids was also higher. These results indicate that PKNLS had excellent biological activity. Cell experiments showed that MC3T3-E1 cell adhesion, proliferation, and differentiation of PKNLS were significantly enhanced compared with PKLS and PK. *In vivo* results showed that new bone grew onto the surface of PKNLS, and the volume of new bone in PKNLS was the highest out of PKLS and PK [131]. Zhang et al. coated the surface of PEEK with a bioactive composite containing lithium-doped silica nanospheres (LSNs) and PDA. *In vitro* testing showed that compared with PEEK and PEEK coated with PDA, modified PEEK significantly promoted apatite mineralization and stimulation of rate bone marrow stromal cells (rBMSCs). *In vivo* experiments have shown that modified PEEK notably promotes bone tissue response [132]. Dai et al. created a bioactive coating of nano silicon nitride (Si_3N_4, Sn) with micro/nanostructure on PEEK (CSNPK) by suspension coating and melt bonding. Compared with pure PEEK, the surface roughness, hydrophilicity, and protein adsorption of CSNPK were greatly improved. Cell experiments showed that MC3T3-E1 cell adhesion, proliferation, differentiation, and bone-related gene expression on CSNPK were remarkably increased. In addition, microcomputed tomography and histological evaluation demonstrated that the SN coating of CSNPK stimulated bone regeneration and integration *in vivo* by using a rat model of skull defects [133].

Femtosecond laser (FSL) irradiation enables the formation of structures with nanotopography on the surface of biomaterials [134]. The advantages of FSL include simplicity, fast scanning speed, high accuracy, reproducibility, and minimal oxidation during processing [135]. Xie et al. constructed submicron nanostructures on PEEK surfaces by FSL. Cellular experiments showed that the adhesion, proliferation, and osteogenic differentiation of MC3T3-E1 cells were enhanced [136].

2.2. PEEK composites

In the surface modification of PEEK, due to the weak bonding strength between the coating and PEEK, the coating may separate from the PEEK surface, which significantly reduces the osteogenic activity of PEEK [56,59,103,137]. In addition, dislodged coating fragments may lead to bone resorption and subsequent implant failure [56,59,103,137]. In the past few decades, inorganic/organic biocomposites have been developed for bone repair by incorporating inorganic bioactive materials into organic polymers, which greatly improves the osteogenic activity of biocomposites [138,139]. Increasingly researchers have incorporated bioactive materials into PEEK to prepare PEEK composites, and compared with pure PEEK, the mechanical properties and bioactivity of PEEK composites have been improved.

2.2.1. CFR-PEEK composites

CF is widely used as a filler for reinforced polymers because of its high strength and high modulus. CFR-PEEK is often used as an orthopedic implant material due to its mechanical properties and close bone proximity. Yet recently, Some studies have shown that CFR-PEEK exhibits cytotoxicity when the carbon fiber content exceeds 25% of CFR-PEEK [21,22]. In detail, with the increase of carbon fiber content, the cytotoxicity of CFR-PEEK composites will become more and more obvious [22], and short carbon fibers have higher cytotoxicity than long carbon fibers [21]. While considering the excellent mechanical properties of CFR-PEEK, the addition of active fillers or surface modification may increase its biological activity. Below are examples of CFR-PEEK modification.

Injection molding is a fast and versatile manufacturing technique used in the plastics industry to produce objects of different sizes, and shapes [141]. Since this process involves high temperature and pressure, it can self-sterilize and facilitate the interaction of the dispersion with the polymer [142]. Qin et al. prepared CF-PEEK composites by injection molding and then treated them with concentrated sulfuric acid to form a porous structure. Subsequently, the sulfonated CF-PEEK composites were immersed in the GO solution to form filamentous wrinkles. The results of *in vitro* experiments showed that modified PEEK increased hydrophilicity. Cell experiments demonstrated that modified PEEK promoted adhesion, proliferation, alkaline phosphatase activity, and mineralization of bone marrow mesenchymal stem cells. Animal experiments showed that modified PEEK effectively promoted new bone formation [140]. The experimental program diagram is shown in Fig. 7. Yu et al. used plasma-enhanced chemical vapor deposition technology to modify CFR-PEEK with amino groups. Cell experiments showed that spreading, adhesion, proliferation and osteogenic differentiation of MG-63 cells were significantly increased on modified PEEK [143]. Ma et al. modified CFR-PEEK with nitric acid (HNO_3) and calcium chloride ($CaCl_2$). The hydrophilicity test showed that modified CFR-PEEK hydrophilicity was significantly improved. They soaked the treated samples in SBF and found that apatite formation capacity also increased [144]. Yan et al. coated graphene on CFR-PEEK. *In vitro* experiments showed that the graphene-modified version of CFR-PEEK increased proliferation and accelerated the differentiation of bone marrow stromal cells. Animal experiments demonstrated that the mineral deposition rate of graphene-modified CFR-PEEK implant was higher than that of bare CFR-PEEK. Through Van Gieson staining, they also found that there was a greater formation of new bone around the graphene-modified CFR-PEEK [145]. Miyazaki et al. soaked both pure PEEK and CFR-PEEK composites containing 30% CF in concentrated sulfuric acid, followed by ultrapure water, before drying. Lastly, they were immersed in a solution of $CaCl_2$. The modified CFR-PEEK in SBF had more apatite formation than the modified pure PEEK group and untreated pure PEEK [146]. Swaminathan et al. modified PEEK/HA composites using CF and carbon nanotubes (CNT). The cytotoxicity test demonstrated that their modified PEEK did not show cytotoxicity. Cell experiments showed that modified PEEK increased the adhesion of bone marrow cells when compared to binary PEEK/HA composites [147].

As mentioned earlier, CFR-PEEK can increase the elastic modulus of PEEK, and HA and GO can increase the surface bioactivity of PEEK. Combining the advantages of CFR-PEEK with HA and GO surface coating, Asante et al. sulfonated 30% CFR-PEEK and coated it with HA and GO. The experimental results showed that the modified PEEK improved hydrophilicity and *in vitro* bioactivity [148].

2.2.2. PEEK/HA composites

HA has excellent biocompatibility and bioactivity, allowing for use as a bone or tooth inducer. It has a certain degree of solubility in body fluid, releasing harmless ions to the surrounding tissue. HA can also participate in body metabolic processes and accelerate bone healing [149]. Since the surface-coated HA is only a thin layer, the surface coating with hydroxyapatite hardly affects the mechanical properties of PEEK. However, studies have shown that the surface coating may debond from the body [150]. Coating and bulk debonding on HA-coated PEEK have not been reported. For mechanical properties, by adjusting the amount of HA powder, the elastic modulus of HA powder injection molding PEEK is in the range of 4–16 GPa and the tensile strength is in the range of 49–83 MPa, which is close to human cortical bone tissue [151–153]. Recent studies have shown that PEEK mixed with HA whiskers can improve tensile and fatigue properties compared to conventional HA powders [154,155]. The elastic moduli of HA-PEEK reinforced with 0–50 vol% HA whiskers ranged from 4 to 23 GPa, and the tensile strengths ranged from 42 to 99 MPa [156]. In the future, it is also necessary to investigate

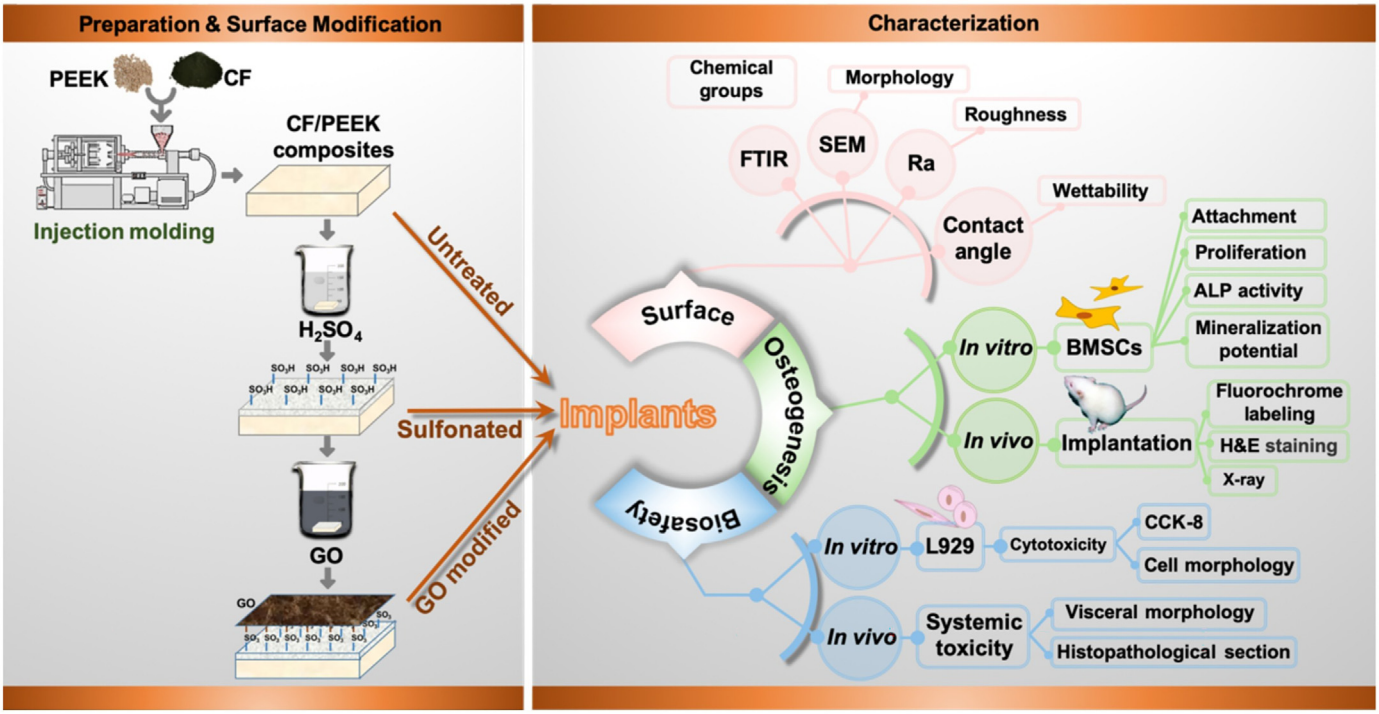

Fig. 7. Schematic diagram of preparation and characterization of graphene-coated sulfonated CF-PEEK [140]. Ra: Roughness average. Reproduced with permission of Ref.

whether the HA coating is easy to debond with PEEK bulk and compare the bioactivity of the two modification methods of HA surface coating and melt blending.

Oladapo et al. synthesized PEEK-HA composites by adding HA particles into PEEK materials. *In vitro* experiments showed that PEEK/HA composites improved cell adhesion, proliferation, and differentiation in comparison to pure PEEK. Furthermore, PEEK/HA composites improved apatite formation in SBF [157]. Walsh et al. used ovine animal models to evaluate whether PEEK and HA composites improved bone growth and fusion. They found that compared with pure PEEK, the composite improved cervical fusion and provided a better environment for bone growth [158]. Shuai et al. added HA to a PEEK/polyglycolic acid (PGA) mixture, then synthesized (PEEK/PGA)-HA composites by laser sintering. They dipped (PEEK/PGA)-HA composites into SBF and found that (PEEK/PGA)-HA increased apatite formation. Cell experiments showed that (PEEK/PGA)-HA significantly increased the adhesion and proliferation ability of MG-63 cells when compared with PEEK/PGA. This indicates that the addition of HA can increase composite biocompatibility [159].

2.2.3. 3D printing of PEEK composites

3D printing can produce bespoke products that are well suited to orthopedic implants. In the past decade, 3D printing technology has developed rapidly within the biomedical engineering discipline. 3D printing technology can now create new types of engineered bone tissue implants with custom shapes and more favorable macro-and microscopic structures [160]. Han et al. used fused-filament fabrication (FFF) 3D printing to produce PEEK, which was then polished and sandblasted. Cell assay results showed that human osteosarcoma cells (SAOS-2 osteoblasts) exhibited increased adhesion, proliferation, and osteoblast density on untreated FFF-3D-printed PEEK versus the polished and sandblasted groups [161].

Fused Deposition Modeling (FDM), also known as FFF, is one of the most widely used 3D printing processes. Compared with the traditional injection molding process, it has the advantages of a simplified process, timeliness, lower cost, and easier customization [162,163]. In the same year, their research group utilized FDM 3D printing techniques to print pure PEEK and CFR-PEEK composites. They also used polishing and sandblasting methods to modify the sample surface. Cell experiments showed that L929 fibroblast density of printed PEEK and CFR-PEEK samples without polishing and sandblasting were significantly higher than that of polished and sandblasting samples. Cytotoxicity tests showed that pure PEEK and CFR-PEEK composites with or without polishing and sandblasting were not cytotoxic [164]. The reason why CFR-PEEK did not show cytotoxicity in this study is that the content of carbon fiber is only five percent of CFR-PEEK. In previous studies [21,22], CFR-PEEK exhibited cytotoxicity because CFR accounted for more than 25% of the CFR-PEEK content.

Introducing a three-dimensional porous structure into PEEK material can provide space for bone ingrowth, which will enhance the bonding strength of the bone implant [165,166]. Magnesium ions can promote angiogenesis [167,168] and accelerate osteogenesis [169–171]. Wei et al. fabricated porous PEEK scaffolds by the FDM technique. The magnesium ion-chelated PDA was then coated on the porous PEEK scaffold. *In vitro* results showed that the activated surface promoted the proliferation, adhesion, and differentiation of MC3T3-E1 cells. At the same time, magnesium ions released by the graft promoted angiogenesis. Rabbit femur implantation experiments also showed that modified PEEK significantly promoted osseointegration [172].

However, 3D printing also has some disadvantages. First, the layer-by-layer approach of 3D printing leads to anisotropy, which causes materials with different mechanical properties in different directions. Second, 3D printing technology requires laboratories to be equipped with digital file acquisition equipment and CAD software, which increases the cost of 3D printing technology. Third, 3D printing requires sophisticated technology, expensive material costs, and time-consuming post-processing. A lack of trained operators may also hinder the application of 3D printing in medicine [173].

In clinical applications, 3D scanners and CT will be better integrated with 3D printing technology, which can simplify the production process, reduce labor costs and make products more accurate [174]. In addition to this, virtual reality (VR) designs can interact with 3D printing technology

in the field of orthopedics. For example, individuals can design 3D printing data directly in VR to better estimate product viability and reduce wasted time and resources [173].

2.2.4. PEEK nano-composites

By adding nanomaterials to PEEK, it is possible to change the biological inertia of PEEK itself and improve its biological activity. As mentioned earlier, nanoparticles have a higher specific surface area than microparticles, which can enhance particle-matrix interaction [122]. LV et al. mixed molybdenum disulfide (MoS_2, MS) nanosheets into PEEK to produce MS/PEEK composite material (MPC). The hydrophilicity test showed that the surface roughness and hydrophilicity of the MPC increased. In addition, cell culture experiments showed that adhesion and proliferation of MPC on rat bone marrow stromal cells increased, indicating good cytocompatibility [175]. Zhang et al. fabricated macro-microporous bone implants (mBPC) with nano-bioglass (NBG) and PEEK using a sol-gel method and cool-pressed sintering and particle leaching. They then added the hinokitiol (HK) drug to mBPC (dmBPC). Antibacterial experiments found that dmBPC possessed excellent antibacterial activity against *Staphylococcus aureus in vitro*. Compared with macroporous NBG/PEEK Composite (BPC) and macroporous PEEK (MPK), mBPC and dmBPC significantly promoted the proliferation and ALP activity of MC3T3-E1 cells. In animal experiments, microscopic CT and histological evaluations revealed that both mBPC and dmBPC induced greater new bone formation than MPK and BPC. Immunohistochemical analysis showed that BMP-2 expression levels increased in mBPC and dmBPC in comparison with MPK and BPC [176]. Cao et al. prepared multi-walled carbon nanotubes (MWCNTs)/PEEK composites by co-precipitation and injection molding techniques. The roughness and hydrophilicity of the synthesized composites were increased. Cell experiments showed that the adhesion and proliferation of MC3T3-E1 osteoblasts on the synthesized composites were also increased [177]. Ma et al. prepared nano-hydroxyapatite PEEK (n-HA/PEEK) and nano-calcium silicate PEEK (n-CS/PEEK) composites using composite and injection molding techniques. Through a rabbit skull defect model, both n-CS/PEEK and n-HA/PEEK promoted osseointegration more than pure PEEK [178]. Tang et al. used the injection-molding machine to synthesize nano-calcium silicate (n-CS)/PEEK composite material. The surface of the n-CS/PEEK composite was treated with sandpaper and sandblasting. The hydrophilicity test showed that the surface treatment significantly increased hydrophilicity. Assessment of apatite formation demonstrated that the mineralization of treated n-CS/PEEK is significantly enhanced in SBF. Furthermore, cell experiments showed that treated n-CS/PEEK remarkably promoted attachment, proliferation, and differentiation of MC3T3-E1 cells when compared with the untreated material [179].

2.2.5. PEEK and inorganic ion composites

The incorporation of inorganic ions in PEEK may increase its biological activity. The following studies outline recent developments in the area. Ren et al. synthesized cubic sodium tantalate (ST) submicron particles by a hydrothermal method. They then prepared ST/(PEEK) composites (TPC) by melting and blending. *In vitro* results showed that the compressive strength, surface roughness, thermal properties, hydrophilicity, surface energy, and protein adsorption of TPC were significantly enhanced compared to pure PEEK. Cell experiments showed that adhesion, proliferation, and differentiation of rBMSCs on TPC were greatly promoted [180]. Ge et al. synthesized niobium pentoxide (Nb_2O_5) submicron-particles by sol-gel method. Then PEEK/Nb_2O_5 composites (PNC) were fabricated by pressing and sintering. *In vitro* experiments showed that in comparison with PEEK, the hydrophilicity, surface energy, surface roughness, and protein absorbability of PNC composites were improved. Cytotoxicity tests showed that PNC had no adverse effects on cell proliferation and morphology. Furthermore, adherence, proliferation, and osteogenic differentiation of rBMSCs on PNC were also higher than normal PEEK [181]. Pezzotti et al. incorporated Si_3N_4 particles into PEEK by melting and blending. Antibacterial experiments showed that the growth of live Staphylococcus epidermidis was greatly reduced on PEEK/Si_3N_4 composites versus normal PEEK. *In vitro* experiments showed that human osteosarcoma cell proliferation and differentiation were significantly enhanced by the composite [182]. Sikder et al. synthesized the AMP-PEEK complex by melting and mixing PEEK with novel AMP particles. They dipped AMP-PEEK into SBF liquid and found that the apatite formation was significantly higher in comparison to pure PEEK. Cell experiments found that the adhesion and proliferation of MC3T3-E1 cells on the AMP-PEEK composite were also increased. Femoral implantation experiments in rats showed that the AMP-PEEK composite had higher osseointegration and new bone formation compared with pure PEEK [183]. Mei et al. synthesized PEEK/Ta_2O_5 composites (PTC) by mixing tantalum pentoxide (Ta_2O_5) into PEEK via cold press sintering and then sandblasting to roughen the surface. *In vitro* experiments demonstrated that surface hydrophilicity, energy, roughness as well as protein adsorption of the composite were all improved. The adhesion, proliferation and osteogenic differentiation of BMSCs on the composite were also significantly increased [184]. Feng et al. mixed poly(L-lactide) (PLLA) powder and β-tricalcium phosphate (β-TCP) powder into PEEK and prepared PEEK/β-TCP/PLLA composite by laser sintering. Cell culture experiments showed that PEEK/β-TCP/PLLA composite promoted osteoblast adhesion, proliferation, and differentiation. *In vivo* experiments, microscopic CT, X-ray, and histological evaluations found that PEEK/β-TCP/PLLA composites remarkably promoted bone formation and regeneration [185]. Cai et al. mixed mesoporous diopside (MD) into PEEK and produced macro-mesoporous PEEK/MD (PM) composites using cold-press- and salt-leaching. Cell experiments showed that the macro-mesoporous PM composite promoted the adhesion, proliferation, and osteogenic differentiation of MC3T3-E1 cells. In rabbit femur defects, porous PM composites significantly enhanced osteogenic properties. In addition, immunohistochemistry showed higher expression of type I collagen and vascular endothelial growth factor (VEGF), suggesting that macro-mesoporous PM greatly enhances osteogenic potential and vascularization [186]. Half a year later, Cai et al. synthesized mesoporous magnesium calcium silicate (M-MCS)/PEEK composite (MPC) by cold pressing and sintering, before roughening the surface by sandblasting. They then loaded genistein into nanopores of the sand-blasted MPC. The findings were that compared with MPC, surface roughness and hydrophilicity of sandblasted MPC significantly increased. Apatite mineralization in SBF solution was also enhanced. Cell experiments showed that adhesion, proliferation, and differentiation of MC3T3-E1 cells increased. In comparison with the first two complexes, genistein-loaded MPC promoted higher cell adhesion, proliferation, and differentiation. In beagle dog femur defect experiments, the osteogenic ability of the materials was as follows in increasing order, MPC, sandblasted MPC, and genistein-loaded MPC [187]. Jung et al. fabricated PEEK and titanium particle composites by compression molding. They tested titanium particles in a range of 0 vol% to 60 vol%. The mechanical tests demonstrated that the compressive strength and stiffness of the composites increased with titanium content. Furthermore, the adhesion, proliferation, and differentiation of MC3T3-E1 cells on the composite material were significantly improved [188].

3. Anti-infective function

In orthopedic surgery, implants in the body are highly susceptible to infections, which is a major cause of implant failure [189]. The incidence of surgical area infections is steadily increasing, with estimates ranging from 2.1% to 8.5% in instrumental procedures [190]. The researchers estimate the additional cost per infected patient to be as high as $100,000 [191]. This leads to increased morbidity and mortality and increased global healthcare costs [192]. Surgical area infection remains a serious challenge in orthopedics. Some studies have shown that *S. aureus* is the most common pathogen after orthopedic surgery, followed by *E. coli* [193]. The bacteria are presumed to have come from the skin near the

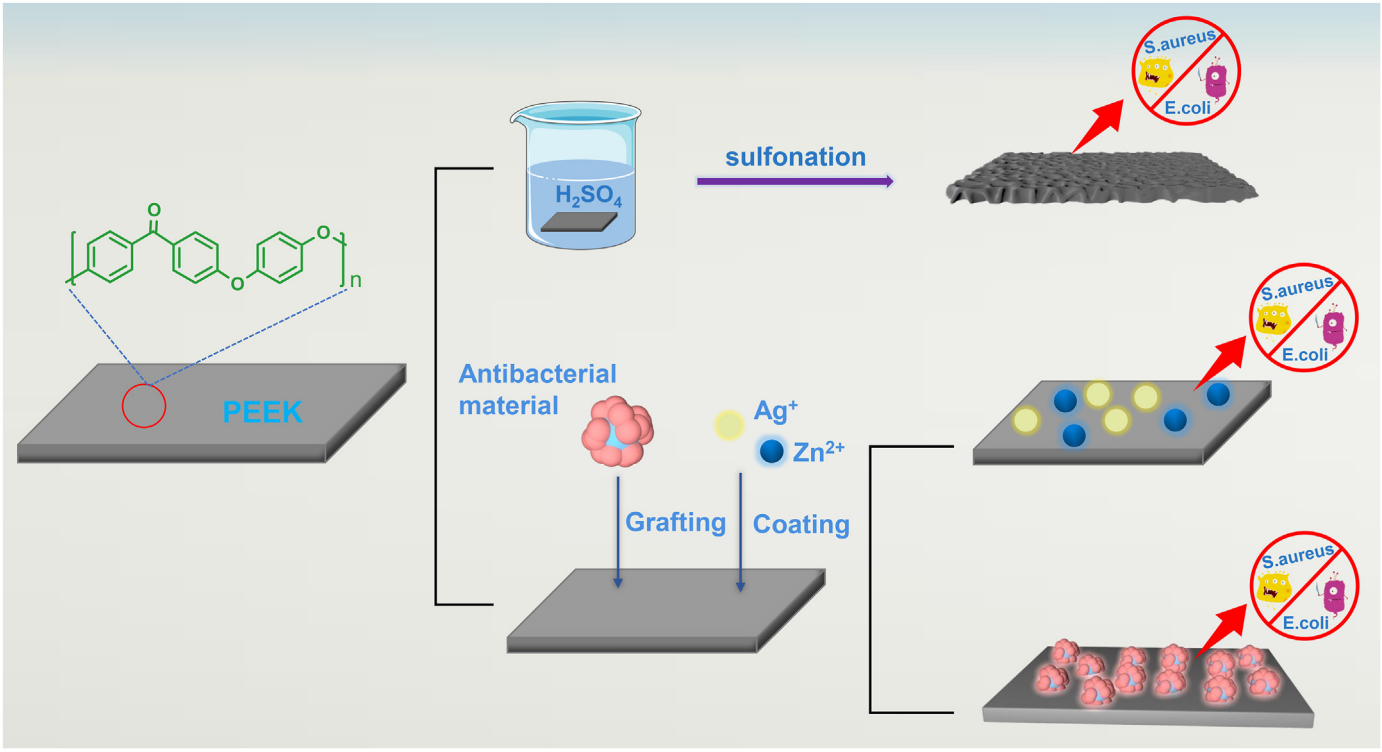

Fig. 8. Modification strategies of PEEK to improve antibacterial property.

surgical site [194]. Studies have also shown that infection rates are 28% higher in patients with implants than in those without because the surfaces of implants provide a convenient place for bacteria to grow and biofilm to form [195]. The infection is particularly difficult to control because biofilm bacteria are highly resistant to antibiotic treatment [196,197]. Therefore, it is of great significance to develop implant materials with antibacterial properties and osteogenic ability [198]. The methods of enhancing PEEK antimicrobial performance include sulfonation treatment, coating antibiotics/antimicrobial peptides/antimicrobial polymers, coating metal nanoparticles, etc. (Fig. 8, Table 3).

3.1. Study on antibacterial activity of sulfonated PEEK

3.1.1. Study on surface modification of sulfonated PEEK

Concentrated sulfuric acid can corrode PEEK and form three-dimensional morphology on PEEK [199]. This process is called sulfonation. The three-dimensional porous structure formed by sulfonation can get better cell adhesion on the PEEK surface [88]. A previous study showed that sulfur-containing compounds have excellent bactericidal properties [200]. Sulfonated PEEK disrupts bacterial cell membranes to achieve bactericidal effects [82]. Ouyang et al. sulfonated PEEK with concentrated sulfuric acid and adjusted the temperature to obtain different sulfur concentrations. *In vitro* cell proliferation and real-time PCR analysis showed increased proliferation and osteogenic differentiation of rBMSCs on samples with low sulfur content. *In vitro* antibacterial evaluation demonstrated that sulfonated samples with different sulfur concentrations all had excellent antibacterial activity against *S. aureus* and *E. coli.* Rat femoral implantation experiment showed that sulfonated PEEK not only killed the pre-injected bacteria but also enhanced new bone formation [82]. Montero et al. tested the effects of PEEK with different sulfonation times on biofilm growth. Biofilm evaluation found that sulfonation times between 2 h and 3 h were most effective in inhibiting growth [84]. Wang et al. prepared PEEK with layered micro/nano morphology by simple sulfonation combined with argon plasma treatment. PEEK showed good antibacterial activity *in vitro*. Cell adhesion experiments showed that PEEK improved MG-63 cell adhesion, proliferation, and osteogenic differentiation [85]. Liu et al. used custom magnetron sputtering technology to fix copper nanoparticles on the sulfonated PEEK surface. In vitro and *in vivo* antibacterial experiments showed that sulfonated PEEK showed good antibacterial activity against MRSA, and the sulfonated PEEK mixed with copper could play a better bactericidal role. Meanwhile, macrophages cultured on the modified PEEK could be polarized into a pro-inflammatory phenotype, which could improve the ability of macrophages to phagocytose MRSA [83].

3.1.2. Study on sulfonation of composite materials

Although the mechanical properties and bioactivity of PEEK composites containing bioactive fillers were improved, most of the bioactive fillers were dispersed into the PEEK matrix and did not significantly improve the surface bioactivity because only a few bioactive materials were exposed on the surface [201,202]. The surface properties (such as chemical composition and morphology) of non-degradable biomaterials for permanent implantation in the human body have a crucial impact on their biological properties [201]. Therefore, some researchers sulfonated PEEK complexes to further improve osteogenic activity and antibacterial activity. Niu et al. synthesized PEEK/nano-magnesium silicate (PEEK/n-MS) composites (PC), which were subjected to surface treatment by particle impact (PCP), before modification with concentrated sulfuric acid (PCPS). The surface roughness, hydrophilicity, and apatite mineralization of PCPS were greatly enhanced compared with PC and PCP. Antibacterial experiments showed that PCPS had antibacterial activity against *E. coli* and *S. aureus.* Cell culture experiments also found that the adhesion, proliferation, and differentiation of rBMSCs on PCPS were improved [203].

In recent years, tantalum (Ta) biomaterials have been increasingly used in bone repair due to their good biocompatibility and osteogenic activity [204]. Luo et al. prepared Ta/PEEK composite material (TP) by blending Ta nanoparticles with PEEK and then treated with concentrated sulfuric acid to form a microporous surface containing Ta particles on TP (TPS). Genistein, which has antibacterial properties, was then loaded onto the microporous surface of TPS (TPSG). Due to the presence of sulfonic groups, TPS showed low antibacterial performance, while TPSG

showed excellent antibacterial performance. In addition, compared with TP, TPS significantly promoted the adhesion and proliferation of MG63 cells *in vitro*, while TPSG and genistein significantly induced osteogenic differentiation of MG63 cells. *In vivo* experiments showed that TPS promoted new bone regeneration and bone integration compared with TP, while TPSG further enhanced bone regeneration and bone integration *in vivo* [86]. Mei et al. prepared PEEK/nanoporous tantalum pentoxide (NTP) composite (PN) by sol-gel method and cold press-sintering. PN was treated with concentrated sulfuric acid to form SPN. They then added genistein to the SPN surface forming SPNG. *In vitro* antibacterial experiments showed that SPNG had excellent antibacterial activity due to the synergistic effect of both the sulfonic acid (SO_3H) group and the continuous release of genistein. Cell experiments demonstrated that when compared with PN, the adhesion, proliferation, and osteogenic differentiation of rBMSCs on SPN and SPNG were enhanced. In animal experiments, SPN and SPNG had greater bone formation than PN [205].

Notwithstanding the above studies showed that sulfonated PEEK had excellent osteogenic and antibacterial properties. However, it has been reported that the sulfur functional groups produced by sulfonation have negative effects on human cells [79–81]. For example, low-valence sulfur compounds may produce oxygen free radicals that damage cells [79]. Researchers need more *in vitro* and *in vivo* studies to study the safety of sulfonated PEEK.

3.2. Coating antibacterial material

3.2.1. Coating antibiotics

Intra-wound antibiotic powders have been used in many orthopedic procedures [206], which also minimize systemic exposure and side effects [207]. Although the use of intrawound antibiotic powder is effective in killing bacteria, it has potential adverse effects, including antibiotic resistance [208], circulatory collapse, and decreased bone healing [209]. However, combining antibiotics and bone repair materials, such as demineralized bone matrix (DBM), into implants gives the best of both worlds [209]. Gentamicin sulfate (GS) is widely used in orthopedic surgery due to its broad-spectrum antibacterial activity [210]. Xue et al. coated PEEK with layers of $CaHPO_4{\cdot}2H_2O$ (CAP) containing GS to obtain PEEK/CAP-GS. This was done via an LBL deposition method. *In vitro* antibacterial experiments showed that PEEK/CAP-GS samples had incredible antibacterial properties. Cell experiments demonstrated that PEEK/CAP-GS had good biocompatibility with MG-63 cells and enhanced osteogenic differentiation. Animal experiments involving rat femoral defects again revealed that PEEK/CAP-GS exhibited excellent antibacterial activity, as well as better osteointegration [211]. Yan et al. coated porous PEEK's surface with silver nanoparticles (AgNPs) bound to silk fibroin (SF)/GS. Antimicrobial experiments found that the modified PEEK had remarkable biocidal activity against Gram-positive and Gram-negative bacteria. Cell experiments showed that MC3T3-E1 cells exhibited increased adhesion, proliferation, and differentiation on modified PEEK compared with bare PEEK [212]. Sun et al. grafted GS on sulfonated PEEK using the self-polymerization of dopamine technique. The modified PEEK exhibited excellent antibacterial and osteogenic activities *in vitro* and *in vivo* [213]. Yin et al. developed a multifunctional PEEK with triple antitumor, antibacterial, and osteogenic effects. They coated MXene nanosheets, gelatin methacrylate (GelMA) hydrogel, and tobramycin on sulfonated PEEK. Under near-infrared irradiation, the modified PEEK can kill osteosarcoma cells. Meanwhile, the tobramycin coating showed strong *in vitro* antibacterial properties. In vivo and *in vitro* experiments showed that this multifunctional PEEK has excellent osteogenic ability [214]. The researchers did not individually evaluate the antibacterial ability of sulfonated PEEK [214]. Xu et al. immobilized dexamethasone plus minocycline-loaded liposomes (Dex/Mino liposomes) on the PEEK surface with PDA. Cell experiments showed that human mesenchymal stem cells had improved osteoblast differentiation on the modified PEEK in comparison with bare PEEK. *In vivo* experiments demonstrated that modified PEEK had excellent antibacterial activity. Furthermore, the Dex/Mino liposome coating enhanced the anti-inflammatory and osteointegration properties of the implant through subcutaneous foreign body reactions and beagle femoral implant models [215].

3.2.2. Coating antimicrobial peptides

Antimicrobial peptides (AMPs) have broad-spectrum and powerful antibacterial abilities [216]. They can exert antibacterial effects on various microorganisms including drug-resistant microorganisms [217]. Some studies have pointed out that antimicrobial peptides also have the dual effects of eliminating biofilms and immunomodulatory attenuating inflammatory responses [218,219]. Meng et al. coated PEEK's surface with the antimicrobial peptide KR-12 and PDA. *In vivo* and *in vitro* antibacterial experiments showed that the coated PEEK had significantly enhanced its antibacterial activity against *S. aureus* (ATCC 25923) versus unmodified PEEK. Cell experiments demonstrated that modified PEEK greatly enhanced adherence, proliferation, and osteogenic differentiation of rBMSCs. Animal experiments showed that PEEK with KR-12 coating also promoted femoral osteointegration in rats [220]. Mouse beta-defensin-14 (MBD-14) is a natural antimicrobial peptide with similar broad-spectrum activity against Gram-positive, Gram-negative, multidrug-resistant bacteria, fungi, and viruses [221–223]. Yuan et al. coated mouse MBD-14 on a sulfonated PEEK surface. *In vitro* antibacterial experiments showed that modified PEEK had increased antibacterial activity against *S. aureus* and *Pseudomonas aeruginosa*. Furthermore, the proliferation and osteogenic differentiation of rBMSCs on modified PEEK were also enhanced. In an infected rat femur model, modified PEEK enhanced the osteointegration ability of the rat femur while successfully inhibiting bacterial growth [224].

3.2.3. Coating natural antibacterial materials

Some natural antibacterial materials have remarkable antibacterial properties, such as butyrate [225], and chlorogenic acid [226]. Some researchers modified PEEK with these natural antibacterial materials and achieved excellent antibacterial properties and osteogenic activity.

Butyrate is involved in a variety of biological processes and exerts anti-inflammatory, antibacterial, and immunomodulatory effects [227–230]. Several studies have shown that butyrate can increase the secretion of reactive oxygen species (ROS) from macrophages and enhance the phagocytic capacity of macrophages [231–233]. Yang et al. loaded sodium butyrate onto porous sulfonated PEEK. The study found that in the presence of bacteria, the phagocytic activity of macrophages increased with the concentration of sodium butyrate by generating ROS. After bacterial clearance, the modified PEEK could polarize macrophages to the M2 phenotype and then stimulate anti-inflammatory cytokine secretion. Therefore, sodium butyrate has a dual role here. In addition, the modified PEEK increased the expression of osteogenic genes and proteins in rBMSCs. In a rat model of osteomyelitis, the modified PEEK exhibited excellent anti-infective activity and promoted new bone formation [225].

Chlorogenic acid, extracted from plants such as honeysuckle, is an ester compound (consisting of caffeic acid and quinic acid) with anti-inflammatory and antioxidant effects [234]. Besides, it is a non-toxic natural product with excellent antibacterial properties [235,236]. He et al. used grafted peptide hydrogels system to load chlorogenic acid onto sulfonated PEEK surfaces. Cell experiments showed that MC3T3-E1 cells exhibited enhanced adhesion and proliferation on the modified PEEK. Furthermore, the modified PEEK exhibited excellent antimicrobial activity against both Gram-negative and Gram-positive bacteria due to chlorogenic acid release [226]. In this study, the authors did not separately study the antibacterial activity of sulfonated PEEK [226].

3.2.4. Coating antimicrobial polymers

Several studies have shown that some synthetic lactams, which are structurally similar to furanones [237–239], are active against biofilms of *Enterococcus faecalis*, *Pseudomonas aeruginosa,* and *Staphylococcus*

epidermidis [238,240]. Montero et al. sulfonated PEEK and then combined it with a new lactam-based antibacterial membrane compound. The antibacterial experiments showed that the morphology of *Streptococcus mutans* on sulfonated PEEK was slightly changed, and the growth of *Streptococcus mutans* on the surface of sulfonated PEEK containing the antibacterial film was significantly reduced. Analysis of plankton growth showed that sulfonated PEEK containing the antibacterial film was not toxic [241]. Previous studies have shown that PEEK grafted with antifouling polymer has an antibacterial effect [242,243]. However, some experts believe that grafting antibacterial polymers alone usually only temporarily reduces the number of bacteria that cling to the implant's surface [244]. Buwalda et al. grafted an antifouling polymer (modified poly(ethylene glycol)) and a bactericidal polymer (quaternized poly(-dimethylaminoethyl acrylate)) onto PEEK using UV photo insertion. Antimicrobial experiments showed that the adhesion of *S. aureus* on the PEEK surface was significantly reduced. The cytotoxicity test showed that PEEK was not cytotoxic after modification [244].

Carboxymethyl chitosan (CMC) is a water-soluble chitosan derivative with good biocompatibility, non-immunogenicity, and antibacterial properties, which has a wide range of applications in the biomedical field [245]. In addition, CMC also possesses osteogenic properties [246–248]. Xu et al. synthesized carbon fiber reinforced PEEK/nano-hydroxyapatite (CFR-PEEK/n-HA) composites through a process of compounding and injection-molding. They then grafted CMC and bone-forming peptide (BFP) covalently with PDA. Antimicrobial experiments demonstrated that the modified PEEK significantly inhibited bacterial adhesion of *S. aureus*. While cell culture experiments showed that modified PEEK increased adhesion, proliferation, and osteogenic differentiation of human mesenchymal stem cells more than unmodified PEEK. Animal studies also revealed that the modified PEEK material promoted tibial osseointegration in beagles [249].

3.2.5. Coating graphene oxide

Graphene oxide (GO), an important graphene derivative, contains a large number of reactive oxygen functional groups [250]. GO can significantly improve its interaction with proteins through hydrophobic and electrostatic interactions [251,252], and promote osteogenic differentiation [253]. In addition, GO nanosheets have obvious antibacterial ability against Gram-negative and Gram-positive bacteria [254]. GO has been widely used in various biotechnologies such as nanoprobes [255], biosensors [256], drug delivery [257], cell imaging [258] and tissue engineering [259,260]. However, studies have shown that GO can generate ROS in target cells [261]. Moreover, the GO solution [254] is more toxic than the GO coating matrix [262]. Ouyang et al. coated graphene oxide on sulfonated PEEK. After detailed characterization, PEEK showed an excellent inhibitory effect on *E. coli.* PEEK could significantly accelerate the proliferation and osteogenic differentiation of MG-63 cells. However, the author did not conclude that sulfonated PEEK had antibacterial properties in the experiment, nor did he give an explanation [263]. Wang et al. assembled graphene oxide nanosheets, PDA nanofilms, and oligopeptides onto the surface of porous sulfonated PEEK. In vitro experiments showed that the modified PEEK increased cytocompatibility, alkaline phosphatase activity, calcium matrix deposition, and osteogenesis-related gene expression. Experiments in rabbit femur defect animal models confirmed that modified PEEK promoted osseointegration and bone remodeling *in vivo*. Furthermore, graphene oxide and PDA coatings were anchored to the sulfonated PEEK surface, resulting in a powerful antibacterial phototherapy effect [264]. The authors also did not evaluate the antibacterial effect of sulfonated PEEK alone [264].

3.3. Coating or filling with metal nanoparticles or inorganic particles

3.3.1. Zinc-modified PEEK

Zinc (Zn) is a structural or functional component of several proteins that promote cell proliferation, differentiation, and bone-related gene expression [265,266]. In addition, Zn is a broad-spectrum antibacterial agent, and Zn does not cause bacterial mutation [267]. Therefore, the addition of Zn at reasonable doses is promising to stimulate bone formation and inhibit bacterial growth [268,269]. Due to the reactive nature of zinc, the outer layer of the zinc coating reacts with oxygen to form zinc oxide. Studies have shown that ZnO nanomaterials also have excellent antibacterial effects [270–272], especially against Gram-positive bacteria [273]. In addition, zinc oxide is FDA-approved for *in vivo* applications [274]. Ye et al. synthesized antimicrobial PEEK by an anodic aluminum oxide (AAO) template printing and a hydrothermal two-step method. The bottom sheet was solid PEEK material, the middle structure was a cicada wing-like nanopillar array, and lastly the top layer was decorated with catkin-like ZnO nanoslices. *In vivo* implantation experiments showed that the composite material can effectively kill inoculated *S. aureus* [275]. Deng et al. coated silver ions and zinc ions on sulfonated PEEK via LBL self-assembly. The antibacterial experiments revealed that the sulfonated PEEK modified by Ag and Ag/ZnO inhibited the growth of Gram-negative and Gram-positive bacteria. They also found that proliferation and osteogenic differentiation of MG-63 cells were significantly enhanced on Ag/ZnO modified sulfonated PEEK compared with Ag and ZnO modified sulfonated PEEK [225]. In this study, the researchers did not individually test sulfonated PEEK for antibacterial activity [276]. Lu et al. modified CFR-PEEK using dual zinc and oxygen plasma immersion ion implantation (Zn/O-PIII). Both MC3T3-E1 cells and rBMSCs showed enhanced adherence, proliferation, and differentiation on the modified CFR-PEEK. *In vitro* antibacterial experiments demonstrated that the modified CFR-PEEK exhibited strong antibacterial activity against *S. aureus* (ATCC 25923), *MRSA* (ATCC 43300), and *S. epidermidis* (ATCC 35984) [277]. Yang et al. loaded zinc oxide and graphene oxide on sulfonated PEEK. The results show that the modified PEEK samples have good biocompatibility. Meanwhile, the modified PEEK has an obvious inhibitory effect on *S. sanguinis, F. nucleatum,* and *P. gingivalis* [278]. The researchers also did not study the antibacterial ability of sulfonated PEEK alone [278]. Zhang et al. coated acrylic acid with zinc ions on PEEK by plasma-induced graft polymerization technique. Cell experiments showed that the modified PEEK promoted the proliferation and differentiation of MC3T3-E1 cells. Antibacterial tests showed that the modified PEEK effectively inhibited the growth of *S. aureus* with the release of zinc ions [279].

However, excess zinc ions can have negative effects on the body. For example, the liver of mice showed transient pathological changes following oral administration of ZnO (2.5 g/kg) [280]. Intratracheal infusion of ZnO increases LDH release and neutrophil numbers [281]. Furthermore, ZnO damages alveolar epithelial cells by increasing ROS and causing mitochondrial dysfunction [282]. Zinc ions released from the implant are transported to the organ through the blood and may negatively affect the organ. Although similar studies have not been conducted, we should still pay attention. Therefore, it is necessary for researchers to measure the concentration of zinc ions in the blood and simultaneously test the toxic effects of organs when using zinc ion-modified implants.

3.3.2. Silver-modified PEEK

Silver has been a common disinfectant for thousands of years because it is highly toxic to a wide variety of microorganisms [283]. It is difficult for bacteria to develop resistance to it. However, silver-resistant bacteria still appear [284,285]. It has also been shown to have the ability to interfere with different pathways of bacterial metabolism [286,287]. For example, some researchers have coated silver ions on titanium substrates, and the electron transfer generated by silver and titanium can generate large amounts of ROS in bacterial cells and culture medium, resulting in bacterial death [287]. Today, silver ions have been shown to produce synergistic antibacterial activity with antibiotics and even expand the antibacterial spectrum [288]. Liu et al. coated the surface of PEEK with silver nanoparticles by magnetron sputtering. Through a water contact angle test, it was demonstrated that the modified PEEK's water contact angle was significantly increased in comparison with the naked PEEK.

Cytotoxicity testing showed that the modified samples were not cytotoxic. Results from antibacterial experiments suggested that the modified PEEK significantly improved antibacterial properties [289]. Deng et al. developed 3D-printed PEEK with silver decoration using catecholamine chemical technology. Antibacterial testing revealed that their modified PEEK had excellent antibacterial activity against *E. coli* and *S. aureus*. Cell culture experiments showed that cell proliferation and differentiation of MG-63 cells were enhanced on the modified PEEK [290]. Yan et al. synthesized copper oxide microspheres decorated with silver nanoparticles and then used silk fibroin to coat the porous PEEK's surface. *In vitro* antibacterial experiments showed that the modified PEEK had great antibacterial properties and could prevent the formation of biofilm. Through experimentation with cultured Adipose-derived mesenchymal stem cells and human umbilical vein stem cells, the modified PEEK can induce the production of ALP, NO, collagen, and calcium deposition. These findings suggested that the modified PEEK can promote bone formation and angiogenesis. A rabbit tibia model then demonstrated that the modified PEEK promoted bone regeneration and osseointegration [291]. Yang et al. obtained a sulfonated porous PEEK by sulfonating PEEK and then modified it with an in situ synthesis of zeolite imidazolium framework-8 (ZIF-8), which was loaded with silver ions. The antibacterial test results showed that PEEK had excellent antibacterial performance against *E. coli* and *S. aureus*. The excellent antibacterial activity was attributed to the synergistic effect of silver and zinc ions continuously released from the modified PEEK [292]. The researchers did not specify the antibacterial properties of sulfonated PEEK [292].

Despite the excellent antibacterial properties of silver ions, some studies have shown that excess silver ions have cytotoxic effects on mammalian cells [293–296]. Some experts pointed out that silver ions can disrupt the mitochondrial respiratory chain, leading to the interruption of ROS production and ATP synthesis, resulting in DNA damage [297,298]. Therefore, implants with silver ions must incorporate an optimal amount of silver to have good antibacterial activity and a non-cytotoxic effect.

3.3.3. Zirconium-modified PEEK

Nanostructured zirconia (ZrO_2) and ZrO_2 coatings have good bioactivity [299–302]. ZrO_2 has not been reported to exhibit any toxic effects and immune responses *in vitro* [303,304]. Moreover, the nanostructured ZrO_2 and ZrO_2 coatings have good bioactivity and cytocompatibility [301,302,305–308]. In addition, ZrO_2 has good osseointegration ability [309–311]. Most importantly, ZrO_2 nanoparticles have antibacterial effects against both Gram-negative and Gram-positive bacteria [312,313]. Li et al. introduced bioactive ZrO_2 onto the surface of CFR-PEEK by zirconium plasma immersion ion implantation (Zr-PIII). Cell culture experiments showed that adherence, proliferation, and differentiation of rBMSCs were significantly increased on CFR-PEEK after PIII treatment. The treated CFR-PEEK showed clear antibacterial activity against *S. aureus* [314].

3.3.4. Nitrogen-modified PEEK

Studies have shown that nitrogen PIII can introduce nitrogen-containing functional groups into the surface of polymer materials, and the formed surface has osteogenic and antibacterial properties [315,316]. Gan et al. used PIII to introduce nitrogen-containing functional groups into PEEK. *In vitro* experiments showed that adherence, proliferation, and osteoblastic differentiation of MG-63 cells were remarkably increased on PEEK after modification. The obtained PEEK surface layer showed excellent antimicrobial activity against *S. aureus* [317]. Likely reasons include greater surface roughness, improved hydrophilicity, and nitrogen-containing functional groups that can inhibit the adhesion of bacteria.

4. Future prospects and challenges

Although PEEK has been approved by the FDA as an implantable biomaterial since the late 1990s, more studies are needed to strengthen the application of modified PEEK materials in clinical practice. First of all, adding porosity has involved a trade-off in the mechanical performance of orthopedic load-bearing PEEK for tissue ingrowth around an implant. For this reason, the first medical device containing porous PEEK only got FDA approval in 2014. More processing methods should be developed to connect a porous surface to a solid base thus providing shear strength closer to cortical/trabecular bone.

Secondly, enhanced surface roughness can promote the attachment of both bony and bacterial cells. Thus, the roughness/pore shape of the PEEK surface should be optimized to inhibit bacterial adhesion and biofilm formation.

Thirdly, it is worth noting that the unrestrained release of antibiotics has led to bacterial resistance. Moreover, Ag/ZnO nanoparticles and high concentrations of Ag^{+} and Zn^{2+} can produce ROS and cause oxidative stress in bone cells. Hence, extensive studies are needed to improve drug/nanoparticle encapsulation in the PEEK matrix and provide controlled release of antibacterial therapy.

5. Conclusions

PEEK has stable chemical and physical properties, excellent X-ray transmittance, and mechanical properties similar to human bones. Because of these characteristics, PEEK is widely used as an orthopedic implant material. However, PEEK itself is biologically inert, which can lead to poor osseointegration after implantation. In addition, PEEK alone has no antimicrobial properties, which could lead to implant failure. PEEK modification methods mainly include surface modification and composite preparation. When using these two methods to modify PEEK, attention should be paid to maintaining the stability of the surface coating and the mechanical properties of the composite material. Improving the bioactivity and antibacterial properties without affecting mechanical properties is the main challenge. Furthermore, the complexity and manufacturing costs of modifying PEEK should be taken into account.

Author contributions

ZZ and SKZ conceived the idea. ZZ collected the related references and wrote the manuscript. ZZ and YJW drew the figures. JGX, XHM, and SLZ made the table. PJL, XMZ, and XSZ supervised and revised the manuscript. All authors agree with the content of the final version.

Funding

This work was supported by the program of the First Hospital of Jilin University (JDYYJCHX2020020).

Declaration of competing interest

The authors declare that they have no known competing financial interests or personal relationships that could have appeared to influence the work reported in this paper.

References

[1] T. Kokubo, H.-M. Kim, M. Kawashita, Novel bioactive materials with different mechanical properties, Biomaterials 24 (13) (2003) 2161–2175.
[2] S.M. Kurtz, J.N. Devine, PEEK biomaterials in trauma, orthopedic, and spinal implants, Biomaterials 28 (32) (2007) 4845–4869.
[3] I.V. Panayotov, V. Orti, F. Cuisinier, J. Yachouh, Polyetheretherketone (PEEK) for medical applications, J. Mater. Sci. Mater. Med. 27 (7) (2016) 118.
[4] S. Vadapalli, K. Sairyo, V.K. Goel, M. Robon, A. Biyani, A. Khandha, N.A. Ebraheim, Biomechanical rationale for using polyetheretherketone (PEEK) spacers for lumbar interbody fusion-A finite element study, Spine 31 (26) (2006) E992–E998.
[5] Y. Deng, W. Tang, Z. Li, Repairing a facial cleft by polyether-ether-ketone implant combined with titanium mesh, J. Craniofac. Surg. 29 (6) (2018) e582–e585.

[6] K. Mozaffari, S. Rana, A. Chow, N. Mahgerefteh, C. Duong, J.P. Sheppard, H.W. Phillips, R. Jarrahy, I. Yang, Customized polyetheretherketone (PEEK) implants are associated with similar hospital length of stay compared to autologous bone used in cranioplasty procedures, J. Neurol. Sci. 434 (2022), 120169.
[7] S. Najeeb, M.S. Zafar, Z. Khurshid, F. Siddiqui, Applications of polyetheretherketone (PEEK) in oral implantology and prosthodontics, Journal of prosthodontic research 60 (1) (2016) 12–19.
[8] A.A. Stratton-Powell, K.M. Pasko, C.L. Brockett, J.L. Tipper, The biologic response to polyetheretherketone (PEEK) wear particles in total joint replacement: a systematic review, Clin. Orthop. Relat. Res. 474 (11) (2016) 2394–2404.
[9] M. Saracco, C. Fulchignoni, C. Velluto, L. Rocchi, Safety and reliability of carbon-peek plate for the treatment of distal radius fractures: a review of the literature, Orthop. Rev. 13 (2) (2021), 28362.
[10] K. Topuz, A. Colak, S. Kaya, H. Simşek, M. Kutlay, M.N. Demircan, M. Velioğlu, Two-level contiguous cervical disc disease treated with peek cages packed with demineralized bone matrix: results of 3-year follow-up, Eur. Spine J. 18 (2) (2009) 238–243.
[11] L. Mastronardi, A. Ducati, L. Ferrante, Anterior cervical fusion with polyetheretherketone (PEEK) cages in the treatment of degenerative disc disease. Preliminary observations in 36 consecutive cases with a minimum 12-month follow-up, Acta Neurochir. 148 (3) (2006) 307–312, discussion 312.
[12] W. Jacobs, P.C. Willems, M. Kruyt, J. van Limbeek, P.G. Anderson, P. Pavlov, R. Bartels, C. Oner, Systematic review of anterior interbody fusion techniques for single- and double-level cervical degenerative disc disease, Spine 36 (14) (2011) E950–E960.
[13] J.J. Yang, C.H. Yu, B.S. Chang, J.S. Yeom, J.H. Lee, C.K. Lee, Subsidence and nonunion after anterior cervical interbody fusion using a stand-alone polyetheretherketone (PEEK) cage, Clin. Orthop. Surg. 3 (1) (2011) 16–23.
[14] P.D. Kim, E.M. Baron, M. Levesque, Extrusion of expandable stacked interbody device for lumbar fusion: case report of a complication, Spine 37 (18) (2012) E1155–E1158.
[15] O. Noiset, Y.J. Schneider, J. Marchand-Brynaert, Fibronectin adsorption or/and covalent grafting on chemically modified PEEK film surfaces, J. Biomater. Sci. Polym. Ed. 10 (6) (1999) 657–677.
[16] J.M. Toth, M. Wang, B.T. Estes, J.L. Scifert, H.B. Seim 3rd, A.S. Turner, Polyetheretherketone as a biomaterial for spinal applications, Biomaterials 27 (3) (2006) 324–334.
[17] J. Sandler, A.H. Windle, P. Werner, V. Altstadt, M.V. Es, M.S.P. Shaffer, Carbon-nanofibre-reinforced poly(ether ether ketone) fibres, J. Mater. Sci. 38 (10) (2003) 2135–2141.
[18] H.B. Skinner, Composite technology for total hip arthroplasty, Clin. Orthop. Relat. Res. (235) (1988) 224–236.
[19] A.K. Bembey, M.L. Oyen, C.C. Ko, A.J. Bushby, A. Boyde, Elastic Modulus and Mineral Density of Dentine and Enamel in Natural Caries Lesions, Symposium on Structure and Mechanical Behavior of Biological Materials Held at the 2005 MRS Spring Meeting, Materials Research Society, San Francisco, CA, 2005, pp. 125–130.
[20] H. Sano, B. Ciucchi, W.G. Matthews, D.H. Pashley, Tensile properties of mineralized and demineralized human and bovine dentin, J. Dent. Res. 73 (6) (1994) 1205–1211.
[21] Y. Li, D. Wang, W. Qin, H. Jia, Y. Wu, J. Ma, B. Tang, Mechanical properties, hemocompatibility, cytotoxicity and systemic toxicity of carbon fibers/poly(ether-ether-ketone) composites with different fiber lengths as orthopedic implants, J. Biomater. Sci. Polym. Ed. 30 (18) (2019) 1709–1724.
[22] W. Qin, Y. Li, J. Ma, Q. Liang, B. Tang, Mechanical properties and cytotoxicity of hierarchical carbon fiber-reinforced poly (ether-ether-ketone) composites used as implant materials, J. Mech. Behav. Biomed. Mater. 89 (2019) 227–233.
[23] M.M. Hanasono, N. Goel, F. DeMonte, Calvarial reconstruction with polyetheretherketone implants, Ann. Plast. Surg. 62 (6) (2009) 653–655.
[24] M. Punchak, L.K. Chung, C. Lagman, T.T. Bui, J. Lazareff, K. Rezzadeh, R. Jarrahy, I. Yang, Outcomes following polyetheretherketone (PEEK) cranioplasty: systematic review and meta-analysis, J. Clin. Neurosci. 41 (2017) 30–35.
[25] N. Sharma, S. Aghlmandi, S. Cao, C. Kunz, P. Honigmann, F.M. Thieringer, Quality characteristics and clinical relevance of in-house 3D-printed customized polyetheretherketone (PEEK) implants for craniofacial reconstruction, J. Clin. Med. 9 (9) (2020).
[26] J. Parthasarathy, 3D modeling, custom implants and its future perspectives in craniofacial surgery, Annals of maxillofacial surgery 4 (1) (2014) 9–18.
[27] Y. Chen, L. Zhang, T. Qin, Z. Wang, Y. Li, B. Gu, Evaluation of neurosurgical implant infection rates and associated pathogens: evidence from 1118 postoperative infections, Neurosurg. Focus 47 (2) (2019) E6.
[28] J. Zhang, W. Tian, J. Chen, J. Yu, J. Zhang, J. Chen, The application of polyetheretherketone (PEEK) implants in cranioplasty, Brain Res. Bull. 153 (2019) 143–149.
[29] Y. Zhao, H.M. Wong, S.C. Lui, E.Y. Chong, G. Wu, X. Zhao, C. Wang, H. Pan, K.M. Cheung, S. Wu, P.K. Chu, K.W. Yeung, Plasma surface functionalized polyetheretherketone for enhanced osseo-integration at bone-implant interface, ACS Appl. Mater. Interfaces 8 (6) (2016) 3901–3911.
[30] Y.G. Koh, K.M. Park, J.A. Lee, J.H. Nam, H.Y. Lee, K.T. Kang, Total knee arthroplasty application of polyetheretherketone and carbon-fiber-reinforced polyetheretherketone: a review, Mater Sci Eng C Mater Biol Appl 100 (2019) 70–81.
[31] C.S. Li, C. Vannabouathong, S. Sprague, M. Bhandari, The use of carbon-fiber-reinforced (CFR) PEEK material in orthopedic implants: a systematic review, clinical medicine insights, Arthritis and musculoskeletal disorders 8 (2015) 33–45.
[32] H.B. Skinner, Composite technology for total hip arthroplasty, Clin. Orthop. Relat. Res. 235 (1988) 224–236.
[33] E. Ingham, J. Fisher, Biological reactions to wear debris in total joint replacement, Proc. IME H J. Eng. Med. 214 (1) (2000) 21–37.
[34] C. Skjöldebrand, J.L. Tipper, P. Hatto, M. Bryant, R.M. Hall, C. Persson, Current status and future potential of wear-resistant coatings and articulating surfaces for hip and knee implants, Materials today, Bio 15 (2022), 100270.
[35] T. Suzuki, W.R. Smith, P.F. Stahel, S.J. Morgan, A.J. Baron, D.J. Hak, Technical problems and complications in the removal of the less invasive stabilization system, J. Orthop. Trauma 24 (6) (2010) 369–373.
[36] S.S. Van Nortwick, J. Yao, A.L. Ladd, Titanium integration with bone, welding, and screw head destruction complicating hardware removal of the distal radius: report of 2 cases, J. Hand Surg. 37 (7) (2012) 1388–1392.
[37] R. Mugnai, L. Tarallo, F. Capra, F. Catani, Biomechanical comparison between stainless steel, titanium and carbon-fiber reinforced polyetheretherketone volar locking plates for distal radius fractures, Orthopaedics & traumatology, surgery & research : OTSR 104 (6) (2018) 877–882.
[38] D. Perugia, M. Guzzini, D. Mazza, C. Iorio, C. Civitenga, A. Ferretti, Comparison between Carbon-Peek volar locking plates and titanium volar locking plates in the treatment of distal radius fractures, Injury 48 (Suppl 3) (2017) S24–s29.
[39] T. Gultan, M.C. Yurtsever, M. Gumusderelioglu, NaOH-etched/boron-doped nanohydroxyapatite-coated PEEK implants enhance the proliferation and differentiation of osteogenic cells, Biomed. Mater. 15 (3) (2020), 035019.
[40] M.K. Bartelstein, D.W. Van Citters, M.C. Weiser, C.S. Moucha, Failure of a polyaryletheretherketone-cobalt-chromium composite femoral stem due to coating separation and subsidence: a case report, JBJS case connector 7 (4) (2017) e83.
[41] H. Lyu, N. Jiang, Y. Li, D. Zhang, Enhancing CF/PEEK interfacial adhesion by modified PEEK grafted with carbon nanotubes, Compos. Sci. Technol. 210 (2021).
[42] C. Lu, S. Qiu, X. Lu, J. Wang, L. Xiao, T. Zheng, X. Wang, D. Zhang, Enhancing the interfacial strength of carbon fiber/poly(ether ether ketone) hybrid composites by plasma treatments, Polymers 11 (5) (2019).
[43] W.Z. Nie, J. Li, Effects of plasma and nitric acid treatment of carbon fibers on the mechanical properties of thermoplastic polymer composites, Mech. Compos. Mater. 46 (3) (2010) 251–256.
[44] J. Li, Interfacial studies on the ozone and air-oxidation-modified carbon fiber reinforced PEEK composites, Surf. Interface Anal. 41 (4) (2009) 310–315.
[45] G. Wolinne, C. Harnisch, E. Heripre, S. Ruch, A. Salito, M. Jeandin, L. Corte, Mechanical study of novel VPS-titanium coating on polyethylene substrates, J. Therm. Spray Technol. 24 (1–2) (2015) 206–214.
[46] L.L. Hench, J. Wilson, Surface-active biomaterials, Science (New York, N.Y.) 226 (4675) (1984) 630–636.
[47] J.W. Durham 3rd, S.A. Montelongo, J.L. Ong, T. Guda, M.J. Allen, A. Rabiei, Hydroxyapatite coating on PEEK implants: biomechanical and histological study in a rabbit model, Mater Sci Eng C Mater Biol Appl 68 (2016) 723–731.
[48] P. Johansson, S. Barkarmo, M. Hawthan, N. Peruzzi, P. Kjellin, A. Wennerberg, Biomechanical, histological, and computed X-ray tomographic analyses of hydroxyapatite coated PEEK implants in an extended healing model in rabbit, J. Biomed. Mater. Res. 106 (5) (2018) 1440–1447.
[49] P. Johansson, R. Jimbo, Y. Naito, P. Kjellin, F. Currie, A. Wennerberg, Polyether ether ketone implants achieve increased bone fusion when coated with nano-sized hydroxyapatite: a histomorphometric study in rabbit bone, Int. J. Nanomed. 11 (2016) 1435–1442.
[50] K.M. Buettner, A.M. Valentine, Bioinorganic chemistry of titanium, Chem. Rev. 112 (3) (2012) 1863–1881.
[51] J.J. Jacobs, N.J. Hallab, A.K. Skipor, R.M. Urban, Metal degradation products: a cause for concern in metal-metal bearings? Clin. Orthop. Relat. Res. 417 (2003) 139–147.
[52] D.G. Olmedo, D.R. Tasat, M.B. Guglielmotti, R.L. Cabrini, Biodistribution of titanium dioxide from biologic compartments, J. Mater. Sci. Mater. Med. 19 (9) (2008) 3049–3056.
[53] S. Redline, B.P. Barna, J.F. Tomashefski Jr., J.L. Abraham, Granulomatous disease associated with pulmonary deposition of titanium, Br. J. Ind. Med. 43 (10) (1986) 652–656.
[54] H.D. Jung, T.S. Jang, J.E. Lee, S.J. Park, Y. Son, S.H. Park, Enhanced bioactivity of titanium-coated polyetheretherketone implants created by a high-temperature 3D printing process, Biofabrication 11 (4) (2019), 045014.
[55] T. Hasegawa, H. Ushirozako, E. Shigeto, T. Ohba, H. Oba, K. Mukaiyama, S. Shimizu, Y. Yamato, K. Ide, Y. Shibata, T. Ojima, J. Takahashi, H. Haro, Y. Matsuyama, The titanium-coated PEEK cage maintains better bone fusion with the endplate than the PEEK cage 6 Months after PLIF surgery, Spine 45 (15) (2020) E892–E902.
[56] T. Shimizu, S. Fujibayashi, S. Yamaguchi, K. Yamamoto, B. Otsuki, M. Takemoto, M. Tsukanaka, T. Kizuki, T. Matsushita, T. Kokubo, S. Matsuda, Bioactivity of sol-gel-derived TiO2 coating on polyetheretherketone: in vitro and in vivo studies, Acta Biomater. 35 (2016) 305–317.
[57] S. Liu, Y. Zhu, H. Gao, P. Ge, K. Ren, J. Gao, Y. Cao, D. Han, J. Zhang, One-step fabrication of functionalized poly(etheretherketone) surfaces with enhanced biocompatibility and osteogenic activity, Mater Sci Eng C Mater Biol Appl 88 (2018) 70–78.
[58] J. Wen, T. Lu, X. Wang, L. Xu, Q. Wu, H. Pan, D. Wang, X. Liu, X. Jiang, In vitro and in vivo evaluation of silicate-coated polyetheretherketone fabricated by electron beam evaporation, ACS Appl. Mater. Interfaces 8 (21) (2016) 13197–13206.

[59] Y. Ren, P. Sikder, B. Lin, S.B. Bhaduri, Microwave assisted coating of bioactive amorphous magnesium phosphate (AMP) on polyetheretherketone (PEEK), Mater Sci Eng C Mater Biol Appl 85 (2018) 107–113.
[60] A. Oyane, M. Nakamura, I. Sakamaki, Y. Shimizu, S. Miyata, H. Miyaji, Laser-assisted wet coating of calcium phosphate for surface-functionalization of PEEK, PLoS One 13 (10) (2018), e0206524.
[61] C.D. Mu, J.M. Guo, X.Y. Li, W. Lin, D.F. Li, Preparation and properties of dialdehyde carboxymethyl cellulose crosslinked gelatin edible films, Food Hydrocolloids 27 (1) (2012) 22–29.
[62] P. Hiwale, S. Lampis, G. Conti, C. Caddeo, S. Murgia, A.M. Fadda, M. Monduzzi, In vitro release of lysozyme from gelatin microspheres: effect of cross-linking agents and thermoreversible gel as suspending medium, Biomacromolecules 12 (9) (2011) 3186–3193.
[63] M. Mehdizadeh Omrani, H. Kumar, M.G.A. Mohamed, K. Golovin, S.M. A, A. Hadjizadeh, K. Kim, Polyether ether ketone surface modification with plasma and gelatin for enhancing cell attachment, J. Biomed. Mater. Res. B Appl. Biomater. 109 (5) (2021) 622–629.
[64] J. Wu, L. Li, C. Fu, F. Yang, Z. Jiao, X. Shi, Y. Ito, Z. Wang, Q. Liu, P. Zhang, Micro-porous polyetheretherketone implants decorated with BMP-2 via phosphorylated gelatin coating for enhancing cell adhesion and osteogenic differentiation, Colloids Surf. B Biointerfaces 169 (2018) 233–241.
[65] C. Wang, S. Wang, Y. Yang, Z. Jiang, Y. Deng, S. Song, W. Yang, Z.G. Chen, Bioinspired, biocompatible and peptide-decorated silk fibroin coatings for enhanced osteogenesis of bioinert implant, J. Biomater. Sci. Polym. Ed. 29 (13) (2018) 1595–1611.
[66] W. Liu, J. Li, M. Cheng, Q. Wang, K.W.K. Yeung, P.K. Chu, X. Zhang, Zinc-modified sulfonated polyetheretherketone surface with immunomodulatory function for guiding cell fate and bone regeneration, Adv. Sci. 5 (10) (2018), 1800749.
[67] X. Liu, F. Han, P. Zhao, C. Lin, X. Wen, X. Ye, Layer-by-layer self-assembled multilayers on PEEK implants improve osseointegration in an osteoporosis rabbit model, Nanomedicine 13 (4) (2017) 1423–1433.
[68] H. Yajima, Y. Kobata, K. Shigematsu, K. Kawamura, K. Kawate, S. Tamai, Y. Takakura, Vascularized fibular grafting in the treatment of methicillin-resistant Staphylococcus aureus osteomyelitis and infected nonunion, J. Reconstr. Microsurg. 20 (1) (2004) 13–20.
[69] E. Buache, F. Velard, E. Bauden, C. Guillaume, E. Jallot, J.M. Nedelec, D. Laurent-Maquin, P. Laquerriere, Effect of strontium-substituted biphasic calcium phosphate on inflammatory mediators production by human monocytes, Acta Biomater. 8 (8) (2012) 3113–3119.
[70] S. Pasqualetti, G. Banfi, M. Mariotti, The effects of strontium on skeletal development in zebrafish embryo, J. Trace Elem. Med. Biol. : organ of the Society for Minerals and Trace Elements (GMS) 27 (4) (2013) 375–379.
[71] M. Yamaguchi, M.N. Weitzmann, The intact strontium ranelate complex stimulates osteoblastogenesis and suppresses osteoclastogenesis by antagonizing NF-κB activation, Mol. Cell. Biochem. 359 (1–2) (2012) 399–407.
[72] Y. Deng, F. Ma, L.I. Ruiz-Ortega, Y. Peng, Y. Tian, W. He, B. Tang, Fabrication of strontium Eucommia ulmoides polysaccharides and in vitro evaluation of their osteoimmunomodulatory property, Int. J. Biol. Macromol. 140 (2019) 727–735.
[73] Z. Mengdi, L. Jiayi, L. Canfeng, W. Guofeng, W. Yutong, H. Pengzhou, Z. Yikun, Z. Xintao, T. Bin, Surface modification of polyetheretherketone (PEEK) to enhance osteointegration by grafting strontium Eucommia ulmoides polysaccharides, Int. J. Biol. Macromol. 211 (2022) 230–237.
[74] J. Egea, A.G. García, J. Verges, E. Montell, M.G. López, Antioxidant, antiinflammatory and neuroprotective actions of chondroitin sulfate and proteoglycans, Osteoarthritis Cartilage 18 (Suppl 1) (2010) S24–S27.
[75] S. Li, F. Ma, X. Pang, B. Tang, L. Lin, Synthesis of chondroitin sulfate magnesium for osteoarthritis treatment, Carbohydr. Polym. 212 (2019) 387–394.
[76] M. Bishnoi, A. Jain, P. Hurkat, S.K. Jain, Chondroitin sulphate: a focus on osteoarthritis, Glycoconj. J. 33 (5) (2016) 693–705.
[77] Z. Zheng, L. Hu, Y. Ge, J. Qi, Q. Sun, Z. Li, L. Lin, B. Tang, Surface modification of poly(ether ether ketone) by simple chemical grafting of strontium chondroitin sulfate to improve its anti-inflammation, angiogenesis, osteogenic properties, Adv Healthc Mater 11 (13) (2022), e2200398.
[78] R. Ma, J. Wang, C. Li, K. Ma, J. Wei, P. Yang, D. Guo, K. Wang, W. Wang, Effects of different sulfonation times and post-treatment methods on the characterization and cytocompatibility of sulfonated PEEK, J. Biomater. Appl. 35 (3) (2020) 342–352.
[79] Z. Meng, Y. Liu, D. Wu, Effect of sulfur dioxide inhalation on cytokine levels in lungs and serum of mice, Inhal. Toxicol. 17 (6) (2005) 303–307.
[80] Z. Meng, G. Qin, B. Zhang, DNA damage in mice treated with sulfur dioxide by inhalation, Environ. Mol. Mutagen. 46 (3) (2005) 150–155.
[81] Z. Meng, G. Qin, B. Zhang, J. Bai, DNA damaging effects of sulfur dioxide derivatives in cells from various organs of mice, Mutagenesis 19 (6) (2004) 465–468.
[82] L. Ouyang, Y. Zhao, G. Jin, T. Lu, J. Li, Y. Qiao, C. Ning, X. Zhang, P.K. Chu, X. Liu, Influence of sulfur content on bone formation and antibacterial ability of sulfonated PEEK, Biomaterials 83 (2016) 115–126.
[83] W. Liu, J. Li, M. Cheng, Q. Wang, Y. Qian, K.W.K. Yeung, P.K. Chu, X. Zhang, A surface-engineered polyetheretherketone biomaterial implant with direct and immunoregulatory antibacterial activity against methicillin-resistant Staphylococcus aureus, Biomaterials 208 (2019) 8–20.
[84] J.F. Montero, H.A. Tajiri, G.M. Barra, M.C. Fredel, C.A. Benfatti, R.S. Magini, A.L. Pimenta, J.C. Souza, Biofilm behavior on sulfonated poly(ether-ether-ketone) (sPEEK), Mater Sci Eng C Mater Biol Appl 70 (Pt 1) (2017) 456–460.
[85] S. Wang, Y. Deng, L. Yang, X. Shi, W. Yang, Z.G. Chen, Enhanced antibacterial property and osteo-differentiation activity on plasma treated porous polyetheretherketone with hierarchical micro/nano-topography, J. Biomater. Sci. Polym. Ed. 29 (5) (2018) 520–542.
[86] S. Luo, P. Wang, M. Ma, Z. Pan, L. Lu, F. Yin, J. Cai, Genistein loaded into microporous surface of nano tantalum/PEEK composite with antibacterial effect regulating cellular response in vitro, and promoting osseointegration in vivo, J. Mech. Behav. Biomed. Mater. 125 (2022), 104972.
[87] T. Wan, Z. Jiao, M. Guo, Z. Wang, Y. Wan, K. Lin, Q. Liu, P. Zhang, Gaseous sulfur trioxide induced controllable sulfonation promoting biomineralization and osseointegration of polyetheretherketone implants, Bioact. Mater. 5 (4) (2020) 1004–1017.
[88] Y. Zhao, H.M. Wong, W. Wang, P. Li, Z. Xu, E.Y. Chong, C.H. Yan, K.W. Yeung, P.K. Chu, Cytocompatibility, osseointegration, and bioactivity of three-dimensional porous and nanostructured network on polyetheretherketone, Biomaterials 34 (37) (2013) 9264–9277.
[89] Y. Zhu, Z. Cao, Y. Peng, L. Hu, T. Guney, B. Tang, Facile surface modification method for synergistically enhancing the biocompatibility and bioactivity of poly(ether ether ketone) that induced osteodifferentiation, ACS Appl. Mater. Interfaces 11 (31) (2019) 27503–27511.
[90] S. Wang, Y. Yang, Y. Li, J. Shi, J. Zhou, L. Zhang, Y. Deng, W. Yang, Strontium/adiponectin co-decoration modulates the osteogenic activity of nano-morphologic polyetheretherketone implant, Colloids Surf. B Biointerfaces 176 (2019) 38–46.
[91] Q. Cheng, B. Yuan, X. Chen, X. Yang, H. Lin, X. Zhu, K. Zhang, X. Zhang, Regulation of surface micro/nano structure and composition of polyetheretherketone and their influence on the behavior of MC3T3-E1 pre-osteoblasts, J. Mater. Chem. B 7 (37) (2019) 5713–5724.
[92] Z. Sun, L. Ouyang, X. Ma, Y. Qiao, X. Liu, Controllable and durable release of BMP-2-loaded 3D porous sulfonated polyetheretherketone (PEEK) for osteogenic activity enhancement, Colloids Surf. B Biointerfaces 171 (2018) 668–674.
[93] Y. Yu, K. Xie, L. Xie, Y. Deng, Endowing polyetheretherketone with anti-inflammatory ability and improved osteogenic ability, J. Biomater. Sci. Polym. Ed. (2020) 1–18.
[94] L. Hallmann, P. Ulmer, F. Lehmann, S. Wille, O. Polonskyi, M. Johannes, S. Köbel, T. Trottenberg, S. Bornholdt, F. Haase, H. Kersten, M. Kern, Effect of surface modifications on the bond strength of zirconia ceramic with resin cement resin, Dent. Mater. 32 (5) (2016) 631–639.
[95] R.M. Melo, R.O. Souza, E. Dursun, E.B. Monteiro, L.F. Valandro, M.A. Bottino, Surface treatments of zirconia to enhance bonding durability, Operat. Dent. 40 (6) (2015) 636–643.
[96] B. Stawarczyk, P. Jordan, P.R. Schmidlin, M. Roos, M. Eichberger, W. Gernet, C. Keul, PEEK surface treatment effects on tensile bond strength to veneering resins, J. Prosthet. Dent 112 (5) (2014) 1278–1288.
[97] J. Uhrenbacher, P.R. Schmidlin, C. Keul, M. Eichberger, M. Roos, W. Gernet, B. Stawarczyk, The effect of surface modification on the retention strength of polyetheretherketone crowns adhesively bonded to dentin abutments, J. Prosthet. Dent 112 (6) (2014) 1489–1497.
[98] R. Zandparsa, N.A. Talua, M.D. Finkelman, S.E. Schaus, An in vitro comparison of shear bond strength of zirconia to enamel using different surface treatments, J. Prosthodont. 23 (2) (2014) 117–123.
[99] F.S.F. Dos Santos, M. Vieira, H.N. da Silva, H. Tomás, M.V.L. Fook, Surface bioactivation of polyether ether ketone (PEEK) by sulfuric acid and piranha solution: influence of the modification route in capacity for inducing cell growth, Biomolecules 11 (9) (2021).
[100] Y. Zheng, L. Liu, L. Xiao, Q. Zhang, Y. Liu, Enhanced osteogenic activity of phosphorylated polyetheretherketone via surface-initiated grafting polymerization of vinylphosphonic acid, Colloids Surf. B Biointerfaces 173 (2019) 591–598.
[101] N. Fukuda, M. Kanazawa, K. Tsuru, A. Tsuchiya, Sunarso, R. Toita, Y. Mori, Y. Nakashima, K. Ishikawa, Synergistic effect of surface phosphorylation and micro-roughness on enhanced osseointegration ability of poly(ether ether ketone) in the rabbit tibia, Sci. Rep. 8 (1) (2018), 16887.
[102] N. Fukuda, A. Tsuchiya, Sunarso, R. Toita, K. Tsuru, Y. Mori, K. Ishikawa, Surface plasma treatment and phosphorylation enhance the biological performance of poly(ether ether ketone), Colloids Surf. B Biointerfaces 173 (2019) 36–42.
[103] H. Mahjoubi, E. Buck, P. Manimunda, R. Farivar, R. Chromik, M. Murshed, M. Cerruti, Surface phosphonation enhances hydroxyapatite coating adhesion on polyetheretherketone and its osseointegration potential, Acta Biomater. 47 (2017) 149–158.
[104] L.F. Cooper, Y. Zhou, J. Takebe, J. Guo, A. Abron, A. Holmén, J.E. Ellingsen, Fluoride modification effects on osteoblast behavior and bone formation at TiO2 grit-blasted c.p. titanium endosseous implants, Biomaterials 27 (6) (2006) 926–936.
[105] S. Huo, X. Meng, S. Zhang, B. Yue, Y. Zhao, T. Long, B. Nie, Y. Wang, Hydrofluoric acid and nitric acid cotreatment for biofunctionalization of polyetheretherketone in M2 macrophage polarization and osteogenesis, J. Biomed. Mater. Res. 109(6) (2020) 879–892.
[106] D.D. Wang, Y.Q. Zou, L. Tao, Y.Q. Zhang, Z.J. Liu, S.Q. Du, S.Q. Zang, S.Y. Wang, Low-temperature plasma technology for electrocatalysis, Chin. Chem. Lett. 30 (4) (2019) 826–838.
[107] Z. Novotna, S. Rimpelova, P. Jurik, M. Vesely, Z. Kolska, T. Hubacek, J. Borovec, V. Svorcik, Tuning surface chemistry of polyetheretherketone by gold coating and plasma treatment, Nanoscale Res. Lett. 12 (2017) 9.
[108] D.G. Petlin, S.I. Tverdokhlebov, Y.G. Anissimov, Plasma treatment as an efficient tool for controlled drug release from polymeric materials: a review, J. Contr. Release : official journal of the Controlled Release Society 266 (2017) 57–74.
[109] Q. Fu, M. Gabriel, F. Schmidt, W.D. Müller, A.D. Schwitalla, The impact of different low-pressure plasma types on the physical, chemical and biological surface properties of PEEK, Dent. Mater. 37 (1) (2021) e15–e22.

[110] C. Liu, J. Bai, Y. Wang, L. Chen, D. Wang, S. Ni, H. Liu, The effects of three cold plasma treatments on the osteogenic activity and antibacterial property of PEEK, Dent. Mater. 37 (1) (2021) 81–93.
[111] Q. Fu, M. Gabriel, F. Schmidt, W.D. Muller, A.D. Schwitalla, The Impact of Different Low-Pressure Plasma Types on the Physical, Chemical and Biological Surface Properties of PEEK, Dent Mater, 2020.
[112] K. Masamoto, S. Fujibayashi, T. Yabutsuka, T. Hiruta, B. Otsuki, Y. Okuzu, K. Goto, T. Shimizu, Y. Shimizu, C. Ishizaki, K. Fukushima, T. Kawai, M. Hayashi, K. Morizane, T. Kawata, M. Imamura, S. Matsuda, In vivo and in vitro bioactivity of a "precursor of apatite" treatment on polyetheretherketone, Acta Biomater. 91 (2019) 48–59.
[113] M. Chen, L. Ouyang, T. Lu, H. Wang, F. Meng, Y. Yang, C. Ning, J. Ma, X. Liu, Enhanced bioactivity and bacteriostasis of surface fluorinated polyetheretherketone, ACS Appl. Mater. Interfaces 9 (20) (2017) 16824–16833.
[114] T. Lu, S. Qian, F. Meng, C. Ning, X. Liu, Enhanced osteogenic activity of poly ether ether ketone using calcium plasma immersion ion implantation, Colloids Surf. B Biointerfaces 142 (2016) 192–198.
[115] J. Czwartos, B. Budner, A. Bartnik, P. Wachulak, B.A. Butruk-Raszeja, A. Lech, T. Ciach, H. Fiedorowicz, Effect of extreme ultraviolet (EUV) radiation and EUV induced, N(2) and O(2) based plasmas on a PEEK surface's physico-chemical properties and MG63 cell adhesion, Int. J. Mol. Sci. 22 (16) (2021).
[116] A. Kirkpatrick, S. Kirkpatrick, M. Walsh, S. Chau, M. Mack, S. Harrison, R. Svrluga, J. Khoury, Investigation of accelerated neutral atom beams created from gas cluster ion beams, Nucl. Instrum. Methods Phys. Res. Sect. B Beam Interact. Mater. Atoms 307 (2013) 281–289.
[117] J. Khoury, I. Selezneva, S. Pestov, V. Tarassov, A. Ermakov, A. Mikheev, M. Lazov, S.R. Kirkpatrick, D. Shashkov, A. Smolkov, Surface bioactivation of PEEK by neutral atom beam technology, Bioact. Mater. 4 (2019) 132–141.
[118] S. Ajami, M.J. Coathup, J. Khoury, G.W. Blunn, Augmenting the bioactivity of polyetheretherketone using a novel accelerated neutral atom beam technique, J. Biomed. Mater. Res. B Appl. Biomater. 105 (6) (2017) 1438–1446.
[119] A.G. Guglya, I.G. Marchenko, ION beam-assisted depositION technology as a method of nanocrystalline coating formatION, Problems of Atomic Science and Technology (2) (2014) 125–136.
[120] J.W. Durham 3rd, M.J. Allen, A. Rabiei, Preparation, characterization and in vitro response of bioactive coatings on polyether ether ketone, J. Biomed. Mater. Res. B Appl. Biomater. 105 (3) (2017) 560–567.
[121] R. Ma, T. Tang, Current strategies to improve the bioactivity of PEEK, Int. J. Mol. Sci. 15 (4) (2014) 5426–5445.
[122] A.M. Diez-Pascual, C. Xu, R. Luque, Development and characterization of novel poly(ether ether ketone)/ZnO bionanocomposites, J. Mater. Chem. B 2 (20) (2014) 3065–3078.
[123] C.R. Pedrosa, D. Arl, P. Grysan, I. Khan, S. Durrieu, S. Krishnamoorthy, M.C. Durrieu, Controlled nanoscale topographies for osteogenic differentiation of mesenchymal stem cells, ACS Appl. Mater. Interfaces 11 (9) (2019) 8858–8866.
[124] B. Yuan, Q. Cheng, R. Zhao, X. Zhu, X. Yang, X. Yang, K. Zhang, Y. Song, X. Zhang, Comparison of osteointegration property between PEKK and PEEK: effects of surface structure and chemistry, Biomaterials 170 (2018) 116–126.
[125] Y. Li, J. Wang, D. He, GuoxiongZhu, G. Wu, L. Chen, Surface sulfonation and nitrification enhance the biological activity and osteogenesis of polyetheretherketone by forming an irregular nano-porous monolayer, J. Mater. Sci. Mater. Med. 31 (1) (2019) 11.
[126] M. Gu, Y. Liu, T. Chen, F. Du, X. Zhao, C. Xiong, Y. Zhou, Is graphene a promising nano-material for promoting surface modification of implants or scaffold materials in bone tissue engineering?, Tissue engineering, Part B, Reviews 20 (5) (2014) 477–491.
[127] C.G. Galbraith, K.M. Yamada, J.A. Galbraith, Polymerizing actin fibers position integrins primed to probe for adhesion sites, Science (New York, N.Y.) 315 (5814) (2007) 992–995.
[128] M.J. Dalby, N. Gadegaard, R.O. Oreffo, Harnessing nanotopography and integrin-matrix interactions to influence stem cell fate, Nat. Mater. 13 (6) (2014) 558–569.
[129] S. Zhang, Z. Feng, Y. Hu, D. Zhao, X. Guo, F. Du, N. Wang, C. Sun, C. Liu, H. Liu, Endowing polyetheretherketone implants with osseointegration properties: in situ construction of patterned nanorod arrays, Small 18 (5) (2022), e2105589.
[130] A. Gao, Q. Liao, L. Xie, G. Wang, W. Zhang, Y. Wu, P. Li, M. Guan, H. Pan, L. Tong, P.K. Chu, H. Wang, Tuning the surface immunomodulatory functions of polyetheretherketone for enhanced osseointegration, Biomaterials 230 (2020), 119642.
[131] L. Wang, K. Zhang, Y. Hao, M. Liu, W. Wu, Osteoblast/bone-tissue responses to porous surface of polyetheretherketone-nanoporous lithium-doped magnesium silicate blends' integration with polyetheretherketone, Int. J. Nanomed. 14 (2019) 4975–4989.
[132] J. Zhang, L. Cai, T. Wang, S. Tang, Q. Li, T. Tang, S. Wei, J. Qian, J. Wei, J. Su, Lithium doped silica nanospheres/poly(dopamine) composite coating on polyetheretherketone to stimulate cell responses, improve bone formation and osseointegration, Nanomedicine 14 (3) (2018) 965–976.
[133] Y. Dai, H. Guo, L. Chu, Z. He, M. Wang, S. Zhang, X. Shang, Promoting osteoblasts responses in vitro and improving osteointegration in vivo through bioactive coating of nanosilicon nitride on polyetheretherketone, J Orthop Translat 24 (2020) 198–208.
[134] R.A. Gittens, T. McLachlan, R. Olivares-Navarrete, Y. Cai, S. Berner, R. Tannenbaum, Z. Schwartz, K.H. Sandhage, B.D. Boyan, The effects of combined micron-/submicron-scale surface roughness and nanoscale features on cell proliferation and differentiation, Biomaterials 32 (13) (2011) 3395–3403.
[135] P. Chen, T. Aso, R. Sasaki, M. Ashida, Y. Tsutsumi, H. Doi, T. Hanawa, Adhesion and differentiation behaviors of mesenchymal stem cells on titanium with micrometer and nanometer-scale grid patterns produced by femtosecond laser irradiation, J. Biomed. Mater. Res. 106 (10) (2018) 2735–2743.
[136] D. Xie, C. Xu, C. Ye, S. Mei, L. Wang, Q. Zhu, Q. Chen, Q. Zhao, Z. Xu, J. Wei, L. Yang, Fabrication of submicro-nano structures on polyetheretherketone surface by femtosecond laser for exciting cellular responses of mc3t3-E1 cells/gingival epithelial cells, Int. J. Nanomed. 16 (2021) 3201–3216.
[137] S. Kargozar, F. Kermani, S. Mollazadeh Beidokhti, S. Hamzehlou, E. Verné, S. Ferraris, F. Baino, Functionalization and surface modifications of bioactive glasses (BGs): tailoring of the biological response working on the outermost surface layer, Materials 12 (22) (2019).
[138] H. Pang, H. Tian, S. Qiu, N. Wang, Y.Q. Wang, Progress of titanium strut for cervical reconstruction with nano-graphene oxide loaded hydroxyapatite/polyamide composite and interbody fusion after corpectomy with anterior plate fixation, Artif. Cell Nanomed. Biotechnol. 47 (1) (2019) 3094–3100.
[139] F. Hajiali, S. Tajbakhsh, A. Shojaei, Fabrication and properties of polycaprolactone composites containing calcium phosphate-based ceramics and bioactive glasses in bone tissue engineering: a review, Polym. Rev. 58 (1) (2018) 164–207.
[140] W. Qin, Y. Li, J. Ma, Q. Liang, X. Cui, H. Jia, B. Tang, Osseointegration and biosafety of graphene oxide wrapped porous CF/PEEK composites as implantable materials: the role of surface structure and chemistry, Dent. Mater. 36 (10) (2020) 1289–1302.
[141] L. Zema, G. Loreti, A. Melocchi, A. Maroni, A. Gazzaniga, Injection Molding and its application to drug delivery, J. Contr. Release : official journal of the Controlled Release Society 159 (3) (2012) 324–331.
[142] C. König, K. Ruffieux, E. Wintermantel, J. Blaser, Autosterilization of biodegradable implants by injection molding process, J. Biomed. Mater. Res. 38 (2) (1997) 115–119.
[143] W. Yu, H. Zhang, L. A, S. Yang, J. Zhang, H. Wang, Z. Zhou, Y. Zhou, J. Zhao, Z. Jiang, Enhanced bioactivity and osteogenic property of carbon fiber reinforced polyetheretherketone composites modified with amino groups, Colloids Surf. B Biointerfaces 193 (2020), 111098.
[144] J. Ma, Q. Liang, W. Qin, P.O. Lartey, Y. Li, X. Feng, Bioactivity of nitric acid and calcium chloride treated carbon-fibers reinforced polyetheretherketone for dental implant, J. Mech. Behav. Biomed. Mater. 102 (2020), 103497.
[145] J.H. Yan, C.H. Wang, K.W. Li, Q. Zhang, M. Yang, W.L. Di-Wu, M. Yan, Y. Song, J.J. Ba, L. Bi, Y.S. Han, Enhancement of surface bioactivity on carbon fiber-reinforced polyether ether ketone via graphene modification, Int. J. Nanomed. 13 (2018) 3425–3440.
[146] T. Miyazaki, C. Matsunami, Y. Shirosaki, Bioactive carbon-PEEK composites prepared by chemical surface treatment, Mater Sci Eng C Mater Biol Appl 70 (Pt 1) (2017) 71–75.
[147] P.D. Swaminathan, M.N. Uddin, P. Wooley, R. Asmatulu, Fabrication and biological analysis of highly porous PEEK bionanocomposites incorporated with carbon and hydroxyapatite nanoparticles for biological applications, Molecules 25 (16) (2020).
[148] N. Addai Asante, Y. Wang, S. Bakhet, S. Kareem, K.A. Owusu, Y. Hu, M. Appiah, Ambient temperature sulfonated carbon fiber reinforced PEEK with hydroxyapatite and reduced graphene oxide hydroxyapatite composite coating, J. Biomed. Mater. Res. B Appl. Biomater. 109 (12) (2021) 2174–2183.
[149] D. Arcos, M. Vallet-Regí, Substituted hydroxyapatite coatings of bone implants, J. Mater. Chem. B 8 (9) (2020) 1781–1800.
[150] M.K. Bartelstein, D.W. Van Citters, M.C. Weiser, C.S. Moucha, Failure of a polyaryletheretherketone-cobalt-chromium composite femoral stem due to coating separation and subsidence: a case report, JBJS case connector 7 (4) (2017) e83.
[151] S.M. Tang, P. Cheang, M.S. AbuBakar, K.A. Khor, K. Liao, Tension-tension fatigue behavior of hydroxyapatite reinforced polyetheretherketone composites, Int. J. Fatig. 26 (1) (2004) 49–57.
[152] M.S. Abu Bakar, P. Cheang, K.A. Khor, Mechanical properties of injection molded hydroxyapatite-polyetheretherketone biocomposites, Compos. Sci. Technol. 63 (3–4) (2003) 421–425.
[153] M.S. Abu Bakar, M.H. Cheng, S.M. Tang, S.C. Yu, K. Liao, C.T. Tan, K.A. Khor, P. Cheang, Tensile properties, tension-tension fatigue and biological response of polyetheretherketone-hydroxyapatite composites for load-bearing orthopedic implants, Biomaterials 24 (13) (2003) 2245–2250.
[154] R.K. Roeder, M.M. Sproul, C.H. Turner, Hydroxyapatite whiskers provide improved mechanical properties in reinforced polymer composites, J. Biomed. Mater. Res. 67 (3) (2003) 801–812.
[155] R.J. Kane, G.L. Converse, R.K. Roeder, Effects of the reinforcement morphology on the fatigue properties of hydroxyapatite reinforced polymers, J. Mech. Behav. Biomed. Mater. 1 (3) (2008) 261–268.
[156] G.L. Converse, W. Yue, R.K. Roeder, Processing and tensile properties of hydroxyapatite-whisker-reinforced polyetheretherketone, Biomaterials 28 (6) (2007) 927–935.
[157] B.I. Oladapo, S.O. Ismail, O.K. Bowoto, F.T. Omigbodun, M.A. Olawumi, M.A. Muhammad, Lattice design and 3D-printing of PEEK with Ca10(OH)(PO4)3 and in-vitro bio-composite for bone implant, Int. J. Biol. Macromol. 165 (Pt A) (2020) 50–62.
[158] W.R. Walsh, M.H. Pelletier, N. Bertollo, C. Christou, C. Tan, Does PEEK/HA enhance bone formation compared with PEEK in a sheep cervical fusion model? Clin. Orthop. Relat. Res. 474 (11) (2016) 2364–2372.
[159] C. Shuai, C. Shuai, P. Wu, F. Yuan, P. Feng, Y. Yang, W. Guo, X. Fan, T. Su, S. Peng, C. Gao, Characterization and bioactivity evaluation of (Polyetheretherketone/Polyglycolicacid)-Hydroxyapatite scaffolds for tissue regeneration, Materials 9 (11) (2016).

[160] C. Wang, W. Huang, Y. Zhou, L. He, Z. He, Z. Chen, X. He, S. Tian, J. Liao, B. Lu, Y. Wei, M. Wang, 3D printing of bone tissue engineering scaffolds, Bioact. Mater. 5 (1) (2020) 82–91.
[161] X. Han, N. Sharma, Z. Xu, L. Scheideler, J. Geis-Gerstorfer, F. Rupp, F.M. Thieringer, S. Spintzyk, An in vitro study of osteoblast response on fused-filament fabrication 3D printed PEEK for dental and cranio-maxillofacial implants, J. Clin. Med. 8 (6) (2019).
[162] C. Zhang, L. Wang, J. Kang, O.M. Fuentes, D. Li, Bionic design and verification of 3D printed PEEK costal cartilage prosthesis, J. Mech. Behav. Biomed. Mater. 103 (2020), 103561.
[163] D. Liu, J. Fu, H. Fan, D. Li, E. Dong, X. Xiao, L. Wang, Z. Guo, Application of 3D-printed PEEK scapula prosthesis in the treatment of scapular benign fibrous histiocytoma: a case report, Journal of bone oncology 12 (2018) 78–82.
[164] X. Han, D. Yang, C. Yang, S. Spintzyk, L. Scheideler, P. Li, D. Li, J. Geis-gerstorfer, F. Rupp, carbon fiber reinforced PEEK composites based on 3D-printing technology for orthopedic and dental applications, J. Clin. Med. 8 (2) (2019).
[165] E. Buck, H. Li, M. Cerruti, Surface modification strategies to improve the osseointegration of poly(etheretherketone) and its composites, Macromol. Biosci. 20 (2) (2020), e1900271.
[166] M. He, Y. Huang, H. Xu, G. Feng, L. Liu, Y. Li, D. Sun, L. Zhang, Modification of polyetheretherketone implants: from enhancing bone integration to enabling multi-modal therapeutics, Acta Biomater. 129 (2021) 18–32.
[167] A.P. Kusumbe, S.K. Ramasamy, R.H. Adams, Coupling of angiogenesis and osteogenesis by a specific vessel subtype in bone, Nature 507 (7492) (2014) 323–328.
[168] S. Stegen, N. van Gastel, G. Carmeliet, Bringing new life to damaged bone: the importance of angiogenesis in bone repair and regeneration, Bone 70 (2015) 19–27.
[169] U. Riaz, I. Shabib, W. Haider, The current trends of Mg alloys in biomedical applications-A review, J. Biomed. Mater. Res. B Appl. Biomater. 107 (6) (2019) 1970–1996.
[170] M.P. Staiger, A.M. Pietak, J. Huadmai, G. Dias, Magnesium and its alloys as orthopedic biomaterials: a review, Biomaterials 27 (9) (2006) 1728–1734.
[171] D. Zhao, F. Witte, F. Lu, J. Wang, J. Li, L. Qin, Current status on clinical applications of magnesium-based orthopaedic implants: a review from clinical translational perspective, Biomaterials 112 (2017) 287–302.
[172] X. Wei, W. Zhou, Z. Tang, H. Wu, Y. Liu, H. Dong, N. Wang, H. Huang, S. Bao, L. Shi, X. Li, Y. Zheng, Z. Guo, Magnesium surface-activated 3D printed porous PEEK scaffolds for in vivo osseointegration by promoting angiogenesis and osteogenesis, Bioact. Mater. 20 (2023) 16–28.
[173] Y. Tian, C. Chen, X. Xu, J. Wang, X. Hou, K. Li, X. Lu, H. Shi, E.S. Lee, H.B. Jiang, A review of 3D printing in dentistry: technologies, affecting factors, and applications, Scanning 2021 (2021), 9950131.
[174] D. Anssari Moin, W. Derksen, H. Waars, B. Hassan, D. Wismeijer, Computer-assisted template-guided custom-designed 3D-printed implant placement with custom-designed 3D-printed surgical tooling: an in-vitro proof of a novel concept, Clin. Oral Implants Res. 28 (5) (2017) 582–585.
[175] X. Lv, X. Wang, S. Tang, D. Wang, L. Yang, A. He, T. Tang, J. Wei, Incorporation of molybdenum disulfide into polyetheretherketone creating biocomposites with improved mechanical, tribological performances and cytocompatibility for artificial joints applications, Colloids Surf. B Biointerfaces 189 (2020), 110819.
[176] J. Zhang, W. Wei, L. Yang, Y. Pan, X. Wang, T. Wang, S. Tang, Y. Yao, H. Hong, J. Wei, Stimulation of cell responses and bone ingrowth into macro-microporous implants of nano-bioglass/polyetheretherketone composite and enhanced antibacterial activity by release of hinokitiol, Colloids Surf. B Biointerfaces 164 (2018) 347–357.
[177] J. Cao, Y. Lu, H. Chen, L. Zhang, C. Xiong, Preparation, mechanical properties and in vitro cytocompatibility of multi-walled carbon nanotubes/poly(etheretherketone) nanocomposites, J. Biomater. Sci. Polym. Ed. 29 (4) (2018) 428–447.
[178] R. Ma, Z. Yu, S. Tang, Y. Pan, J. Wei, T. Tang, Osseointegration of nanohydroxyapatite- or nano-calcium silicate-incorporated polyetheretherketone bioactive composites in vivo, Int. J. Nanomed. 11 (2016) 6023–6033.
[179] X. Tang, K. Huang, J. Dai, Z. Wu, L. Cai, L. Yang, J. Wei, H. Sun, Influences of surface treatments with abrasive paper and sand-blasting on surface morphology, hydrophilicity, mineralization and osteoblasts behaviors of n-CS/PK composite, Sci. Rep. 7 (1) (2017) 568.
[180] L. Ren, S. Tang, X. Shen, C. Gao, Y.K. Jung, D. Wang, A. He, L. Yang, J.W. Shin, J. Wei, Influences of sodium tantalite submicro-particles in polyetheretherketone based composites on behaviors of rBMSCs/HGE-1 cells for dental application, Colloids Surf. B Biointerfaces 188 (2020), 110723.
[181] J. Ge, F. Wang, Z. Xu, X. Shen, C. Gao, D. Wang, G. Hu, J. Gu, T. Tang, J. Wei, Influences of niobium pentoxide on roughness, hydrophilicity, surface energy and protein absorption, and cellular responses to PEEK based composites for orthopedic applications, J. Mater. Chem. B 8 (13) (2020) 2618–2626.
[182] G. Pezzotti, E. Marin, T. Adachi, F. Lerussi, A. Rondinella, F. Boschetto, W. Zhu, T. Kitajima, K. Inada, B.J. McEntire, R.M. Bock, B.S. Bal, O. Mazda, Incorporating Si3 N4 into PEEK to produce antibacterial, osteocondutive, and radiolucent spinal implants, Macromol. Biosci. 18 (6) (2018), e1800033.
[183] P. Sikder, J.A. Ferreira, E.A. Fakhrabadi, K.Z. Kantorski, M.W. Liberatore, M.C. Bottino, S.B. Bhaduri, Bioactive amorphous magnesium phosphate-polyetheretherketone composite filaments for 3D printing, Dent. Mater. 36 (7) (2020) 865–883.
[184] S. Mei, L. Yang, Y. Pan, D. Wang, X. Wang, T. Tang, J. Wei, Influences of tantalum pentoxide and surface coarsening on surface roughness, hydrophilicity, surface energy, protein adsorption and cell responses to PEEK based biocomposite, Colloids Surf. B Biointerfaces 174 (2019) 207–215.
[185] P. Feng, P. Wu, C. Gao, Y. Yang, W. Guo, W. Yang, C. Shuai, A multimaterial scaffold with tunable properties: toward bone tissue repair, Adv. Sci. 5 (6) (2018), 1700817.
[186] L. Cai, Y. Pan, S. Tang, Q. Li, T. Tang, K. Zheng, A.R. Boccaccini, S. Wei, J. Wei, J. Su, Macro-mesoporous composites containing PEEK and mesoporous diopside as bone implants: characterization, in vitro mineralization, cytocompatibility, and vascularization potential and osteogenesis in vivo, J. Mater. Chem. B 5 (42) (2017) 8337–8352.
[187] L. Cai, J. Zhang, J. Qian, Q. Li, H. Li, Y. Yan, S. Wei, J. Wei, J. Su, The effects of surface bioactivity and sustained-release of genistein from a mesoporous magnesium-calcium-silicate/PK composite stimulating cell responses in vitro, and promoting osteogenesis and enhancing osseointegration in vivo, Biomater. Sci. 6 (4) (2018) 842–853.
[188] H.D. Jung, H.S. Park, M.H. Kang, Y. Li, H.E. Kim, Y.H. Koh, Y. Estrin, Reinforcement of polyetheretherketone polymer with titanium for improved mechanical properties and in vitro biocompatibility, J. Biomed. Mater. Res. B Appl. Biomater. 104 (1) (2016) 141–148.
[189] A.F. Widmer, New developments in diagnosis and treatment of infection in orthopedic implants, Clinical infectious diseases, an official publication of the Infectious Diseases Society of America 33 (Suppl 2) (2001) S94–S106.
[190] A. Di Martino, R. Papalia, E. Albo, L. Diaz, L. Denaro, V. Denaro, Infection after spinal surgery and procedures, Eur. Rev. Med. Pharmacol. Sci. 23 (2 Suppl) (2019) 173–178.
[191] D. Hedequist, A. Haugen, T. Hresko, J. Emans, Failure of attempted implant retention in spinal deformity delayed surgical site infections, Spine 34 (1) (2009) 60–64.
[192] E.N. Perencevich, K.E. Sands, S.E. Cosgrove, E. Guadagnoli, E. Meara, R. Platt, Health and economic impact of surgical site infections diagnosed after hospital discharge, Emerg. Infect. Dis. 9 (2) (2003) 196–203.
[193] E. Mylona, M. Samarkos, E. Kakalou, P. Fanourgiakis, A. Skoutelis, Pyogenic vertebral osteomyelitis: a systematic review of clinical characteristics, Semin. Arthritis Rheum. 39 (1) (2009) 10–17.
[194] J.C. Alverdy, N. Hyman, J. Gilbert, Re-examining causes of surgical site infections following elective surgery in the era of asepsis, the Lancet, Infectious diseases 20 (3) (2020) e38–e43.
[195] J. Chahoud, Z. Kanafani, S.S. Kanj, Surgical site infections following spine surgery: eliminating the controversies in the diagnosis, Front. Med. 1 (2014) 7.
[196] M. Ribeiro, F.J. Monteiro, M.P. Ferraz, Infection of orthopedic implants with emphasis on bacterial adhesion process and techniques used in studying bacterial-material interactions, Biomatter 2 (4) (2012) 176–194.
[197] M.Q. Shah, M.S. Zardad, A. Khan, S. Ahmed, A.S. Awan, T. Mohammad, Surgical site infection in orthopaedic implants and its common bacteria with their sensitivities to antibiotics, in open reduction internal fixation, J. Ayub Med. Coll. Abbottabad : J. Ayub Med. Coll. Abbottabad 29 (1) (2017) 50–53.
[198] X. Liu, C. Chen, H. Zhang, A. Tian, J. You, L. Wu, Z. Lei, X. Li, X. Bai, S. Chen, Biocompatibility evaluation of antibacterial Ti-Ag alloys with nanotubular coatings, Int. J. Nanomed. 14 (2019) 457–468.
[199] D. Daoust, J. Devaux, P. Godard, Mechanism and kinetics of poly(ether ether ketone) (PEEK) sulfonation in concentrated sulfuric acid at room temperature. Part 1. Qualitative comparison between polymer and monomer model compound sulfonation, Polym. Int. 50 (8) (2001) 917–924.
[200] J. Zhang, D. Li, W. Xu, Y. Fu, Effect of SO_2 controlled release packaging on preservation performance of cherry, Packag. Eng. 34 (15) (2013) 49.
[201] A. Xu, X. Liu, X. Gao, F. Deng, Y. Deng, S. Wei, Enhancement of osteogenesis on micro/nano-topographical carbon fiber-reinforced polyetheretherketone-nanohydroxyapatite biocomposite, Mater Sci Eng C Mater Biol Appl 48 (2015) 592–598.
[202] K.W. Chan, C.Z. Liao, H.M. Wong, K.W.K. Yeung, S.C. Tjong, Preparation of polyetheretherketone composites with nanohydroxyapatite rods and carbon nanofibers having high strength, good biocompatibility and excellent thermal stability, RSC Adv. 6 (23) (2016) 19417–19429.
[203] Y. Niu, L. Guo, F. Hu, L. Ren, Q. Zhou, J. Ru, J. Wei, Macro-microporous surface with sulfonic acid groups and micro-nano structures of PEEK/nano magnesium silicate composite exhibiting antibacterial activity and inducing cell responses, Int. J. Nanomed. 15 (2020) 2403–2417.
[204] B.R. Levine, S. Sporer, R.A. Poggie, C.J. Della Valle, J.J. Jacobs, Experimental and clinical performance of porous tantalum in orthopedic surgery, Biomaterials 27 (27) (2006) 4671–4681.
[205] S. Mei, F. Wang, X. Hu, K. Yang, D. Xie, L. Yang, Z. Wu, J. Wei, Construction of a hierarchical micro & nanoporous surface for loading genistein on the composite of polyetheretherketone/tantalum pentoxide possessing antibacterial activity and accelerated osteointegration, Biomater. Sci. 9(1) (2020) 167–185.
[206] A.F. Chen, A. Fleischman, M.S. Austin, Use of intrawound antibiotics in orthopaedic surgery, J. Am. Acad. Orthop. Surg. 26 (17) (2018) e371–e378.
[207] F.A. Sweet, M. Roh, C. Sliva, Intrawound application of vancomycin for prophylaxis in instrumented thoracolumbar fusions: efficacy, drug levels, and patient outcomes, Spine 36 (24) (2011) 2084–2088.
[208] S.A. McEwen, P.J. Collignon, Antimicrobial resistance: a one health perspective, Microbiol. Spectr. 6 (2) (2018).
[209] S.M. Shiels, V.P. Raut, P.B. Patterson, B.R. Barnes, J.C. Wenke, Antibiotic-loaded bone graft for reduction of surgical site infection in spinal fusion, Spine J. 17 (12) (2017) 1917–1925.

[210] Y. Yang, H.Y. Ao, S.B. Yang, Y.G. Wang, W.T. Lin, Z.F. Yu, T.T. Tang, In vivo evaluation of the anti-infection potential of gentamicin-loaded nanotubes on titania implants, Int. J. Nanomed. 11 (2016) 2223–2234.
[211] Z. Xue, Z. Wang, A. Sun, J. Huang, W. Wu, M. Chen, X. Hao, Z. Huang, X. Lin, S. Weng, Rapid construction of polyetheretherketone (PEEK) biological implants incorporated with brushite (CaHPO4.2H2O) and antibiotics for anti-infection and enhanced osseointegration, Mater Sci Eng C Mater Biol Appl 111 (2020), 110782.
[212] J. Yan, W. Zhou, Z. Jia, P. Xiong, Y. Li, P. Wang, Q. Li, Y. Cheng, Y. Zheng, Endowing polyetheretherketone with synergistic bactericidal effects and improved osteogenic ability, Acta Biomater. 79 (2018) 216–229.
[213] A. Sun, X. Lin, Z. Xue, J. Huang, X. Bai, L. Huang, X. Lin, S. Weng, M. Chen, Facile surface functional polyetheretherketone with antibacterial and immunoregulatory activities for enhanced regeneration toward bacterium-infected bone destruction, Drug Deliv. 28 (1) (2021) 1649–1663.
[214] J. Yin, Q. Han, J. Zhang, Y. Liu, X. Gan, K. Xie, L. Xie, Y. Deng, MXene-based hydrogels endow polyetheretherketone with effective osteogenicity and combined treatment of osteosarcoma and bacterial infection, ACS Appl. Mater. Interfaces 12 (41) (2020) 45891–45903.
[215] X. Xu, Y. Li, L. Wang, Y. Li, J. Pan, X. Fu, Z. Luo, Y. Sui, S. Zhang, L. Wang, Y. Ni, L. Zhang, S. Wei, Triple-functional polyetheretherketone surface with enhanced bacteriostasis and anti-inflammatory and osseointegrative properties for implant application, Biomaterials 212 (2019) 98–114.
[216] N. Mookherjee, M.A. Anderson, H.P. Haagsman, D.J. Davidson, Antimicrobial host defence peptides: functions and clinical potential, Nat. Rev. Drug Discov. 19 (5) (2020) 311–332.
[217] Y. Li, Q. Xiang, Q. Zhang, Y. Huang, Z. Su, Overview on the recent study of antimicrobial peptides: origins, functions, relative mechanisms and application, Peptides 37 (2) (2012) 207–215.
[218] B.C. Wu, A.H. Lee, R.E.W. Hancock, Mechanisms of the innate defense regulator peptide-1002 anti-inflammatory activity in a sterile inflammation mouse model, J. Immunol. 199 (10) (2017) 3592–3603.
[219] S.C. Mansour, C. de la Fuente-Núñez, R.E. Hancock, Peptide IDR-1018: modulating the immune system and targeting bacterial biofilms to treat antibiotic-resistant bacterial infections, J. Pept. Sci. : an official publication of the European Peptide Society 21 (5) (2015) 323–329.
[220] X. Meng, J. Zhang, J. Chen, B. Nie, B. Yue, W. Zhang, Z. Lyu, T. Long, Y. Wang, KR-12 coating of polyetheretherketone (PEEK) surface via polydopamine improves osteointegration and antibacterial activity in vivo, J. Mater. Chem. B 8(44) (2020) 10190–10204.
[221] J. Röhrl, D. Yang, J.J. Oppenheim, T. Hehlgans, Human beta-defensin 2 and 3 and their mouse orthologs induce chemotaxis through interaction with CCR2, J. Immunol. 184 (12) (2010) 6688–6694.
[222] K. Hinrichsen, R. Podschun, S. Schubert, J.M. Schröder, J. Harder, E. Proksch, Mouse beta-defensin-14, an antimicrobial ortholog of human beta-defensin-3, Antimicrob. Agents Chemother. 52 (5) (2008) 1876–1879.
[223] R.E. Hancock, G. Diamond, The role of cationic antimicrobial peptides in innate host defences, Trends Microbiol. 8 (9) (2000) 402–410.
[224] X. Yuan, L. Ouyang, Y. Luo, Z. Sun, C. Yang, J. Wang, X. Liu, X. Zhang, Multifunctional sulfonated polyetheretherketone coating with beta-defensin-14 for yielding durable and broad-spectrum antibacterial activity and osseointegration, Acta Biomater. 86 (2019) 323–337.
[225] C. Yang, L. Ouyang, W. Wang, B. Chen, W. Liu, X. Yuan, Y. Luo, T. Cheng, K.W.K. Yeung, X. Liu, X. Zhang, Sodium butyrate-modified sulfonated polyetheretherketone modulates macrophage behavior and shows enhanced antibacterial and osteogenic functions during implant-associated infections, J. Mater. Chem. B 7 (36) (2019) 5541–5553.
[226] X. He, Y. Deng, Y. Yu, H. Lyu, L. Liao, Drug-loaded/grafted peptide-modified porous PEEK to promote bone tissue repair and eliminate bacteria, Colloids Surf. B Biointerfaces 181 (2019) 767–777.
[227] P. Guilloteau, L. Martin, V. Eeckhaut, R. Ducatelle, R. Zabielski, F. Van Immerseel, From the gut to the peripheral tissues: the multiple effects of butyrate, Nutr. Res. Rev. 23 (2) (2010) 366–384.
[228] G. Chen, X. Ran, B. Li, Y. Li, D. He, B. Huang, S. Fu, J. Liu, W. Wang, Sodium butyrate inhibits inflammation and maintains epithelium barrier integrity in a TNBS-induced inflammatory bowel disease mice model, EBioMedicine 30 (2018) 317–325.
[229] R.O. Corrêa, A. Vieira, E.M. Sernaglia, M. Lancellotti, A.T. Vieira, M.J. Avila-Campos, H.G. Rodrigues, M.A.R. Vinolo, Bacterial short-chain fatty acid metabolites modulate the inflammatory response against infectious bacteria, Cell Microbiol. 19 (7) (2017).
[230] J. Ji, D. Shu, M. Zheng, J. Wang, C. Luo, Y. Wang, F. Guo, X. Zou, X. Lv, Y. Li, T. Liu, H. Qu, Microbial metabolite butyrate facilitates M2 macrophage polarization and function, Sci. Rep. 6 (2016), 24838.
[231] N. Alva-Murillo, A. Ochoa-Zarzosa, J.E. López-Meza, Short chain fatty acids (propionic and hexanoic) decrease Staphylococcus aureus internalization into bovine mammary epithelial cells and modulate antimicrobial peptide expression, Vet. Microbiol. 155 (2–4) (2012) 324–331.
[232] N. Alva-Murillo, I. Medina-Estrada, M. Báez-Magaña, A. Ochoa-Zarzosa, J.E. López-Meza, The activation of the TLR2/p38 pathway by sodium butyrate in bovine mammary epithelial cells is involved in the reduction of Staphylococcus aureus internalization, Mol. Immunol. 68 (2 Pt B) (2015) 445–455.
[233] L.N. Nguyen, L.C. Lopes, R.J. Cordero, J.D. Nosanchuk, Sodium butyrate inhibits pathogenic yeast growth and enhances the functions of macrophages, J. Antimicrob. Chemother. 66 (11) (2011) 2573–2580.
[234] X.X. Gong, X.S. Su, K. Zhan, G.Q. Zhao, The protective effect of chlorogenic acid on bovine mammary epithelial cells and neutrophil function, J. Dairy Sci. 101 (11) (2018) 10089–10097.
[235] M. Naveed, V. Hejazi, M. Abbas, A.A. Kamboh, G.J. Khan, M. Shumzaid, F. Ahmad, D. Babazadeh, X. FangFang, F. Modarresi-Ghazani, L. WenHua, Z. XiaoHui, Chlorogenic acid (CGA): a pharmacological review and call for further research, Biomedicine & pharmacotherapy = Biomedecine & pharmacotherapie 97 (2018) 67–74.
[236] E. Tranquillo, F. Barrino, G. Dal Poggetto, I. Blanco, Sol-gel synthesis of silica-based materials with different percentages of PEG or PCL and high chlorogenic acid content, Materials 12 (1) (2019) 12.
[237] M. Hentzer, M. Givskov, Pharmacological inhibition of quorum sensing for the treatment of chronic bacterial infections, J. Clin. Invest. 112 (9) (2003) 1300–1307.
[238] U.A. Pereira, L.C. Barbosa, C.R. Maltha, A.J. Demuner, M.A. Masood, A.L. Pimenta, γ-Alkylidene-γ-lactones and isobutylpyrrol-2(5H)-ones analogues to rubrolides as inhibitors of biofilm formation by gram-positive and gram-negative bacteria, Bioorg. Med. Chem. Lett 24 (4) (2014) 1052–1056.
[239] M. Manefield, T.B. Rasmussen, M. Henzter, J.B. Andersen, P. Steinberg, S. Kjelleberg, M. Givskov, Halogenated furanones inhibit quorum sensing through accelerated LuxR turnover, Microbiol. 148 (Pt 4) (2002) 1119–1127.
[240] U.A. Pereira, L.C. Barbosa, C.R. Maltha, A.J. Demuner, M.A. Masood, A.L. Pimenta, Inhibition of Enterococcus faecalis biofilm formation by highly active lactones and lactams analogues of rubrolides, Eur. J. Med. Chem. 82 (2014) 127–138.
[241] J.F. Montero, L.C. Barbosa, U.A. Pereira, G.M. Barra, M.C. Fredel, C.A. Benfatti, R.S. Magini, A.L. Pimenta, J.C. Souza, Chemical, microscopic, and microbiological analysis of a functionalized poly-ether-ether-ketone-embedding antibiofilm compounds, J. Biomed. Mater. Res. 104 (12) (2016) 3015–3020.
[242] P. Amdjadi, H. Nojehdehian, F. Najafi, A. Ghasemi, M. Seifi, E. Dashtimoghadam, F. Fahimipour, L. Tayebi, Ultraviolet-induced surface grafting of octafluoropentyl methacrylate on polyether ether ketone for inducing antibiofilm properties, J. Biomater. Appl. 32 (1) (2017) 3–11.
[243] A. Yousaf, A. Farrukh, Z. Oluz, E. Tuncel, H. Duran, S.Y. Dogan, T. Tekinay, H.U. Rehman, B. Yameen, UV-light assisted single step route to functional PEEK surfaces, React. Funct. Polym. 83 (2014) 70–75.
[244] S. Buwalda, S. Rotman, D. Eglin, F. Moriarty, A. Bethry, X. Garric, O. Guillaume, B. Nottelet, Synergistic anti-fouling and bactericidal poly(ether ether ketone) surfaces via a one-step photomodification, Mater Sci Eng C Mater Biol Appl 111 (2020), 110811.
[245] R. Jayakumar, M. Prabaharan, S.V. Nair, S. Tokura, H. Tamura, N. Selvamurugan, Novel carboxymethyl derivatives of chitin and chitosan materials and their biomedical applications, Prog. Mater. Sci. 55 (7) (2010) 675–709.
[246] F. Wu, G. Meng, J. He, Y. Wu, F. Wu, Z. Gu, Antibiotic-loaded chitosan hydrogel with superior dual functions: antibacterial efficacy and osteoblastic cell responses, ACS Appl. Mater. Interfaces 6 (13) (2014) 10005–10013.
[247] R. Budiraharjo, K.G. Neoh, E.T. Kang, Hydroxyapatite-coated carboxymethyl chitosan scaffolds for promoting osteoblast and stem cell differentiation, J. Colloid Interface Sci. 366 (1) (2012) 224–232.
[248] D. Mishra, B. Bhunia, I. Banerjee, P. Datta, S. Dhara, T.K. Maiti, Enzymatically crosslinked carboxymethyl-chitosan/gelatin/nano-hydroxyapatite injectable gels for in situ bone tissue engineering application, Mater. Sci. Eng. C-Mater. Biol. Appl. 31 (7) (2011) 1295–1304.
[249] A. Xu, L. Zhou, Y. Deng, X. Chen, X. Xiong, F. Deng, S. Wei, A carboxymethyl chitosan and peptide-decorated polyetheretherketone ternary biocomposite with enhanced antibacterial activity and osseointegration as orthopedic/dental implants, J. Mater. Chem. B 4 (10) (2016) 1878–1890.
[250] D.R. Dreyer, A.D. Todd, C.W. Bielawski, Harnessing the chemistry of graphene oxide, Chem. Soc. Rev. 43 (15) (2014) 5288–5301.
[251] J. Hong, N.J. Shah, A.C. Drake, P.C. DeMuth, J.B. Lee, J. Chen, P.T. Hammond, Graphene multilayers as gates for multi-week sequential release of proteins from surfaces, ACS Nano 6 (1) (2012) 81–88.
[252] D. Li, R.B. Kaner, Materials science. Graphene-based materials, Science (New York, N.Y.) 320 (5880) (2008) 1170–1171.
[253] Y. Luo, H. Shen, Y. Fang, Y. Cao, J. Huang, M. Zhang, J. Dai, X. Shi, Z. Zhang, Enhanced proliferation and osteogenic differentiation of mesenchymal stem cells on graphene oxide-incorporated electrospun poly(lactic-co-glycolic acid) nanofibrous mats, ACS Appl. Mater. Interfaces 7 (11) (2015) 6331–6339.
[254] Z. Jia, Y. Shi, P. Xiong, W. Zhou, Y. Cheng, Y. Zheng, T. Xi, S. Wei, From solution to biointerface: graphene self-assemblies of varying lateral sizes and surface properties for biofilm control and osteodifferentiation, ACS Appl. Mater. Interfaces 8 (27) (2016) 17151–17165.
[255] Y.H. Wang, H.H. Deng, Y.H. Liu, X.Q. Shi, A.L. Liu, H.P. Peng, G.L. Hong, W. Chen, Partially reduced graphene oxide as highly efficient DNA nanoprobe, Biosens. Bioelectron. 80 (2016) 140–145.
[256] S. Ge, M. Yan, J. Lu, M. Zhang, F. Yu, J. Yu, X. Song, S. Yu, Electrochemical biosensor based on graphene oxide-Au nanoclusters composites for L-cysteine analysis, Biosens. Bioelectron. 31 (1) (2012) 49–54.
[257] X.T. Zheng, X.Q. Ma, C.M. Li, Highly efficient nuclear delivery of anti-cancer drugs using a bio-functionalized reduced graphene oxide, J. Colloid Interface Sci. 467 (2016) 35–42.
[258] Q. Liu, L. Wei, J. Wang, F. Peng, D. Luo, R. Cui, Y. Niu, X. Qin, Y. Liu, H. Sun, J. Yang, Y. Li, Cell imaging by graphene oxide based on surface enhanced Raman scattering, Nanoscale 4 (22) (2012) 7084–7089.
[259] L. Feng, Z. Liu, Graphene in biomedicine: opportunities and challenges, Nanomed. 6 (2) (2011) 317–324.

[260] C. Chung, Y.K. Kim, D. Shin, S.R. Ryoo, B.H. Hong, D.H. Min, Biomedical applications of graphene and graphene oxide, Acc. Chem. Res. 46 (10) (2013) 2211–2224.
[261] V.C. Sanchez, A. Jachak, R.H. Hurt, A.B. Kane, Biological interactions of graphene-family nanomaterials: an interdisciplinary review, Chem. Res. Toxicol. 25 (1) (2012) 15–34.
[262] K. Yang, J. Wan, S. Zhang, Y. Zhang, S.T. Lee, Z. Liu, In vivo pharmacokinetics, long-term biodistribution, and toxicology of PEGylated graphene in mice, ACS Nano 5 (1) (2011) 516–522.
[263] L. Ouyang, Y. Deng, L. Yang, X. Shi, T. Dong, Y. Tai, W. Yang, Z.G. Chen, Graphene-oxide-decorated microporous polyetheretherketone with superior antibacterial capability and in vitro osteogenesis for orthopedic implant, Macromol. Biosci. 18 (6) (2018), e1800036.
[264] S. Wang, C. Duan, W. Yang, X. Gao, J. Shi, J. Kang, Y. Deng, X.L. Shi, Z.G. Chen, Two-dimensional nanocoating-enabled orthopedic implants for bimodal therapeutic applications, Nanoscale 12 (22) (2020) 11936–11946.
[265] R.S. MacDonald, The role of zinc in growth and cell proliferation, J. Nutr. 130 (5S Suppl) (2000) 1500s, 8s.
[266] K.B. Hadley, S.M. Newman, J.R. Hunt, Dietary zinc reduces osteoclast resorption activities and increases markers of osteoblast differentiation, matrix maturation, and mineralization in the long bones of growing rats, J. Nutr. Biochem. 21 (4) (2010) 297–303.
[267] K.M. Reddy, K. Feris, J. Bell, D.G. Wingett, C. Hanley, A. Punnoose, Selective toxicity of zinc oxide nanoparticles to prokaryotic and eukaryotic systems, Appl. Phys. Lett. 90 (213902) (2007) 2139021–2139023.
[268] G. Jin, H. Cao, Y. Qiao, F. Meng, H. Zhu, X. Liu, Osteogenic activity and antibacterial effect of zinc ion implanted titanium, Colloids Surf. B Biointerfaces 117 (2014) 158–165.
[269] G. Jin, H. Qin, H. Cao, S. Qian, Y. Zhao, X. Peng, X. Zhang, X. Liu, P.K. Chu, Synergistic effects of dual Zn/Ag ion implantation in osteogenic activity and antibacterial ability of titanium, Biomaterials 35 (27) (2014) 7699–7713.
[270] X.L. Wang, H. Zhu, F. Yang, X.R. Yang, Biofilm-engineered nanostructures, Adv. Mater. 21 (27) (2009) 2815–+.
[271] F. Yu, X. Fang, H. Jia, M. Liu, X. Shi, C. Xue, T. Chen, Z. Wei, F. Fang, H. Zhu, H. Xin, J. Feng, X. Wang, Zn or O? An atomic level comparison on antibacterial activities of zinc oxides, Chem. 22 (24) (2016) 8053–8058.
[272] X. Wang, F. Yang, W. Yang, X. Yang, A study on the antibacterial activity of one-dimensional ZnO nanowire arrays: effects of the orientation and plane surface, Chem. Commun. (42) (2007) 4419–4421.
[273] R. Brayner, R. Ferrari-Iliou, N. Brivois, S. Djediat, M.F. Benedetti, F. Fiévet, Toxicological impact studies based on Escherichia coli bacteria in ultrafine ZnO nanoparticles colloidal medium, Nano Lett. 6 (4) (2006) 866–870.
[274] R. Augustine, H.N. Malik, D.K. Singhal, A. Mukherjee, D. Malakar, N. Kalarikkal, S. Thomas, Electrospun polycaprolactone/ZnO nanocomposite membranes as biomaterials with antibacterial and cell adhesion properties, J. Polym. Res. 21 (3) (2014) 17.
[275] J. Ye, J. Deng, Y. Chen, T. Yang, Y. Zhu, C. Wu, T. Wu, J. Jia, X. Cheng, X. Wang, Cicada and catkin inspired dual biomimetic antibacterial structure for the surface modification of implant material, Biomater. Sci. 7 (7) (2019) 2826–2832.
[276] Y. Deng, L. Yang, X. Huang, J. Chen, X. Shi, W. Yang, M. Hong, Y. Wang, M.S. Dargusch, Z.G. Chen, Dual Ag/ZnO-decorated micro-/nanoporous sulfonated polyetheretherketone with superior antibacterial capability and biocompatibility via layer-by-layer self-assembly strategy, Macromol. Biosci. 18 (7) (2018), e1800028.
[277] T. Lu, J. Li, S. Qian, H. Cao, C. Ning, X. Liu, Enhanced osteogenic and selective antibacterial activities on micro-/nano-structured carbon fiber reinforced polyetheretherketone, J. Mater. Chem. B 4 (17) (2016) 2944–2953.
[278] S. Yang, W. Yu, J. Zhang, X. Han, J. Wang, D. Sun, R. Shi, Y. Zhou, H. Zhang, J. Zhao, The antibacterial property of zinc oxide/graphene oxide modified porous polyetheretherketone againstS, sanguinis, F. nucleatumandP. gingivalis, Biomed Mater 17 (2) (2022).
[279] Y. Zhang, H. Wu, B. Yuan, X. Zhu, K. Zhang, X. Zhang, Enhanced osteogenic activity and antibacterial performance in vitro of polyetheretherketone by plasma-induced graft polymerization of acrylic acid and incorporation of zinc ions, J. Mater. Chem. B 9 (36) (2021) 7506–7515.
[280] C.H. Li, C.C. Shen, Y.W. Cheng, S.H. Huang, C.C. Wu, C.C. Kao, J.W. Liao, J.J. Kang, Organ biodistribution, clearance, and genotoxicity of orally administered zinc oxide nanoparticles in mice, Nanotoxicology 6 (7) (2012) 746–756.
[281] C.M. Sayes, K.L. Reed, D.B. Warheit, Assessing toxicity of fine and nanoparticles: comparing in vitro measurements to in vivo pulmonary toxicity profiles, Toxicol. Sci. : an official journal of the Society of Toxicology 97 (1) (2007) 163–180.
[282] Y.H. Kim, F. Fazlollahi, I.M. Kennedy, N.R. Yacobi, S.F. Hamm-Alvarez, Z. Borok, K.J. Kim, E.D. Crandall, Alveolar epithelial cell injury due to zinc oxide nanoparticle exposure, Am. J. Respir. Crit. Care Med. 182 (11) (2010) 1398–1409.
[283] S. Chernousova, M. Epple, Silver as antibacterial agent: ion, nanoparticle, and metal, Angew. Chem. 52 (6) (2013) 1636–1653.
[284] A. Gupta, K. Matsui, J.F. Lo, S. Silver, Molecular basis for resistance to silver cations in Salmonella, Nat. Med. 5 (2) (1999) 183–188.
[285] K. Mijnendonckx, N. Leys, J. Mahillon, S. Silver, R. Van Houdt, Antimicrobial silver: uses, toxicity and potential for resistance, Biometals : an international journal on the role of metal ions in biology, biochemistry, and medicine 26 (4) (2013) 609–621.
[286] S. Tang, J. Zheng, Antibacterial activity of silver nanoparticles: structural effects, Adv Healthc Mater 7 (13) (2018), e1701503.
[287] G. Wang, W. Jin, A.M. Qasim, A. Gao, X. Peng, W. Li, H. Feng, P.K. Chu, Antibacterial effects of titanium embedded with silver nanoparticles based on electron-transfer-induced reactive oxygen species, Biomaterials 124 (2017) 25–34.
[288] J.R. Morones-Ramirez, J.A. Winkler, C.S. Spina, J.J. Collins, Silver enhances antibiotic activity against gram-negative bacteria, Sci. Transl. Med. 5 (190) (2013), 190ra81.
[289] X. Liu, K. Gan, H. Liu, X. Song, T. Chen, C. Liu, Antibacterial properties of nano-silver coated PEEK prepared through magnetron sputtering, Dent. Mater. 33 (9) (2017) e348–e360.
[290] L. Deng, Y. Deng, K. Xie, AgNPs-decorated 3D printed PEEK implant for infection control and bone repair, Colloids Surf. B Biointerfaces 160 (2017) 483–492.
[291] J. Yan, D. Xia, W. Zhou, Y. Li, P. Xiong, Q. Li, P. Wang, M. Li, Y. Zheng, Y. Cheng, pH-responsive silk fibroin-based CuO/Ag micro/nano coating endows polyetheretherketone with synergistic antibacterial ability, osteogenesis, and angiogenesis, Acta Biomater. 115 (2020) 220–234.
[292] X. Yang, H. Chai, L. Guo, Y. Jiang, L. Xu, W. Huang, Y. Shen, L. Yu, Y. Liu, J. Liu, In situ preparation of porous metal-organic frameworks ZIF-8@Ag on poly-ether-ether-ketone with synergistic antibacterial activity, Colloids Surf. B Biointerfaces 205 (2021), 111920.
[293] L. Zhao, H. Wang, K. Huo, L. Cui, W. Zhang, H. Ni, Y. Zhang, Z. Wu, P.K. Chu, Antibacterial nano-structured titania coating incorporated with silver nanoparticles, Biomaterials 32 (24) (2011) 5706–5716.
[294] M. Ramstedt, B. Ekstrand-Hammarström, A.V. Shchukarev, A. Bucht, L. Osterlund, M. Welch, W.T. Huck, Bacterial and mammalian cell response to poly(3-sulfopropyl methacrylate) brushes loaded with silver halide salts, Biomaterials 30 (8) (2009) 1524–1531.
[295] M. Roy, A. Bandyopadhyay, S. Bose, In vitro antimicrobial and biological properties of laser assisted tricalcium phosphate coating, Mater Sci Eng C Mater Biol Appl 29 (6) (2009) 1965–1968.
[296] K. Das, S. Bose, A. Bandyopadhyay, B. Karandikar, B.L. Gibbins, Surface coatings for improvement of bone cell materials and antimicrobial activities of Ti implants, J. Biomed. Mater. Res. B Appl. Biomater. 87 (2) (2008) 455–460.
[297] P.V. AshaRani, G. Low Kah Mun, M.P. Hande, S. Valiyaveettil, Cytotoxicity and genotoxicity of silver nanoparticles in human cells, ACS Nano 3 (2) (2009) 279–290.
[298] M. Akter, M.T. Sikder, M.M. Rahman, A. Ullah, K.F.B. Hossain, S. Banik, T. Hosokawa, T. Saito, M. Kurasaki, A systematic review on silver nanoparticles-induced cytotoxicity: physicochemical properties and perspectives, J. Adv. Res. 9 (2018) 1–16.
[299] D. Sarkar, S.K. Swain, S. Adhikari, B.S. Reddy, H.S. Maiti, Synthesis, mechanical properties and bioactivity of nanostructured zirconia, Mater Sci Eng C Mater Biol Appl 33 (6) (2013) 3413–3417.
[300] Y.Y. Yan, Y. Han, Structure and bioactivity of micro-arc oxidized zirconia films, Surf. Coat. Technol. 201 (9–11) (2007) 5692–5695.
[301] X. Liu, A. Huang, C. Ding, P.K. Chu, Bioactivity and cytocompatibility of zirconia (ZrO(2)) films fabricated by cathodic arc deposition, Biomaterials 27 (21) (2006) 3904–3911.
[302] G. Wang, X. Liu, H. Zreiqat, C. Ding, Enhanced effects of nano-scale topography on the bioactivity and osteoblast behaviors of micron rough ZrO2 coatings, Colloids Surf. B Biointerfaces 86 (2) (2011) 267–274.
[303] V. Covacci, N. Bruzzese, G. Maccauro, C. Andreassi, G.A. Ricci, C. Piconi, E. Marmo, W. Burger, A. Cittadini, In vitro evaluation of the mutagenic and carcinogenic power of high purity zirconia ceramic, Biomaterials 20 (4) (1999) 371–376.
[304] F. Carinci, F. Pezzetti, S. Volinia, F. Francioso, D. Arcelli, E. Farina, A. Piattelli, Zirconium oxide: analysis of MG63 osteoblast-like cell response by means of a microarray technology, Biomaterials 25 (2) (2004) 215–228.
[305] Y. Josset, Z. Oum'Hamed, A. Zarrinpour, M. Lorenzato, J.J. Adnet, D. Laurent-Maquin, In vitro reactions of human osteoblasts in culture with zirconia and alumina ceramics, J. Biomed. Mater. Res. 47 (4) (1999) 481–493.
[306] L. Saldaña, A. Méndez-Vilas, L. Jiang, M. Multigner, J.L. González-Carrasco, M.T. Pérez-Prado, M.L. González-Martín, L. Munuera, N. Vilaboa, In vitro biocompatibility of an ultrafine grained zirconium, Biomaterials 28 (30) (2007) 4343–4354.
[307] G. Wang, F. Meng, C. Ding, P.K. Chu, X. Liu, Microstructure, bioactivity and osteoblast behavior of monoclinic zirconia coating with nanostructured surface, Acta Biomater. 6 (3) (2010) 990–1000.
[308] C.J. Frandsen, K.S. Brammer, K. Noh, L.S. Connelly, S. Oh, L.H. Chen, S.J. Jin, Zirconium oxide nanotube surface prompts increased osteoblast functionality and mineralization, Mater. Sci. Eng. C-Mater. Biol. Appl. 31 (8) (2011) 1716–1722.
[309] Y. Ichikawa, Y. Akagawa, H. Nikai, H. Tsuru, Tissue compatibility and stability of a new zirconia ceramic in vivo, J. Prosthet. Dent 68 (2) (1992) 322–326.
[310] S. Schultze-Mosgau, H. Schliephake, M. Radespiel-Tröger, F.W. Neukam, Osseointegration of endodontic endosseous cones: zirconium oxide vs titanium, Oral Surg. Oral Med. Oral Pathol. Oral Radiol. Endod. 89 (1) (2000) 91–98.
[311] M. Gahlert, S. Röhling, M. Wieland, C.M. Sprecher, H. Kniha, S. Milz, Osseointegration of zirconia and titanium dental implants: a histological and histomorphometrical study in the maxilla of pigs, Clin. Oral Implants Res. 20 (11) (2009) 1247–1253.
[312] S.L. Jangra, K. Stalin, N. Dilbaghi, S. Kumar, J. Tawale, S.P. Singh, R. Pasricha, Antimicrobial activity of zirconia (ZrO2) nanoparticles and zirconium complexes, J. Nanosci. Nanotechnol. 12 (9) (2012) 7105–7112.
[313] M. Gouda, Nano-zirconium oxide and nano-silver oxide/cotton gauze fabrics for antimicrobial and wound healing acceleration, J. Ind. Textil. 41 (3) (2012) 222–240.

[314] J. Li, S. Qian, C. Ning, X. Liu, rBMSC and bacterial responses to isoelastic carbon fiber-reinforced poly(ether-ether-ketone) modified by zirconium implantation, J. Mater. Chem. B 4 (1) (2016) 96–104.
[315] W. Zhang, H. Wang, A. Oyane, H. Tsurushima, P.K. Chu, Osteoblast differentiation and disinfection induced by nitrogen plasma-treated surfaces, Bio Med. Mater. Eng. 21 (2) (2011) 75–82.
[316] H. Wang, J. Ji, W. Zhang, W. Wang, Y. Zhang, Z. Wu, Y. Zhang, P.K. Chu, Rat calvaria osteoblast behavior and antibacterial properties of O(2) and N(2) plasma-implanted biodegradable poly(butylene succinate), Acta Biomater. 6 (1) (2010) 154–159.
[317] K. Gan, H. Liu, L. Jiang, X. Liu, X. Song, D. Niu, T. Chen, C. Liu, Bioactivity and antibacterial effect of nitrogen plasma immersion ion implantation on polyetheretherketone, Dent. Mater. 32 (11) (2016) e263–e274.
[318] T. Yabutsuka, K. Fukushima, T. Hiruta, S. Takai, T. Yao, Effect of pores formation process and oxygen plasma treatment to hydroxyapatite formation on bioactive PEEK prepared by incorporation of precursor of apatite, Mater Sci Eng C Mater Biol Appl 81 (2017) 349–358.
[319] T. Lu, J. Wen, S. Qian, H. Cao, C. Ning, X. Pan, X. Jiang, X. Liu, P.K. Chu, Enhanced osteointegration on tantalum-implanted polyetheretherketone surface with bone-like elastic modulus, Biomaterials 51 (2015) 173–183.
[320] G. Wu, P. Li, H. Feng, X. Zhang, P.K. Chu, Engineering and functionalization of biomaterials via surface modification, J. Mater. Chem. B 3 (10) (2015) 2024–2042.
[321] J. Khoury, M. Maxwell, R.E. Cherian, J. Bachand, A.C. Kurz, M. Walsh, M. Assad, R.C. Svrluga, Enhanced bioactivity and osseointegration of PEEK with accelerated neutral atom beam technology, J. Biomed. Mater. Res. B Appl. Biomater. 105 (3) (2017) 531–543.
[322] D. Almasi, N. Iqbal, M. Sadeghi, I. Sudin, M.R. Abdul Kadir, T. Kamarul, Preparation methods for improving PEEK's bioactivity for orthopedic and dental application: a review, International journal of biomaterials 2016 (2016), 8202653.
[323] A. Poulsson, R.G. Richards, Surface Modification Techniques of Peek; Including Plasma Surface Treatment, 2011.
[324] J.J. Roeters, A simple method to protect patient and environment when using sandblasting for intraoral repair, J. Adhesive Dent. 2 (3) (2000) 235–238.
[325] Y. Oshida, Y. Oshida, Bioscience and Bioengineering of Titanium Materials, second ed., vol. 25, Elsevier Science Bv, Sara Burgerhartstraat, Amsterdam, 2013. Po Box 211, 1000 Ae Netherlands.